TAMARACK (LARIX LARICINA (DU ROI) K. KOCH) AS A BIOLOGICAL INDICATOR OF WIND

ALEXANDER WOOD ROBERTSON

TAMARACK (*Larix laricina* (Du Roi) K. Koch) AS A BIOLOGICAL INDICATOR OF WIND

by

© ALEXANDER WOOD ROBERTSON

A Thesis submitted to the School of Graduate Studies
in partial fulfillment of the requirements for the
degree of Master of Science

Department of Geography
Memorial University of Newfoundland

St. John's Newfoundland

ABSTRACT

A major obstacle to validation of climatic models involving estimates of wind is the technical and economic constraints which preclude effective and efficient measurement of wind over complex terrain, especially over forested terrain.

This thesis examines tamarack as a biological indicator of wind as an alternative method of estimating the spatial variation of mean wind speed and direction in complex, forested terrain. The deformation of tamarack, including crown deformation and tree-ring asymmetry, was calibrated against the mean wind speed and direction at seven meteorological stations across Newfoundland. The indices were tested in a biological wind survey of the Black Mountain area, Avalon Peninsula, Newfoundland. The results show that tree deformation is caused primarily by summer southwesterlies. A crown deformation ratio, D_r', adapted to tamarack, was found to be a reliable indicator of wind in complex terrain. A compression index, C_i, describing tree-ring asymmetry, gave a reasonably good estimate of wind on level terrain but was not reliable for estimating wind in complex terrain.

ACKNOWLEDGEMENTS

The financial and logistic support provided by the Canadian Forestry Service, Newfoundland and Labrador Region, is gratefully acknowledged.

I am indebted to my supervisors, Dr. Roberts Mednis and Dr. Colin Banfield for their guidance throughout my graduate studies. Also, I thank my colleagues Dr. M.A.K. Khalil and Dr. Surindar Sidhu for their valuable advice.

The patience and expertise of Mrs. Ramona Raske in typing this thesis is greatly appreciated.

TABLE OF CONTENTS

LIST OF TABLES

LIST OF FIGURES

SYMBOLS

A	Angle of stem deflection from plumb line
B'	$\frac{\text{Branch extension leeward}}{\text{Branch extension windward}}$
C_i	Compression index = $\frac{\text{Tree-ring width leeward of pith}}{\text{Tree-ring width windward of pith}}$
C_{DIR}	Maximum width of tree-ring asymmetry
D_r	Wade-Hewson crown deformation ratio
D'_r	Crown deformation ratio modified for tamarack
G_{SL}	Yoshino's deformation grade
H_S	Relative stand height with respect to wind profiles
S_{DIR}	Direction of stem inclination
$\bar{V}_A$	Mean annual wind speed ($m\ s^{-1}$)
$\bar{V}_{AT}$	Mean annual wind speed adjusted to 2/3 tree height
$\bar{v}_{DIR}$	Mean wind vector direction

1.0 INTRODUCTION

1.1 SCOPE OF THESIS

To date, many numerical and theoretical models of wind flow over complex terrain and through forests, derived from wind tunnel studies, lack field validation. A major obstacle to validation of climatic models involving estimates of wind is the technical and economic constraints which preclude effective and efficient measurement of wind over complex terrain, especially over forested terrain.

Despite mankind's age-old preoccupation with climatic effects on plants, notably the destructive forces of wind storms, the use of vegetation as a biological indicator of wind is still primitive. Properly calibrated, biological indices offer a direct and reasonably good estimate of climatic parameters, and would be especially useful in regions with a paucity of meteorological stations.

With respect to environmental research and natural resource utilization, there is of late a growing interest in biological indices of climatic parameters. No doubt part of this interest is associated with recent advances in stochastic modeling techniques. Biological indices, based on tree deformation, have been used successfully in wind energy prospecting (Putnam, 1948; Wade and Hewson, 1979). Wind energy prospectors emphasize convenience and economy as the principal advantage in biological wind prospecting surveys.

Besides direct applications of biological indices for climate modeling and wind energy surveys, other applications could encompass a broad range of studies; for example:

- biomass productivity and distribution relating to forestry, agriculture, wildlife and environmental management;
- prediction of storm damage causing wind throw in forests, the spread of forest fires, and dispersal of insects and diseases;
- estimating the exposure to wind as a factor in energy consumption, snow drifting and parks and recreation activities.

To be quantitatively useful, biological indicators must be calibrated against a standard quantity. Accordingly, this thesis has two main objectives:

- to investigate the relationship between wind flow and tree deformation;
- to test the practicality of these relationships for mapping spatial variations in wind flow over complex, forested terrain using tree deformation indices.

1.2 WIND-RELATED CLIMATOLOGICAL PROBLEMS

The climate of Newfoundland is not easily divisible into homogenous units because of its insular nature, and also because it lies in the path of almost every major cyclone that tracks across and up the eastern seaboard of North America (Sutherland, et.al., 1963; Banfield, 1981) (Figure 1.1). The combination of unsettled weather associated with frontal systems and the complex topography of the island means that comparatively small changes in altitude and aspect result in considerable differences in the gradients of atmospheric properties, such as wind, temperature and humidity. These differences are often reflected by a sharp contrast in vegetation zonation.

The effect of wind on vegetation was discussed by the ancients. In De Ventis, Theophrastus discussed the effects of wind on crops and in mountainous regions (Coutant and Eichenlaub, 1975). Since Theophrastus' time, literature on vegetation zonation as a reflection of climatic gradients has become extensive. Some examples of the effects of climate on vegetation zonation can be found in Wilton (1964) and Daubenmire (1974). Because plants are master integrators of atmospheric properties, Kimbal and Brooks (1959) applies the term 'plant-climate' to this relationship. They defined plantclimate as: "The condition wherein specific groups or association of plants and the physical climate are in complete harmony." The assumption of harmony between plants and climate is analogous to the classical climax theory which implies the existence of a steady-state, or equilibrium, at some stage in plant succession. However, this assumption is anachronistic because it fails to recognize the infinite dynamic processes governing

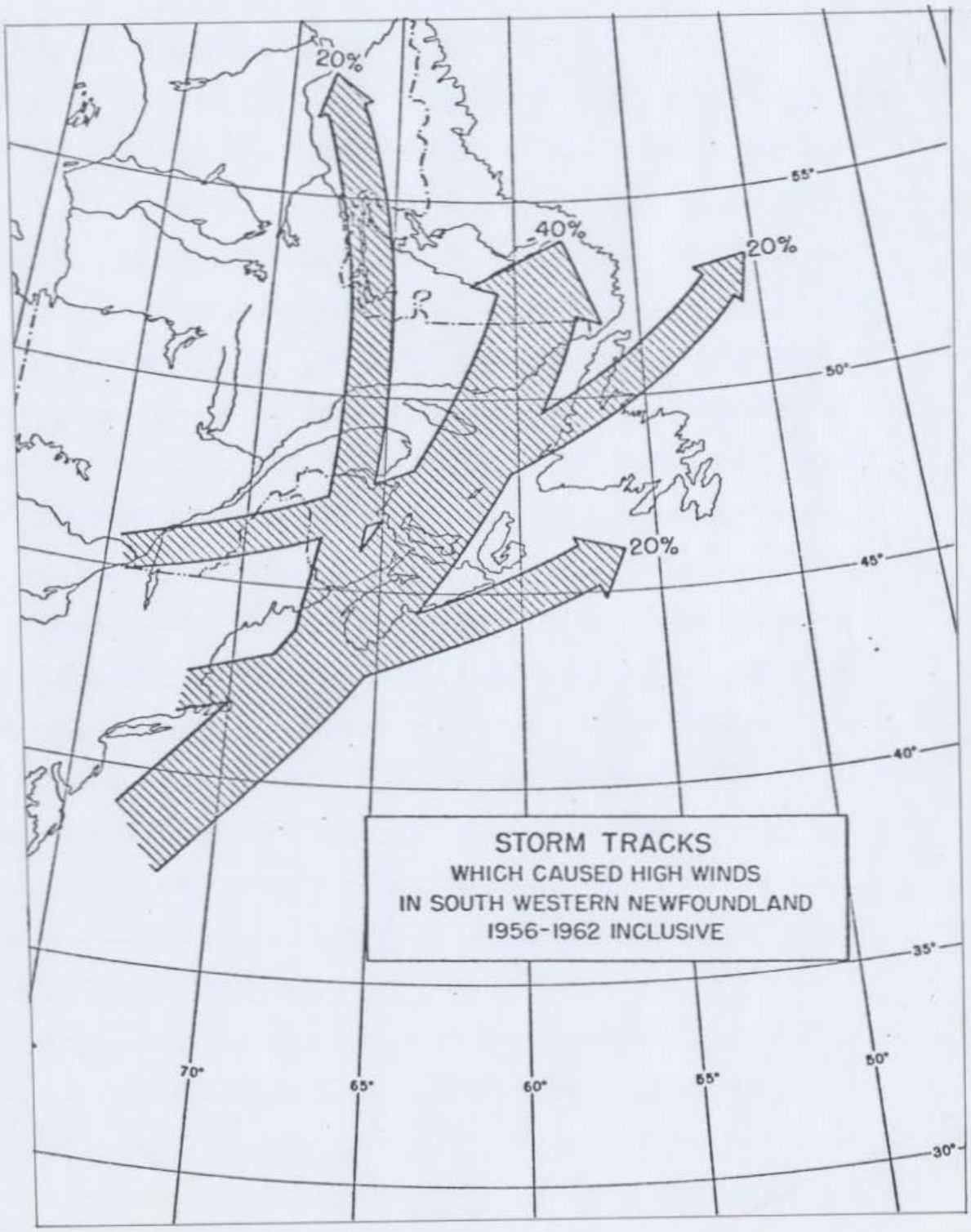

Figure 1.1 Tracks of cyclones which cause strong winds in Atlantic Canada (from Sutherland, et.al., 1963).

the nature of plantclimates.

Contrary to the belief that plants are ever in 'complete harmony' with physical climate, the writer proposes a slightly modified definition of plantclimate; i.e. "a condition wherein plants and atmospheric properties reflect each other." Embodied in this general framework is a restatement of the first law of thermodynamics which emphasizes the dynamic principle whereby plants absorb and temporarily store energy to an extent dictated by a physical climate. The plants and their plantclimate are but a momentary phase in a ceaseless, universal transformation of energy. Therefore, the concept of 'complete harmony' in physical systems is illogical.

'Plantclimate' is a quantitative term used to describe trends in physical climate associated with plant growth and decay. Apparently the dimensions of a plantclimate zone are determined arbitrarily, depending on the object and scale, both temporal and spatial, of inquiry. For example, plantclimates can be stratified to study the climate of a cell, a leaf, a single plant or a group of plants, or parts thereof. In short, the plantclimate zone is an arbitrary interactive layer between plants and physical climate.

Being at the surface of the Earth where frictional forces are greatest, the plantclimate zone occupies the most turbulent part of the so-called planetary boundary layer. The planetary boundary layer is not easily defined because changes in its thickness vary with step changes in surface roughness. Also, the planetary boundary layer varies in height diurnally from approximately 100m over relatively flat, homogenous terrain up to 1 km over mountainous terrain and its height at

any particular time varies with wind speed near the surface.

In reality, it is impossible to separate patterns of atmospheric motion by scale or size because as kinetic energy is dissipated from jet streams in upper-air global circulations systems to the smallest eddies at the turbulent-free laminar layer at the surface, a particular wind flow pattern interacts with all others to some extent. Thus, what is often loosely referred to as the planetary boundary layer actually consists of myriads of smaller boundary layers. Despite the extensive literature on boundary layers in general, a totally satisfactory definition will remain elusive until we have a precise mathematical definition of turbulence, since this is, in effect, what a boundary layer describes. Dutton (1976) notes:

> Everybody knows what turbulence is and yet no one can define it. A turbulent flow is easily recognized if its patterns can be seen visually, but no specification that provides a sharp, mathematical distinction between turbulent and non-turbulent flow is yet available. (pp. 440)

Nevertheless, for general reference, Dutton (1976) distinguished three layers which make up the planetary boundary layer:

- a laminar layer over surfaces where viscous forces predominate and eddy stress is negligible and its thickness is a few millimeters at most;
- a constant stress layer where the wind profile is approximately logarithmic due to a constant eddy stress;
- the Ekman layer where the real wind spirals upwards to the geostrophic wind at which point is considered to be the top of the planetary layer.

Laminar layers also exist between parcels of air that are indepen-

dent of any surface when turbulence is dampened out by the work it has to perform against stably stratified air. This density stratification phenomenon is utilized extensively in wind tunnel experiments that create boundary layers artificially. For example, Grace (1977) defined an artificially-induced boundary layer over a thin, leaf-like plate as: ". . . the point at which velocity [of air] reaches some arbitrary fraction, say 0.99, of its value in the mainstream." Mathematically, the thickness of the boundary layer, δ^*, was defined

$$\delta^* = \int_{\infty}^{\delta} \left(1 - \frac{u}{u_{\infty}}\right) \Delta y$$

where u = local wind velocity

u_{∞} = mainstream wind velocity.

This expression is analogous to the internal boundary layer created by the leading edge effect (Oke, 1978), which involves a step change as wind flow encounters a new surface with a different roughness. The structure of the internal boundary layer depends on the porosity, or bluffness, of the underlying surface. Since plant canopies are usually porous, the air that flows through is referred to as the clothesline effect which readjusts the velocity and properties of air flow within the internal boundary layer. This boundary layer within a boundary layer is called the equilibrium layer. Hence, within the constant stress layer there is actually a series of internal boundary layers, each with its own equilibrium layer that is wholly dependent on the magnitude of surface effects on local wind flow. Wind flow in the

equilibrium layer created by plant canopies does not have a logarithmic profile except near the top of the canopy. This non-logarithmic profile boundary layer will be referred to herein as the plantclimate zone. Figure 1.2 is a schematic representation of layers of turbulent zones within the planetary boundary layer.

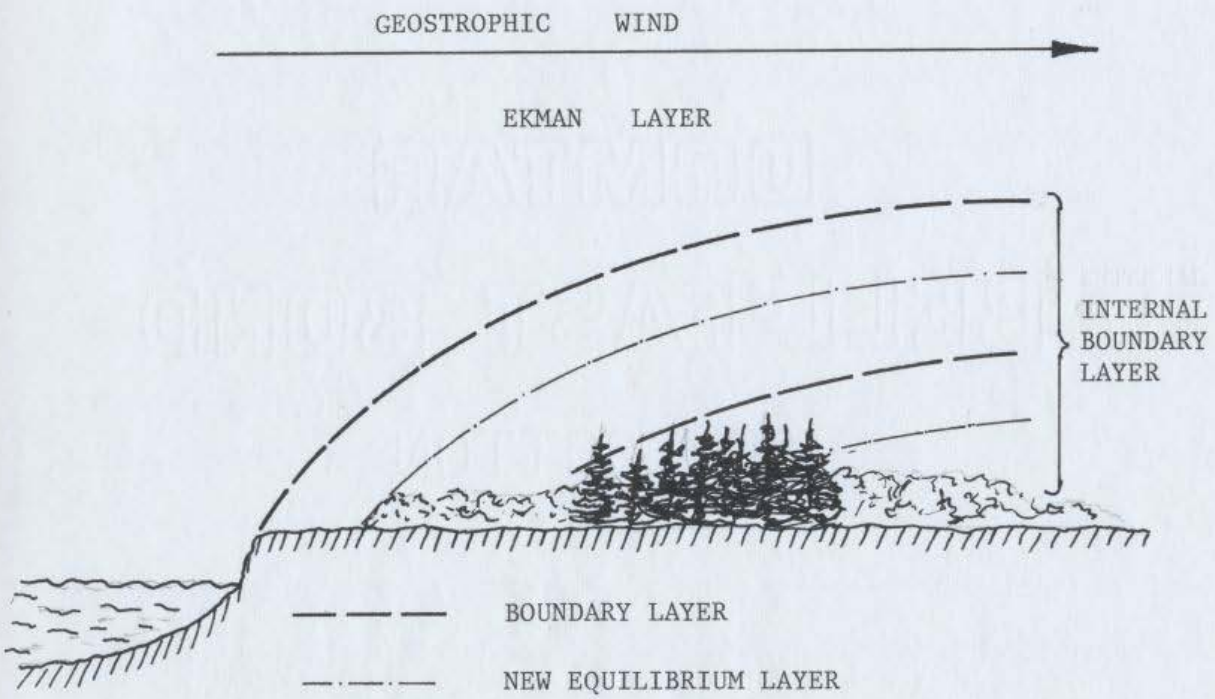

Figure 1.2 Creation of internal boundary layers by step changes in topography and surface texture

Over complex topography with heterogenous surfaces, especially with vegetation, the internal boundary layer will also be complex and poorly differentiated, which means simply that its wind profile will deviate considerably from logarithmic. For example, obstacles such as buildings, isolated hills and windbreaks, create special aerodynamic features by

decreasing wind speed in their leeward side; but by increasing it near the top of the windward side, vortices are generated by flow separation. Such vortices can be observed directly in wind tunnel models. In nature, they can be inferred from tree deformation (Yoshino, 1975) and wind throw (Hutte, 1968). Figure 1.3 illustrates vortices based on Yoshino's observations.

Because the spatial variation of atmospheric properties in plant-climates is extreme, they are difficult to measure. On a microscale the introduction of sensors leads to systematic errors, whereas on a larger scale, such as a forest, directly measuring atmospheric properties over a broad range of conditions and canopy levels is beset with many technical difficulties and often prohibitively expensive. Alternatively, numerical simulation and quasi-empirical models have been developed to predict wind flow in forests and over complex terrain, respectively. Quasi-empirical models of wind flow in forests involved studies of homogenous plantations on relatively flat terrain with an adequate fetch, e.g., Oliver (1971), Thom (1971), Oliver and Mayhead (1974), and so do not adequately reflect wind flow in forests growing on complex hilly terrain. Similarly, the majority of numerical and theoretical models of wind flow over complex terrain derived from wind tunnel experiments lack field validation and, therefore, have limited practical value..

Plantclimate inferred from standard meteorological data is prone to large errors and is often irrelevant. For example, Nicholson and Bryant (1971) used the principal component analysis, a multivariate statistical technique, to explain variation in climate among stations

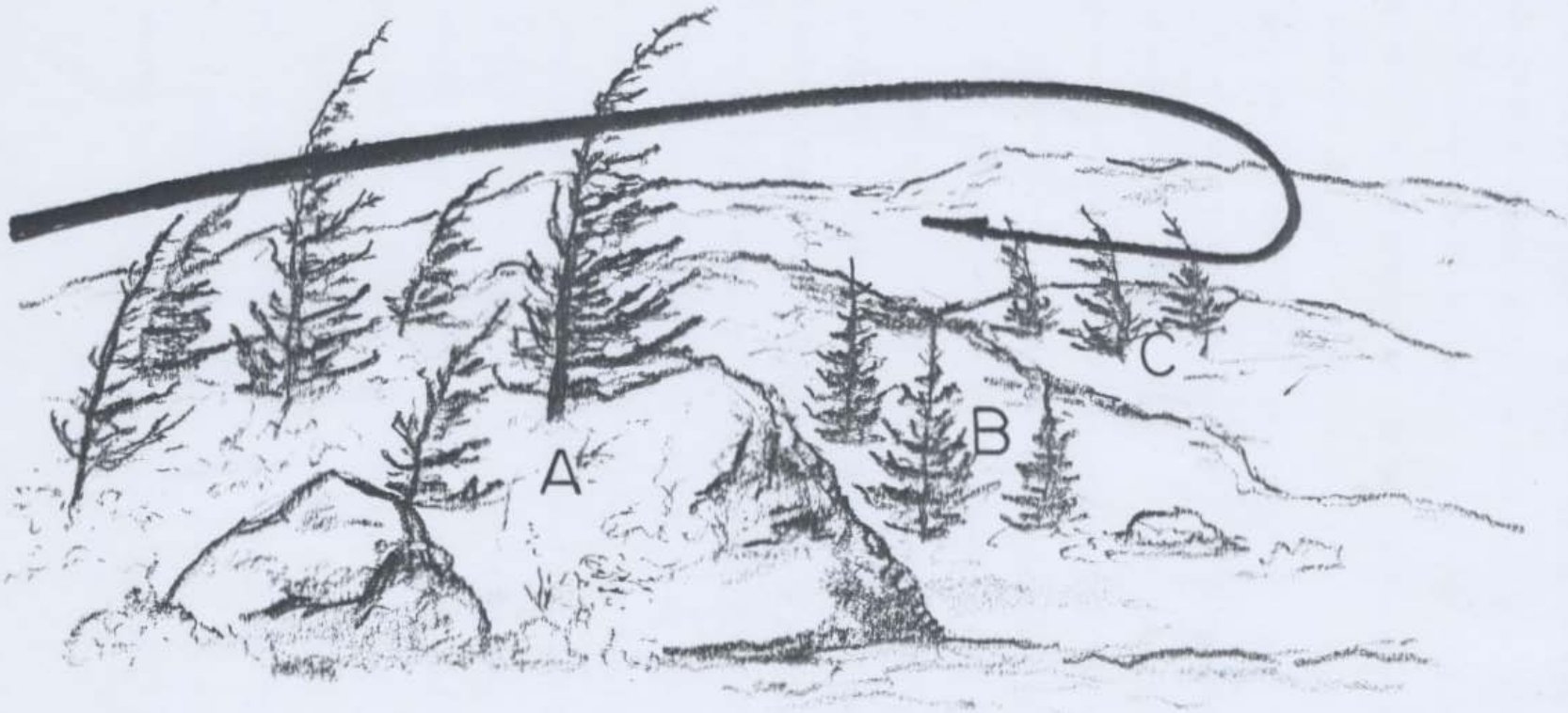

Figure 1.3 Vortices generated by flow separation over a ridge inferred from the direction of stem inclination of deformed tamarack on the Avalon Peninsula, Newfoundland. The phenomenon is similar to that observed by Yoshino (1975) on Mt. Azuma, Japan.

in Newfoundland. Their analyses were restricted to parameters of temperature and precipitation; and they concluded that these were the variables that "explained variation" in Newfoundland climate. Other variables such as humidity, cloud cover, wind and radiation were omitted from the analysis because they were recorded at too few stations. Despite these omissions they maintained that:

> Investigators attempting to relate biological phenomena to the variation of climate in insular Newfoundland need only use the climatic variable that is most heavily weighted in each principal component if climatic relations are to be adequately analyzed.

Considering the relatively high mean annual wind speed in Newfoundland (Banfield, 1981; A.E.S., 1982), it appears that because this important variable was left out of their analysis, their conclusions may be invalid. Also, since the object of the principal component analysis is to reduce a large number of variables into a set of new variables (Newnham, 1968), the sensitivity of the analysis depends on the original choice of variables, especially considering the first two or three eigenvalues account for most of the variation (McAdam, 1980).

Another restriction on the usefulness of standard meteorological data is that complex topography and vegetation zonations preclude interpolation of local climates between meteorological stations primarily because the climate represented by standard meteorological data is uncharacteristic of plantclimates. For example, for measuring standard variables all sensors are located at one level. Furthermore, temperature and humidity sensors are housed in artificial shelters; raingauges are designed to minimize evaporation once rain water is collected; where possible anemometers are located well above the internal boundary layer

and radiation is recorded in the open where horizontal obstructions are less than 15° degrees above the horizon. The main criteria for siting a meteorological station are that it have as large a fetch (i.e., level, open expanse) in all directions as possible and also be readily accessible. Large airports generally provide the best sites. In practice, the condition of an adequate fetch in Newfoundland is rarely met. Furthermore, since much of Newfoundland's interior in uninhabited, the meteorological data have limited value for most of the Island. In addition, the climate of a region as represented by standard meteorological data is not nearly as complex as that of a plantclimate and, therefore, it is not realistic to make direct comparisons. Difficulties inherent in applying standard data on a regional basis were demonstrated by Ryan (1977) who showed that topography precluded interpolation of regional wind flow based on distance and direction as criteria.

Even comparisons between adjacent meteorological stations result in different interpretations of data for the same purpose. For example, Simard (1969) studied the effect that wind speed measurements at airport stations and nearby forestry stations had on forest fire danger ratings. He found that wind speed measurements at nine forestry stations across Canada were significantly lower than at respective adjacent airports. Consequently, the relative frequency of days with severe fire danger ratings was significantly higher at airports than forestry stations.

2.0 LITERATURE REVIEW

2.1 EFFECT OF WIND FLOW ON TREES

In the Rocky Mountains of North America, Rydberg (1913) observed that the tree line was higher on complex mountain terrain than on isolated peaks. He attributed the differences to wind velocity, i.e. being higher around isolated peaks than in complex terrain. Also in the Rocky Mountains, Griggs (1938) observed that some leeward slopes supported trees, whereas windward slopes at corresponding elevations did not. Recent studies on advective processes, contained in Oke (1978), have shown this to be a common occurrence due to spatial variations in the energy balance.

Daubenmire (1974) and Wilton (1964) concluded that the tree line is modified by latitude, implying that temperature regimes were more important than wind.

Tansley (1939), Tranquillini (1963), Wardle (1968), Lawrence (1939) and others have studied the variation of tree deformation caused mainly by wind-pruning.

Despite the obvious effect of wind on tree growth, relatively few studies have been conducted on the relationship between tree growth and wind. Booth (1976) obtained a good correlation between growth of tree plantations and wind speed in a hilly region of Kintyre, Scotland with correlation coefficient of $r = 0.63$ to $r = 0.67$.

Peterson and Billings (1980) showed that geomorphic processes influence patterns of tundra vegetation and alluded to the importance of wind in soil erosion and redistribution of snow. Nichols (1976) suggested that outliers of tree stands persist because of protection from wind.

Figures 2.1 and 2.2 illustrate the extreme effects of exposure on tree growth in western and central Newfoundland.

In dendrochronology, wind as the major factor influencing tree growth is rarely considered, e.g., Jacoby and Cook (1981) and Clague, et.al. (1982). Werren (1981) assumed that spruce growth rings examined up a gradient reflected a cline from low stress to high stress. He also described a 'regular' growth in sheltered sites and 'irregular' growth in exposed sites and attributed growth restraints to 'atmospheric stresses.' Similarly, Kay (1978) found the greatest variation and suppression of tree-rings on more 'exposed' sites, interpreting the climatic stress in terms of the position of Arctic fronts. Grace (1977) notes that the term 'exposure' is used too often without a proper definition. Do Werren and Kay, for example, mean that wind is the dominant factor in their concept of 'exposure' and 'stress'? Nevertheless, Cropper and Fritts (1981) maintain that many Arctic dendrochronologies are of limited value for climatic analysis; even more so since most of them fail to recognize the importance of tree-ring asymmetry as a response to wind.

In north-central USSR, Larix dahurica, L. sibirica and L. s. var. jukaczewi are the main tree species in the upper tree limit (Gorchakovsky and Shiyatov, 1978). Analysis of their vitality, change in growth patterns and associated vegetation indicate latitudinal and altitudinal fluctuations in the tree line in response to cyclical climatic change. The expansion of the boreal forest zone is evident in 60-80 and 140-160 year cycles in tree line fluctuations. In tree ring widths of Larix sibirica at the upper tree limit, 100-year cycles are evident. Short

Figure 2.1 Remains of a coastal balsam fir forest destroyed by a combination of wind, sand, ice and salt at Western Brook, western Newfoundland.

Figure 2.2 Remnants from a forest fire on the Buchan's Plateau, central Newfoundland, indicates the severity and direction of winds that deform trees in this region.

cycles of tree growth, 22-35 years, do not result in significant changes to the tree line.

Cooper (1913) described the forest structure of Isle Royale, Lake Superior, as a mosaic of constant change. Native vegetation was heterogeneous due to small wind throw areas. In an Appalachian virgin forest, tree-ring growth revealed higher than average abrupt changes in the frequency and intensity of forest regeneration. Lorimer (1980) attributed the changes to disturbance which hastens forest succession towards a 'climax' by releasing the understory from suppression. Sprugel (1976) and Sprugel and Bormann (1981) rejected the 'climax' theory and argued that disturbance is a vital process in ecosystem dynamics. On the slopes of the White Mountains, New York, he observed that wind damage was concentrated on the south and east slopes. The canopy was broken by crescent-shaped strips and each band is a slow moving wave in the general direction of the prevailing wind. The highest wave speed occurred near the top of the ridges. Sixty-year wave cycles correspond to the lifespan of balsam fir, the dominant tree species. At maturity balsam fir is weakened by biotic and abiotic stress which makes it vulnerable to wind throw. Waves result from the wind throw of a single mature tree, followed by other mature trees in the vicinity blown down by later storms. Eventually, a crest-shaped wave forms. As another generation of trees matures behind a wave, a new wave is formed slightly out-of-phase with the original wave; hence, the canopy profile has a multi-crescent form. A strong correlation ($r = 0.888$ at $P < 0.01$) exists between slope aspect and angle and wave speed. Figure 2.3 shows wave strips on the lee slope of a small hill at the head of South Brook

Figure 2.3 A series of wave strips near the crest of a hill (foreground) in South Brook Valley, near Pasadena, western Newfoundland. Note the wind thrown stands of decadent balsam fir just below the ridge where regeneration will probably form a new wave.

Valley, western Newfoundland not unlike those described by Sprugel (1976).

In Japan, 100-200 year wave cycles occur in Abies veitchii forests on the southwest slopes of Mt. Shimagare. In fact, Mt. Shimagare means "mountain with the dead trees" on account of the whitish strips that transect the dark green slopes (Oshima, et.al., 1958 and Franklin, et.al., 1979).

Storm damage to forests is a major economic and management problem and may account for a substantial portion of the allowable annual cut. In extreme years, storms may destroy up to 30% of the allowable annual cut of a country (Brunig, 1967). Gilmour (1926) studied wind throw in black spruce pulpwood forests in central Newfoundland. He examined wind throw damage in 24 (2.25 ha) plots left within a logged area. Five years after cutting the volume of wind thrown trees exceeded the growth of the standing timber. Moore (1977) examined factors affecting wind throw in streamside leave strips on Vancouver Island, British Columbia. Wind throw was shown to be a complex phenomena and results primarily from storm winds rather than prevailing winds. Environmentally, extensive wind throw is considered to have undesirable effects on streams and slopes. Sporadic wind throw, however, is considered useful since it dissipates stream energy, collects gravel, forms pools and is beneficial to fish and other fauna (Heede, 1962 and Swanson, et.al., 1976). Alexander (1964) provided guidelines to minimize wind throw around logged areas in spruce-fir forests. Petrie (1951) made silvicultural recommendations to minimize wind throw in the spruce plantations. He noted that canopies with a more uniform height were more susceptible to

wind throw than irregular ones; that trees conditioned to exposure are more wind firm than sheltered trees; stands generally withstand greater forces from prevailing winds than occasional storms from non-prevailing directions. Kennedy (1974) conducted an extensive survey of wind damage in forest plantations in Northern Ireland. He found that wind damage varied significantly with other environmental factors (such as stand age, soil type, slope angle and aspect) besides climate.

Johnson (1982) correlated wind throw with mean wind speed. Comparing field observation with wind tunnel tests, he developed a method for predicting maximum wind speed based on observed damage. The technique is especially useful for understanding surface winds in cyclonic storms, particularly in regions where wind data is scarce.

2.2 TREE INDICES OF WIND

Numerous studies on wind throw tend to confirm general theory on wind flow over complex terrain. For example, it is well-known that wind throw occurs most frequently and to a greater extent on ridges and lee slopes and on the shoulders of bell-shaped hills (Smith and Weitkneckt, 1915; Curtis, 1943; Gratkowski, 1956; Aanensen, 1965; and Hutte, 1968). The reason, according to Hutte (1968), is that turbulence caused by vortex wake detaches from the hill and attacks the tree from its most vulnerable side, i.e. leaning side. Likewise, in the case of flat terrain, and even hilly terrain, storm winds from the non-prevailing direction will generally result in more damage than those from the prevailing direction.

Patterns of wind throw are useful for studying the spatial distribution of storm winds (Onaka, 1949; Curtis, 1943; Hutte, 1968; Weidmann, 1930; and Johnston, et.al., 1982). Alexander and Buell (1955) took compass bearings of wind thrown logs to construct a wind rose frequency. From this they were able to determine the direction of destructive winds in a Rocky Mountain timber stand. Weidmann (1930) did a similar study and found that wind throw was greatest in the section of a valley where the wind tends to be funnelled.

In particularly windy sites tree canopies tend to be asymmetric with the main axis in the direction of the prevailing wind and swept to the leeward. Jefferson (1904) discussed tree deformation of a number of species in relation to different wind systems. He observed that persistent, moderately strong winds causes as much deformation as occational storm winds do. Different direction of tree deformation axis

can distinguish between "trade winds" and westerlies. According to Jefferson, "trade winds" are associated with clear skies, steady temperatures and wind always in the same quarter, i.e. southwest quarter. Westerlies, on the other hand, are associated with fine, stormy weather with winds veering and reversing through all points of the compass. Locally, tree deformation also reflects sea breezes and mountain winds.

Lawrence (1939) described two mechanical effects which causes flagging, i.e. glaze injury plus wind associated with easterly gales and wind only.

In coastal areas, the extent of wind deformation may be masked by salt-spray damage. At Cape Fear, North Carolina, Wells and Shunk (1937) showed that deformation along the coast was largely the result of salt damage rather than wind, per se. They observed injury to shoots during a 50 kph southeasterly which lasted 19 hours. Injury resulted to shrubs along a coastal strand and not to others inland that were equally exposed. Soil moisture was abundant but tests for chlorine content revealed higher Cl concentrations on exposed than sheltered shoots along the strand. They also simulated injury by spraying immature shoots with sea water and showed that only protected, unsprayed lateral shoots develop. Figures 2.4 and 2.5 show the structure of a coastal tuckamore along shore of Ingornachoix Bay, Newfoundland that exhibits salt damage similar to that described by Wells and Shunk (1937).

Studies of deformed trees as indicators of prevailing wind direction include those of Plesnik (1957, 1971) in the Tatra Mountains of Central Europe; Runge (1957, 1959) in the valleys of the Allgauer Alps and Italian Riviera; Plesnik (1973) in the Rocky Mountains of U.S.A.;

Figure 2.4 Coastal tuckamore (Krummholz) of balsam fir along the shore near Daniels Harbour, western Newfoundland (color). The distinctive sweeping profile is attributed to the effects of onshore winds laden with salt and (in winter) with ice crystals.

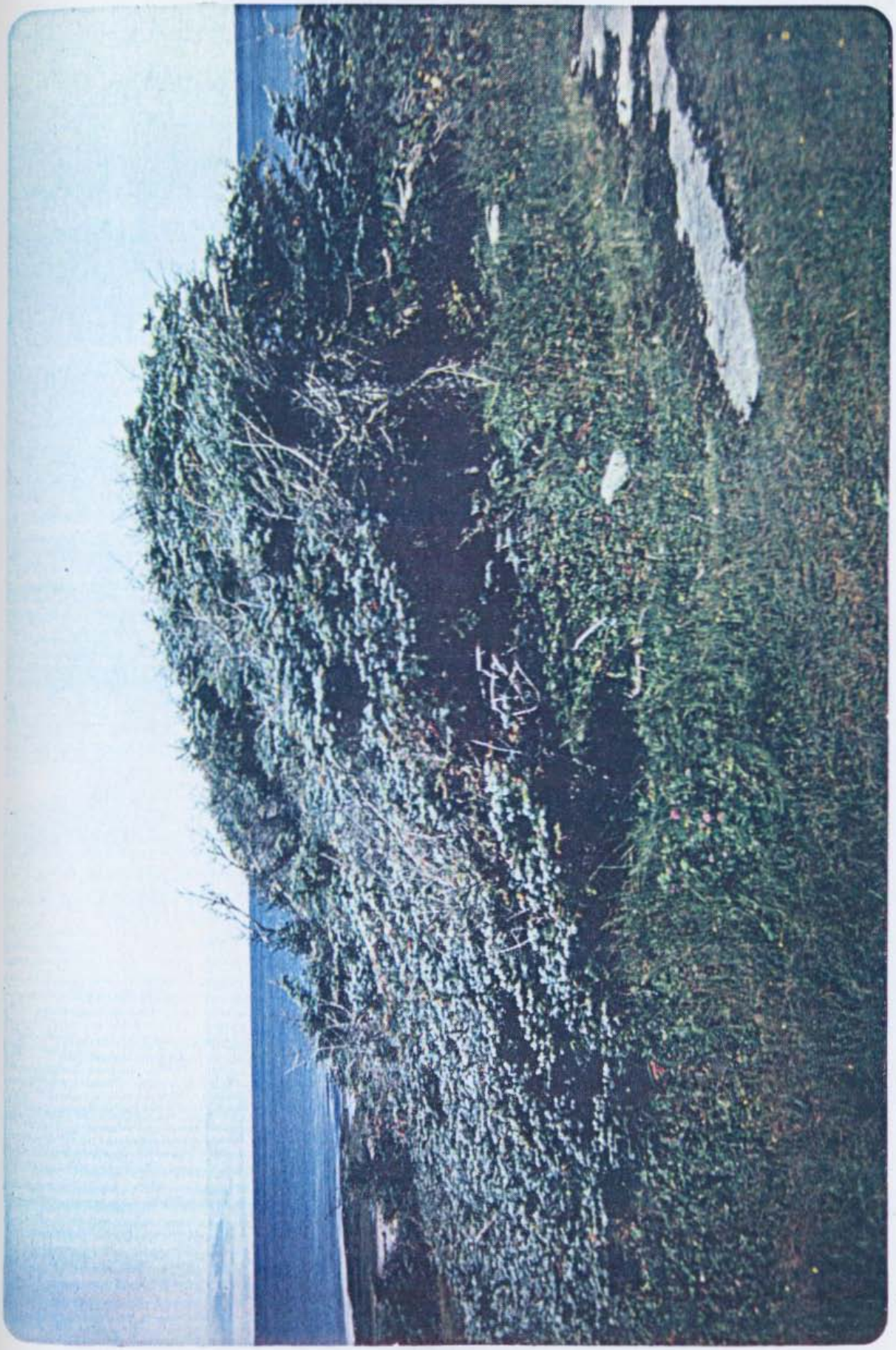

Figure 2.5 The impenetrable structure of a coastal tuckamore is revealed by this burned stand of balsam fir near Hawke Bay, western Newfoundland. Note the branches are predominantly on the landward side of the trunk attributed to the effect of onshore winds laden with salt and (in winter) with ice crystals.

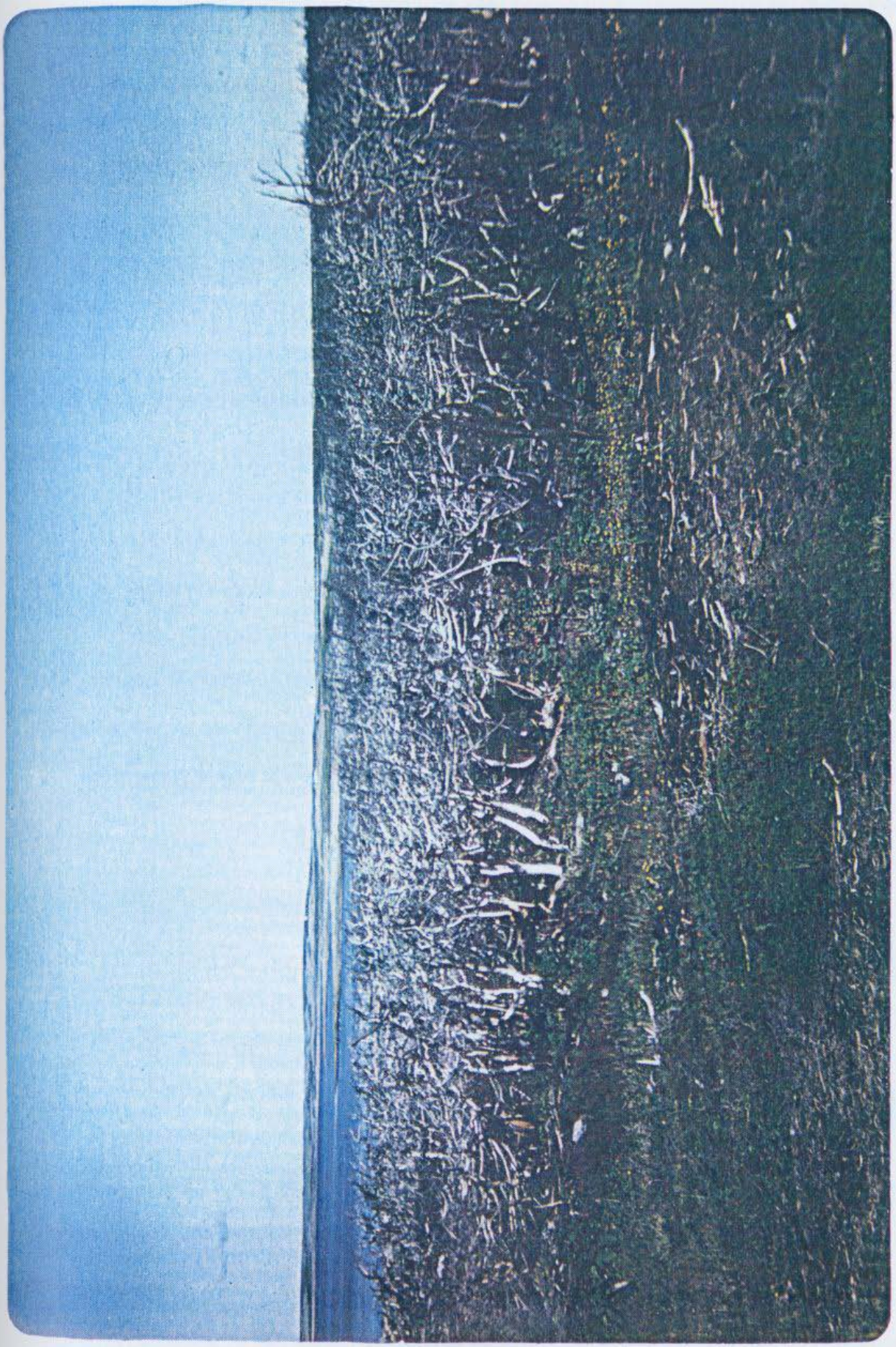

Holroyd (1970) in New York; Yoshino (1975) in Japan and Eastern Europe; Oliver (1960) in England; Thomas (1973) in Wales; and Noguchi (1979) in Hawaii.

Griggs and Putnam (Putnam, 1948) developed a grading system to estimate mean wind speed from deformed conifers (Figure 2.6). Later, Barsch (1963) devised a similar index for broadleaved trees (Figure 2.7). Yoshino (1975) modified these grading systems to account for indirect and direct environmental influences (Figure 2.8).

Weischet (1955) observed that species vary in their tolerance to wind and devised a rather crude grading system based on differences to wind tolerance between genera. He advised that only isolated trees, or trees in shelterbelts of the same species, size and age can be compared.

Owada (1973) appears to be the first to have established a semi-empirical relationship between tree deformation and wind. He calibrated Japanese larch (Larix leptolepis Gord.) to estimate the mean growing season wind speed at a local meteorological station ($\bar{u}_s$)

$$\bar{u}_s = 1.6 + 0.95\ G_{SL}$$

where G_{SL} = deformation grade determined subjectively by Yoshino's classification system for deformed trees

Japanese larch planted on a bog near Stephenville, Newfoundland (Figure 2.9) shows that the mean annual wind speed is approximately 5 m S^{-1}, using Owada's equation.

Wade and Hewson (1979) improved on the original Griggs-Putnam and Barsch indices by calibrating numerous species, mostly of western United States, representing five genera of conifers, four deciduous and one

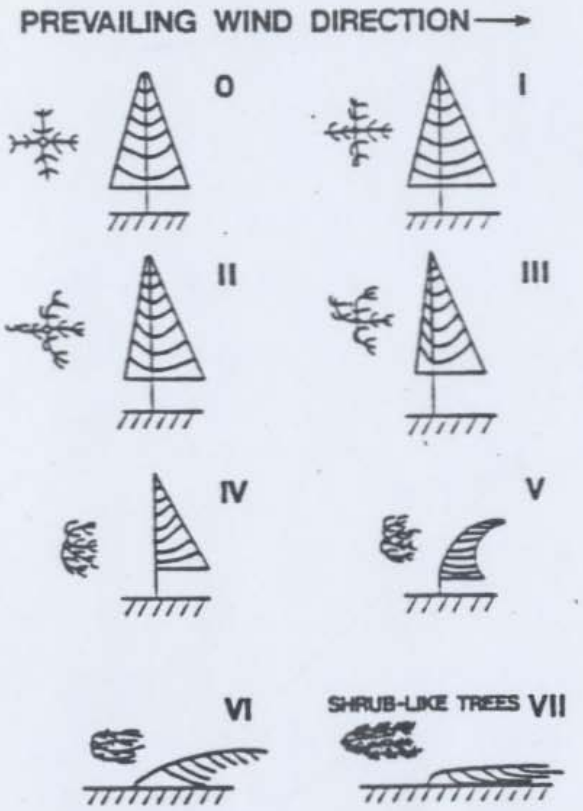

Figure 2.6 Griggs-Putnam index characterizing wind deformation of conifers (from Wade and Hewson, 1980).

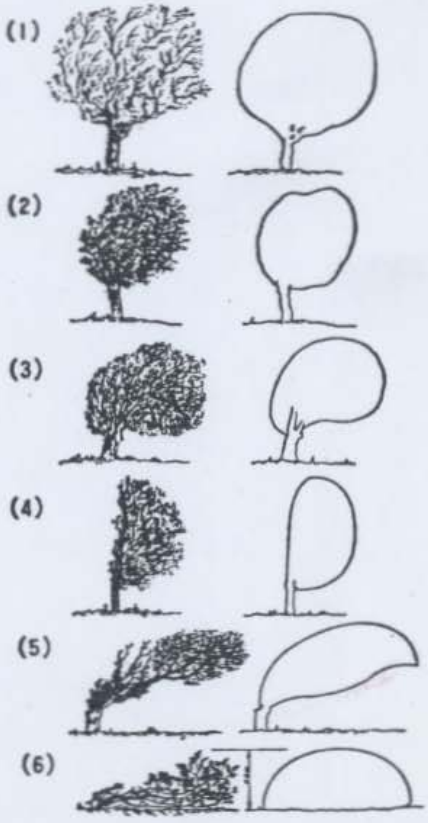

Figure 2.7 Barsch index characterizing wind deformation of broad-leaved trees (Barsch, 1963).

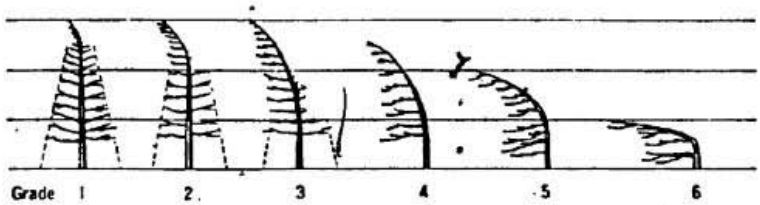

Grade	Type 1	Type 2	Type 3
0	Symmetrical form	Symmetrical form	Symmetrical form
1	Tree-top and twigs are bent slightly to leeward.	Windward side of tree-top has severed slightly.	Trunk or branches are bent slightly to leeward.
2	Tree-top (ca 1/3 of tree height) and twigs are bent apparently to leeward. This form can be called "Brushing."	Windward side of tree-top (ca 1/3 of trunk height*) has no twigs or branches.	Trunk and branches in ca 1/3 tree height are bent markedly to leeward.
3	Imperfect flag-shaped tree. About 2/3 of the height of tree from the tree-top and branches are bent apparently to leeward.	Wind side of trunk in ca 2/3 of trunk height* from the tree-top has no twigs or branches. Imperfect flag-shape.	Trunk and branches in ca 2/3 tree height are bent drastically to leeward. Imperfect flag-shape.
4	Perfect flag-shaped tree. All branches are bent to leeward. Windward side of trunk has no branches. Trunk leans slightly.	Perfect flag-shaped tree, as far as the part over the surface of snow accumulation in winter. Trunk is bare on windward side.	Trunk and branches are bent almost perfectly to leeward. On windward side, trunk is bare.
5	Tree height is lower than length of main branches. Trunk leans leewards. Called *Krüppelform*, *Windflüchter* (Weischet) or "Throwing" (Putnum).	Trunk height* is lower than length of branches. Branches are developing poorly on leeward and none on windward.	Trunk and branches are deformed so as to lean away. Height of tree is lower than length of main trunk or branches. Branches on the extreme leeward part only are living.
6	The shape becomes similar to that of Type 3.	There are no trees in Grade 6 of Type 2.	Trunk and branches grow only leeward very low on the ground level, look like creeping. Called *wind creeping* (Putnum) or *Teppich-form* (Barsch). Called *cushion shape*, *tree-carpet*, and so on.

* Trunk height of Type 2 is measured from the estimated surface of snow accumulation in winter.

Figure 2.8 Yoshino's grading system for tree deformation (from Yoshino, 1975).

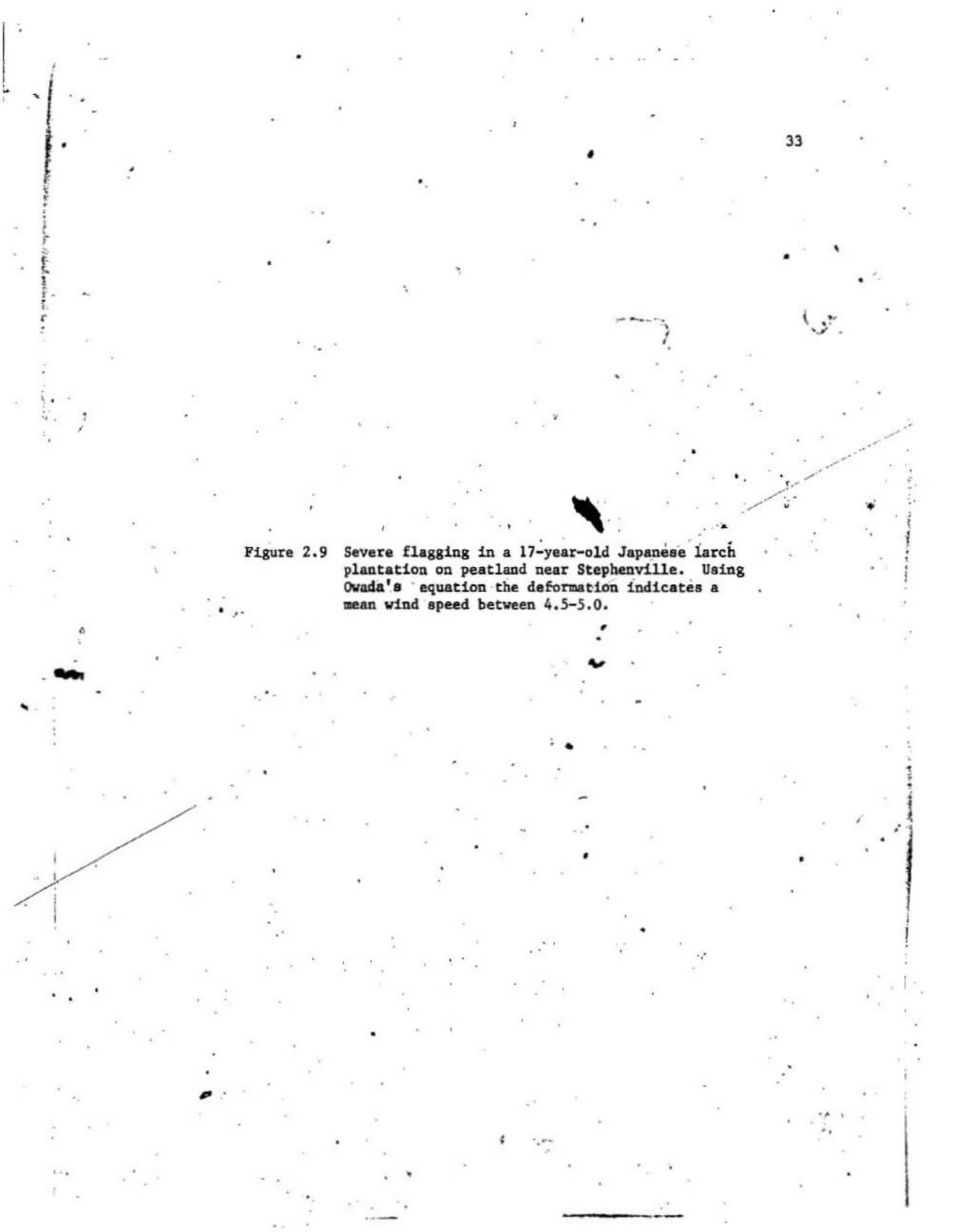

Figure 2.9 Severe flagging in a 17-year-old Japanese larch plantation on peatland near Stephenville. Using Owada's equation the deformation indicates a mean wind speed between 4.5-5.0.

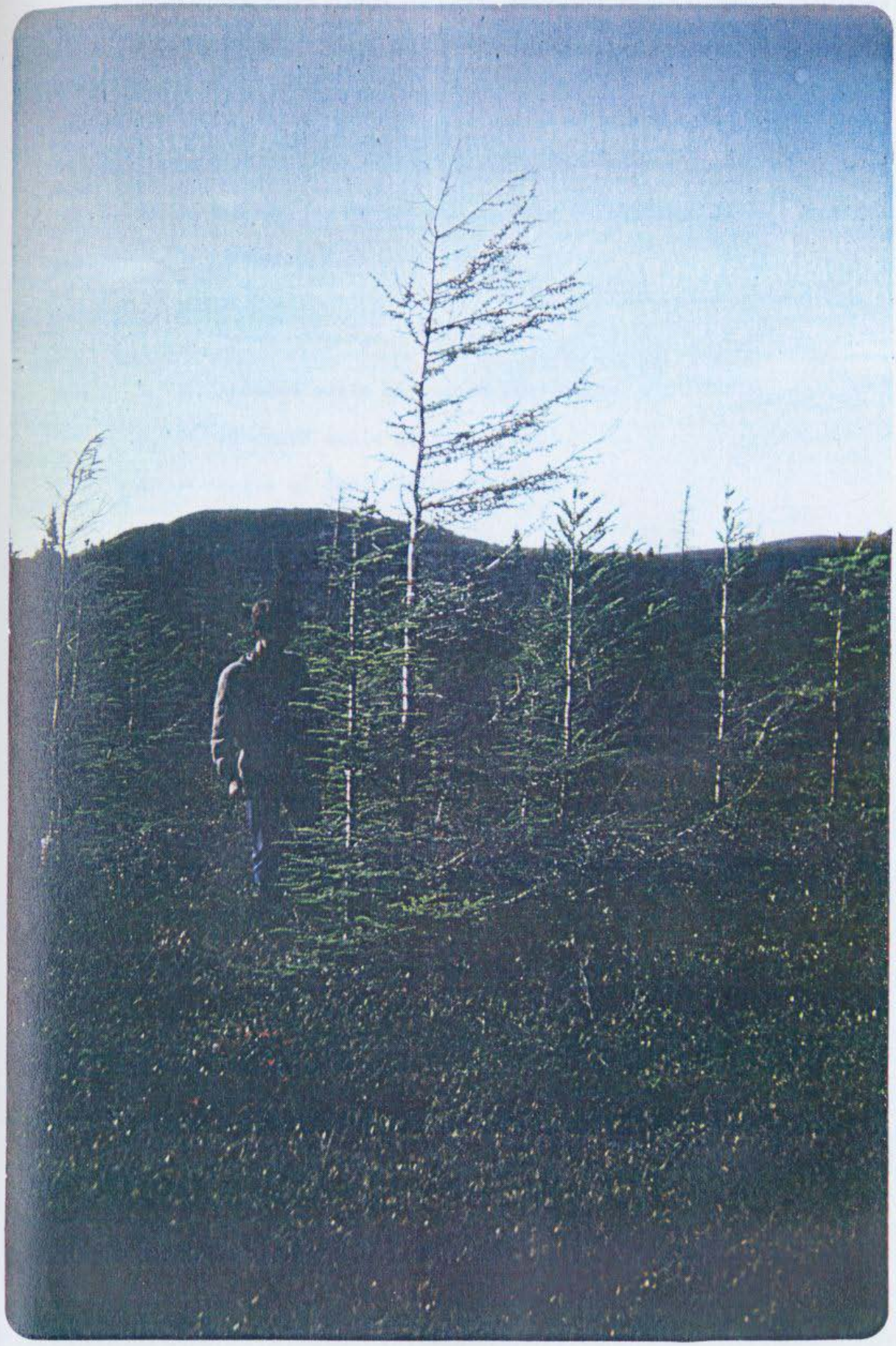

tropical. In addition, they introduced two new indices. The first, called the deformation ratio (D_r), measures the proportion of branches on the leeward and windward side of the trunk, respectively, as well as the angle of inclination of the trunk. The deformation ratio is calculated from

$$D_r = (B_L/B_w) + AT/45^o \qquad (1 \leq (B_L/B_w) \leq 5)$$

where B_L = leeward angle of branch projection

B_w = windward angle of branch projection

AT = angle of inclination of trunk

Figure 2.10 illustrates the measurements required to obtain the deformation ratio.

The other index given by Wade and Hewson (1979) is the compression index (C_i) given by

$$C_i = TR_L/TR_w$$

where TR_L = tree-ring width leeward

TR_w = tree-ring width windward

Sciedo et.al. (1979) adopted a more theoretical basis for estimating wind velocity in open black spruce-lichen forests at Schefferville, Quebec. Their technique involved defining the relative stand height and weighting this with a non-dimensional factor derived from the vertically projected stand density. The relative stand height (H_S) is determined from

$$H_S = A' (\bar{H}/Z) + h'$$

$$D_r = (B_L/B_w) + AT/45^o \qquad (1 \leq (B_L/B_w) \leq 5)$$

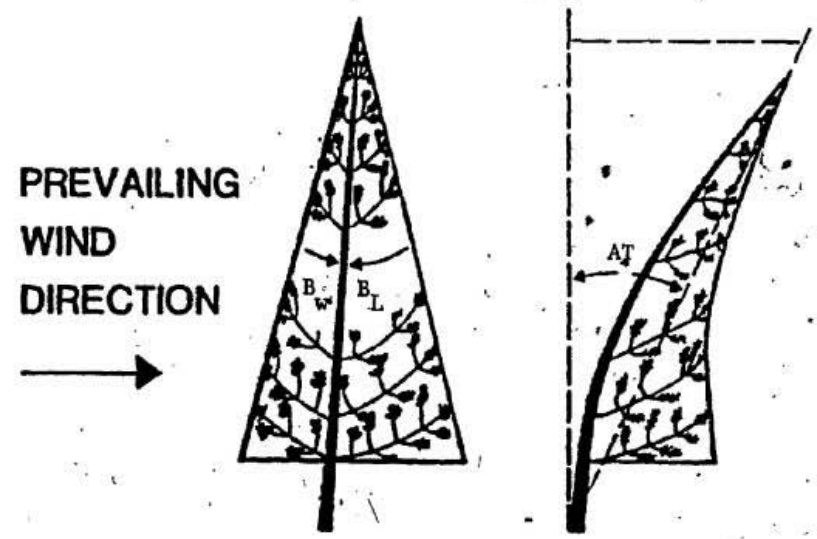

(a)

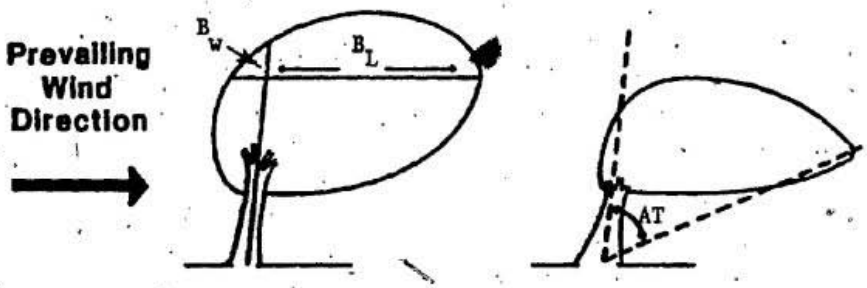

(b)

Figure 2.10 Wade-Hewson deformation ratio for conifers (a) and broad-leaved or hemispherical crowned trees (b) (from Wade and Hewson, 1980).

where A' = fractional vertically projected stand density

$\bar{H}$ = mean tree height

Z = anemometer height (2 m)

h' = correctional factor accounting for height of large boulders and shrubs

Having determined H_S, the mean wind velocity at a given height within the stand ($\bar{u}(Z)$) is calculated from

$$\bar{u}(Z) = u_S \cdot (1 + C_d H_S)^{-2}$$

where u_S = wind velocity at the nearest meteorological station

C_d = drag coefficient derived from measurement at 2 m within the stand

However, although such factors as diameter breast height and crown base diameter enter into the equation, tree deformation indices are not accounted for in their analyses.

2.3 WIND AS A FACTOR IN COMPRESSION WOOD FORMATION

Jaffe (1973) coined the word 'thigmomorphogenesis' meaning "plant growth response to environmental (mechanical) stimulation." For example, Lawrence (1982) argued that shorter, sturdier trees were adaptations to windy, steep environments as a result of phenotypic plasticity and/or genetic differentiation within a population.

It has long been recognized that compression wood formation in coniferous trees is associated with windy and/or steep slopes (Mer, 1888; Kononchuk, 1888; Kienholz, 1930; Low, 1964; Jacobs, 1936; Pillow and Luxford, 1937; and others). In stands thinned by insect infestations and partial logging, compression wood forms in response to greater exposure of individual trees to wind (Hartig, 1896; Low, 1964; Pillow, et.al., 1959; Onaka, 1945; Pillow, 1931).

Compression wood (Rothholz) is reddish wood which forms on the leaning side of the stem and on the lower side of branches. It is generally accepted that compression wood stimulation results from geotropism (Ewart and Mason-Jones, 1906; Hartmann, 1942; Sinnott, 1952; Fielding, 1940; Jaccard, 1920; Larson, 1965; and others).

Geotropism is a directed growth response with respect to a plumb line as opposed to geotonus, which is an undirected growth response resulting from imposed disorientation. Rawitscher (1937) defined geotropism as a growth response proportional to the transverse component of gravity and thus the sine of the angle of deviation from vertical; whereas geotonus is a response proportional to the longitudinal component of gravity and thus the cosine of the angle of deviation from the vertical.

Kononchuk (1888) described the formation of compression wood in Scots pine (Pinus sylvestris L.) and Norway spruce (Picea abies L.) as a function of gravity. Hartig (1901) found that tree-ring asymmetry can result from differential nutrient absorption (due to pruning) but does not stimulate compression wood formation. He observed that artificial shaking did not induce compression wood, although it did reduce growth rate. Keinholz (1930) concluded that compression wood was stimulated by a variety of factors including gravity, moisture, nutrients, phototropism and mechanical forces. Metsger (1939) conceded that while several factors, especially differential solar heating, may be involved, wind was chiefly responsible for compression wood formation.

Experiments on bending stems of several species of conifers into loops found that compression wood always formed on the physically lower side of the shoot (Ewart and Mason-Jones, 1906; White, 1908; Burns, 1920). They concluded that compression wood formed as a result of gravitational stimulation. In similar experiments, Hartmann (1932) and Sinnott (1952) maintained that, although gravity was associated with compression wood formation, the primary cause was disturbance of an inherent equilibrium pattern with an orientation initially set by gravity.

Using a centrifuge, Jaccard (1939) demonstrated experimentally that inertial forces stimulated compression wood formation. This has been corroborated in similar experiments by Hartmann (1942), Scott and Preston (1955), and Westing (1964). Jaccard (1920) found that a stem inclination of only 3°, producing a force equivalent to 0.05 g, resulted in compression wood in Austrian pine (Pinus nigra Ait.). Compression

wood was also found in a longleaf pine (Pinus palustris Mill.) stem inclined 2° (= 0.03 g) (Paul, 1941). Low (1964) studied the distribution of compression wood in plantations in Scotland. He found that compression wood accounted for 21-24% of the standing volume of 25-40 year old Scots pine plantations. Most of the compression wood formed on the leeward side at roughly the centre of mass (i.e. 1/3 the tree height). Wind was chiefly responsible for compression wood content in stands. Larson (1965) confirmed that unidirectional prevailing winds produce asymmetric cross-sections with a high content of compression wood. His greenhouse studies on 4 year old tamarack showed that compression wood distribution in stems is similar to that observed by Low (1964). Furthermore, multidirectional winds did not produce compression wood, primarily because stems did not incline. However, both unidirectional and multidirectional winds caused a downward shift of increment at the expense of the upper stem. Similar growth responses to wind were observed by Kellogg and Steucek (1980), Bannan and Bindra (1970), and Rees and Grace (1980).

The response time for initiation of compression wood cells is about 12 hours (White, 1908; Jaccard, 1919; Larsen, 1953). On the average it takes approximately 7 days for a layer of compression wood cells to mature, while 6-7 layers of xylem cells are being initiated during this period (Westing, 1959).

A number of workers studied the internal stresses associated with the geotrophic righting processes (Fitting, 1905; Münch, 1937; Jacobs 1938, 1939, 1945; Jaccard, 1934; Westing, 1961; and others). Based on the works of others and his own, Westing (1965) outlined the main

factors in the mode of righting by trees:

- radial growth on the lower (leeward) side;
- expanding strains of compression wood;
- radial growth depression on upper (windward) side;
- contracting strains of normal wood on upper (windward) side;
- potential increase in osmotic pressure in the cambial cells on lower side.

Onaka (1935, 1940) maintained that only the first two factors contribute significantly to the righting process. Jacobs (1945) referred to an inclined stem as a giant fulcrum, with the fulcrum at ground level, in which counterbalancing forces decreases as the inclination from vertical decreases. Fitting (1905) proposed a sine law which would relate the dependence of compression wood formation to the vertical component of gravity perpendicular to the longitudinal axis of the stem. Hartmann (1942) implied that compression wood content is proportional to the sine of its angular displacement. Onaka (1949) implied that a similar relationship existed for asymmetry in stems. However, neither presented data to support their thesis.

Knight (1803) demonstrated experimentally that the major axis of asymmetric apple tree cross-sections corresponded to the prevailing wind. This was also observed in conifers by Bannan and Bindra (1970) and many others.

Static forces, resulting from mass loading in the absence of bending, are insignificant compared to dynamic forces resulting mainly from wind (Boyd, 1950; Quirk & Freese, 1976a). Quirk, et.al. (1975) applied torque stress to stems of red pine (Pinus resinosa Ait.) which changed the grain angle by up to 250%; the radial growth rate decreased

by 100% and fiber length decreased by 20%. The growth rate, however, remained unchanged. Torque stress is a vector component of wind and combined with static stress, as indicated by Quirk's experiments, does not produce compression wood. Therefore, we can reasonably assume that, in nature, lateral dynamic stress applied by the horizontal component of wind is a major causal effect of compression wood.

Wind action does not induce compression wood formation unless the geotropic response time is sufficiently long. For example, Burns (1920) and Jaccard (1919) found that momentary shaking by simulated wind did not result in compression wood. The degree of shaking affects height and diameter growth; for example, stems of sheltered trees are tall and thin with symmetric tree-rings, whilst stems of trees exposed to persistent wind are shorter, strong tapered and usually have asymmetrical tree-rings. For example, Figures 2.11-2.13 show how severe bending of stems in a Scots pine plantation near Bonavista, Newfoundland, results in the formation of asymmetrical tree-rings.

Quirk and Freese (1976b) conducted vibration experiments to simulate wind sway in a greenhouse and outdoor situations. Vibrated trees exhibited lower radial growth, wood volume, crown size, and number of cells per growth ring than unvibrated trees. However, vibrating had no effect on the average cell size or cell-wall thickness. Therefore, they concluded the lower radial growth was due simply to a reduction in the number of cells indicating that cambial division was a function of asymmetry and not a physiological phenomenon. This corroborates the findings of Burns (1920) who found that, in an inclined white pine, 165 layers of cells were laid down in the first season on the leaning side,

Figure 2.11 A Scots Pine plantation near Bonaviata deformed mainly by wind. Note the straight stems of Norway Spruce in the background which are less prone to deformation.

Figure 2.12 Inclined stems of Scots Pine in a plantation near Bonavista caused by persistent strong winds.

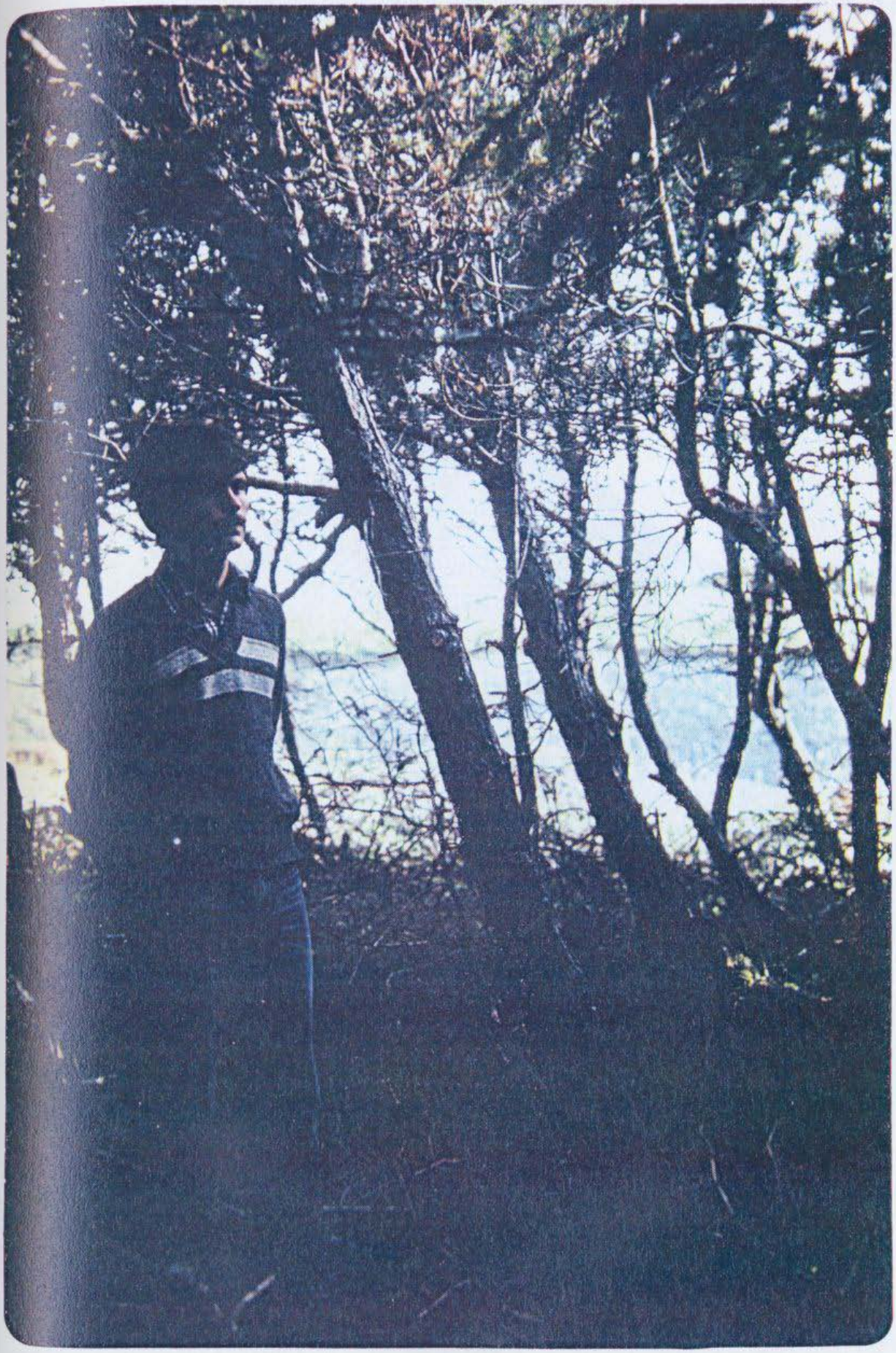

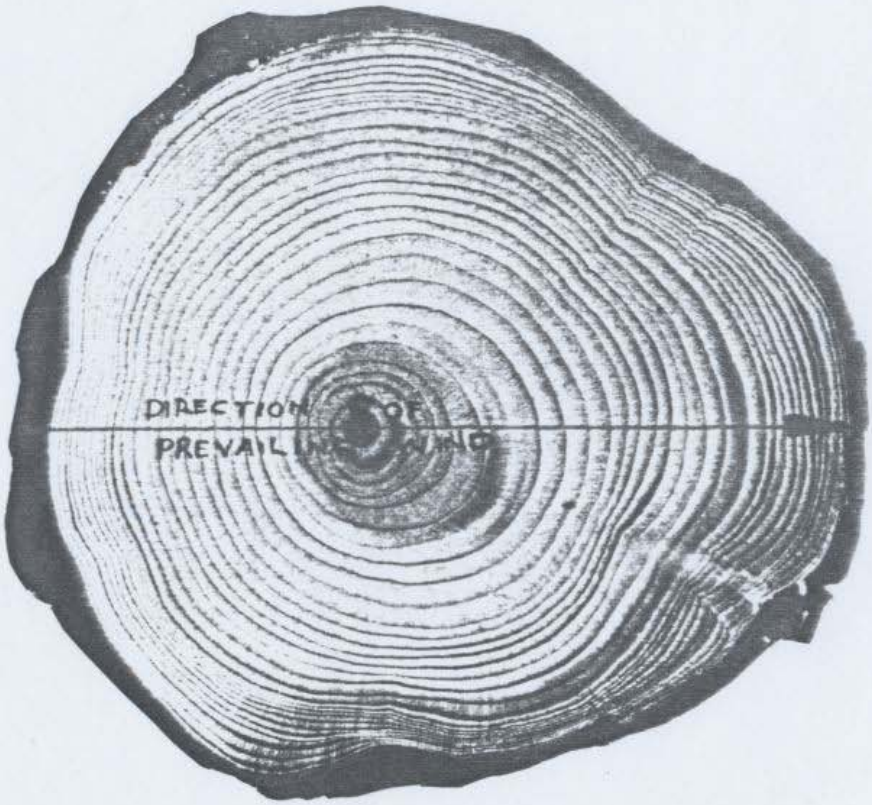

Figure 2.13 Cross-section of a Scots pine tree in a plantation near Bonavista, Newfoundland. Note the asymmetrical tree-rings attributed to the effect of wind. The "prevailing" wind direction drawn across the disc corresponds to the direction of stem inclination.

compared to 25 layers on the opposite side. Similarly, after 7 days of inclination, an average of 9 layers on the leaning side and five on the opposite side developed in a Norway spruce stem (Casperson, 1963).

3.0 METHODS AND MATERIALS

3.1 CHOICE OF TREE SPECIES FOR CALIBRATION

Tamarack (Larix laricina (Du Roi) K. Koch) was chosen because it had a number of attributes which made it suitable as an indicator of wind:

- compared to other tree species its deformation indicates a greater sensitivity to wind (Figures 3.1, 3.2);
- it has a wide geographical distribution throughout Newfoundland;
- it has a wide ecological amplitude ranging from ericaceous shrub bogs, dense spruce and fir forests to thin soils on exposed barrens;
- as a pioneer species it grows as isolated trees (Figure 3.3) or in well-spaced groups (Figure 3.4), rarely forms pure stands (Figure 3.5) and, because it is intolerant of shade, extends well above the canopy when growing in mixture with spruce and fir (Figure 3.6).

3.2 CALIBRATION

3.2.1 Pre-selection of Sampling Plots

Potential sampling sites within 1.5 km of twelve meteorological stations throughout Newfoundland were identified on aerial photographs.

The main criteria for selection were sites with a reasonably homogenous vegetation cover, soils, open-growing tamarack trees and level with an adequate fetch of at least 300 m in all directions. Large ericaceous shrub bogs were found to be ideally suited for calibration

Figure 3.1 The strong flagging of the tamarack (centre) exhibits a greater sensitivity to wind than the balsam fir (left) in the background.

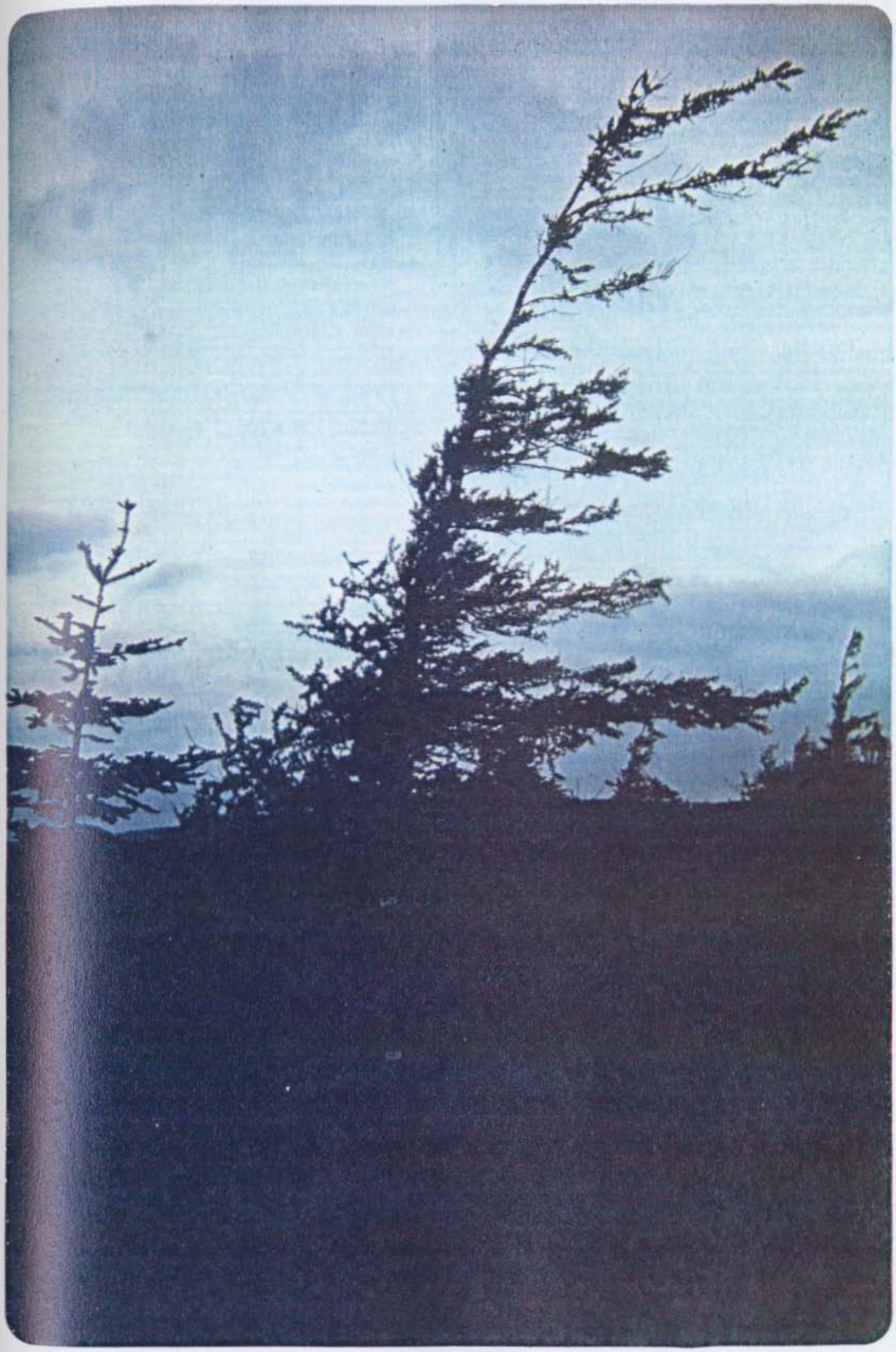

Figure 3.2 The strong flagging of the naturally growing tamarack tree (extreme right) exhibits a greater sensitivity to wind than the Austrian pines in this plantation near Avondale, Newfoundland.

Figure 3.3 An open growing tamarack tree used for calibration against mean wind speed at Bonavista, Newfoundland.

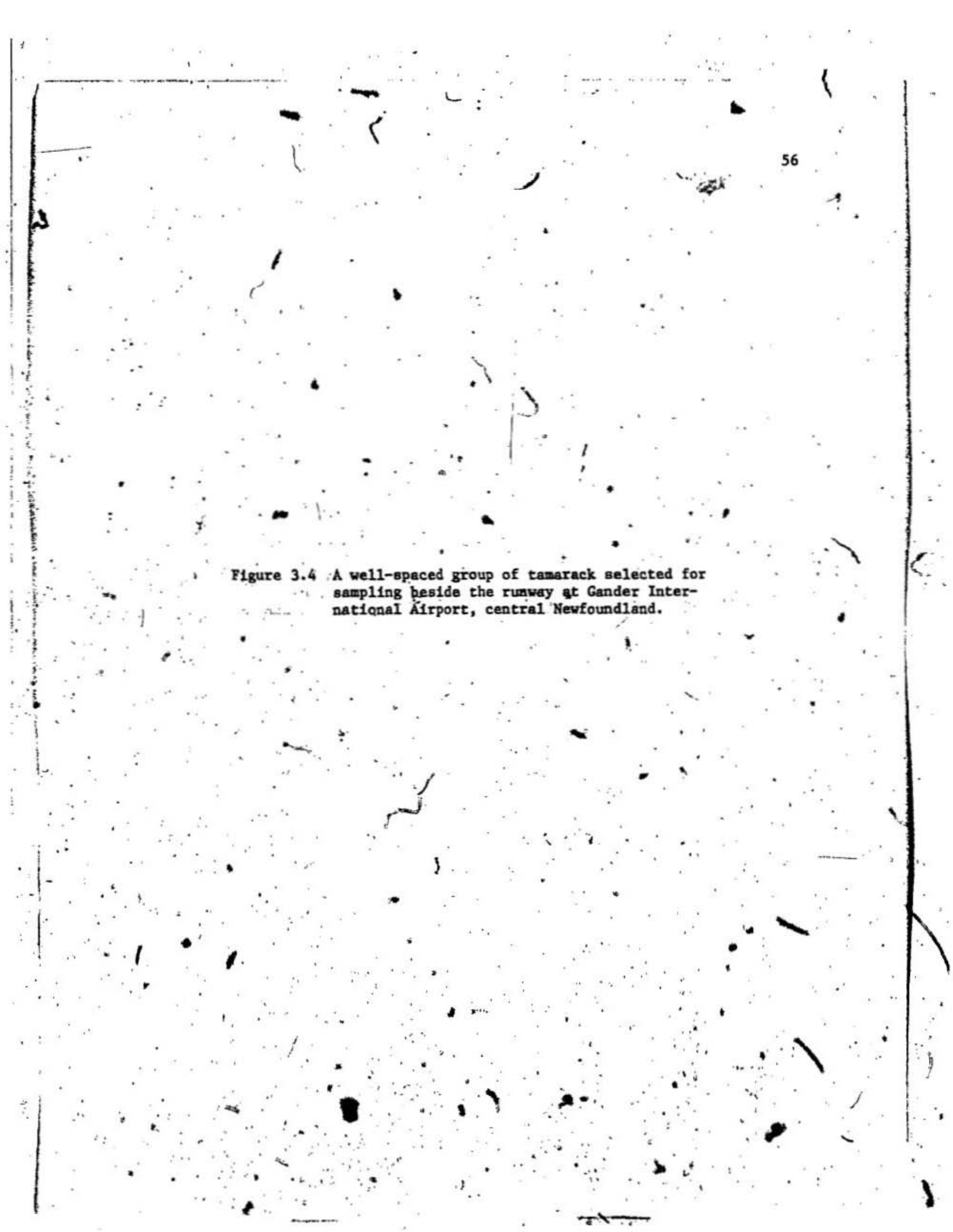

Figure 3.4 A well-spaced group of tamarack selected for sampling beside the runway at Gander International Airport, central Newfoundland.

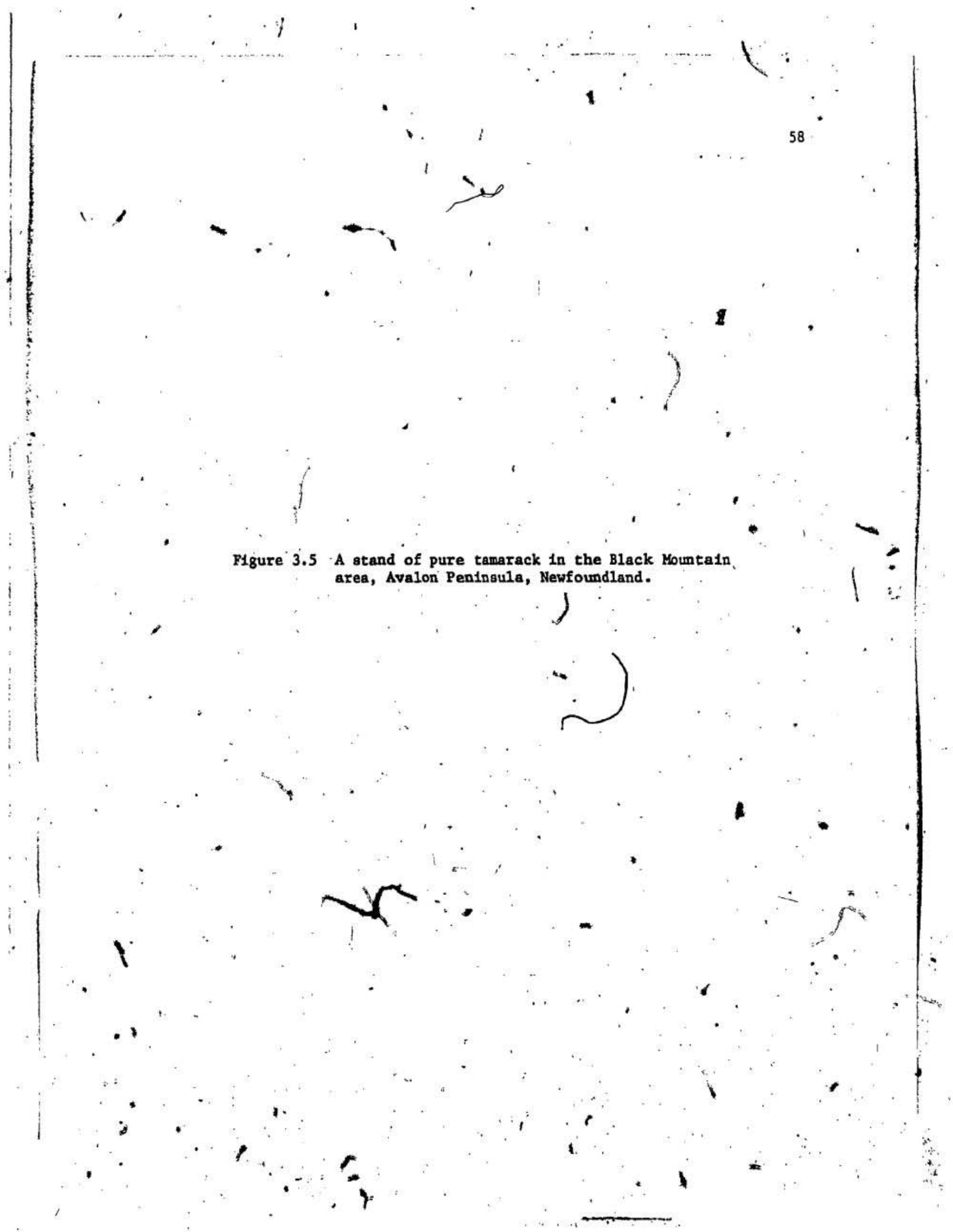

Figure 3.5 A stand of pure tamarack in the Black Mountain area, Avalon Peninsula, Newfoundland.

Figure 3.6 A tamarack tree extending well above the spruce-fir forest near Millertown, central Newfoundland. (Note how the tamarack is deformed while there is no perceptible deformation in the spruce and fir.)

plots. The fact that four of the calibration sites were located adjacent to airports indicates that the surrounding terrain in general had no major hills which would unduly affect the wind flow over the sampling areas.

Another criterion was that all stations must have at least 10 years of continuous climatic data (Wade and Hewson (1979) recommended that stations have at least one year's climatic data). Wind data for all potential calibrating sites is contained in the Canadian Climate Normals 1951-1980 (A.E.S. 1982).

3.2.2. On-site Selection of Sampling Plots

Of the twelve potential sampling plots visited, seven were found to be acceptable; they are listed in Table 1.

Table 1

Selected calibration sites in Newfoundland

Calibration Site	Latitude	Longitude	Elevation (m)
Stephenville	48°32'N	58°33'W	26
Deer Lake A	49°13'N	57°24'W	22
Buchans A	48°51'N	56°50'W	276
Twillingate	46°16N	54°53'W	99
Gander	48°57'N	54°34'W	151
Bonavista	48°42'N	53°05'W	25
St. John's A	47°37'N	52°45'W	140

3.2.3 Characteristics of Calibration Sites

STEPHENVILLE: Sampling plot located 1.2 km north of meteorological

station on a plateau raised bog dominated by ericaceous shrubs 1.0 - 1.5 m high. Tamarack isolated, more or less uniformly spaced about 15-20 m apart and a total of 7 trees available for sampling.

DEER LAKE A: Adjacent to the west end of airport runway and roughly 0.5 km from meteorological station. Mixed, open-growing tamarack-black spruce stand with ericaceous shrub layer. Tamarack 1.3 - 1.5 times taller than black spruce. Stand density approximately 10-15 trees per 250 m^2 and evenly spaced. Shrub layer 0.25 - 0.5 m high with lichen ground cover.

BUCHANS A: Site about 0.75 km southeast of meteorological station on an ericaceous shrub bog. Tamarack widely spaced with a stand density of approximately 10 trees per 250 m^2 with a few small black spruce trees mixed in. Shrub layer about 0.5 m high.

TWILLINGATE: Site located 1.2 km southeast of meteorological station on a typical exposed coastal ericaceous bog. Tamarack widely spaced, approximately 2 trees per 500 m^2; no other species of tree on the site. Shrub layer 0.2 m high.

GANDER: Bog located between service road and end of runway on the east side of airport (about 1.0 km from meteorological station). Tamarack widely spaced at roughly 5-10 trees per 500 m^2 on both sides of road dissecting the plot. Shrub layer 7.0 - 1.5 m high.

BONAVISTA: Site located 0.75 km east of the meteorological station on a coastal ericaceous bog. Tamarack trees very isolated throughout the bog. Shrub layer 0.25 - 0.5 m high.

ST. JOHN'S A: Site adjacent to northwest side of control tower on a disturbed ericaceous bog and on opposite side of a runway to meteorological station (≈ = 100 m). Tamarack trees widely scattered, few in number. Shrub layer 1.0 - 1.5 m high.

3.2.4 Sampling

Aerial photo interpretation of potential calibration sites indicated that tamarack stands varied in density from roughly 2 to 160 trees/ha^{-1}. Consequently, random sampling could only be done at two sites, Deer Lake A and Buchans A, where stand density was high enough to permit this technique to be used.

Since the object is to sample trees which are open-growing and totally exposed to winds from all directions, a maximum stand density of 160 trees/ha^{-1} with trees reasonably evenly spaced were arbitrarily chosen.

For the purpose of random sampling, the plots at Deer Lake A and Buchans A were 50 m x 50 m (0.25 ha) and represented a grid with 5 m x 5 m cells. The sides of the plots were oriented north-south and east-west respectively. A corner of the plot was located arbitrarily from which chosen cells would be located by compass and chain. Particular cells were chosen from a random numbers table and the centre of

selected cells was located with a compass and survey chain. The tamarack tree nearest the center of selected cells was designated the sample tree.

At the remaining five calibrating sites there were usually fewer than 10 widely spaced tamarack trees to choose from. In these cases one tree and its four nearest neighbours nearest the centre of the calibration site were designated for sampling.

The number of sample trees at each calibration site was set at 5. This figure was established partly on the scarcity of trees that was expected at several sites and also based on a pilot study of tree deformation on a bell-shaped hill on the Avalon Peninsula. This figure agrees well with the theoretical estimation of the number of sample trees required for a maximum population of 40 trees per plot. At 95% confidence level the standard error of estimate, ideally, should be less than 12 to be accurate within 30% (Cochrane, 1963). According to the pilot study the maximum value of the deformation ratio was 3.4 and the mean was 2.1. Since the population extremes are expected to be no more than 2.5 standard deviation, the estimated standard deviation ($\hat{\sigma}$) is computed from

$$\hat{\sigma} = (X_{max} - \bar{X}) / SD_{2.5} = (3.4 - 2.1) / 2.5 = 0.51$$

Thus, according to Cochrane (1963), the standard error of estimate, based on sample, $\hat{s}$, for a maximum population of $N = 40$ with an estimated standard deviation of $\hat{\sigma} = 0.51$ is obtained from

$$\hat{s} = \sqrt{(N^2 \hat{\sigma}^2 / n)(1 - n/N)} \qquad (< 12)$$

$$= \sqrt{(139/n)(1 - n/40)}$$

For n=3 the standard error of estimate is 11.3. Therefore, n=5 trees from each of the calibration sites provides good representation.

Prior to felling each sample tree a compass bearing of the direction of stem inclination was taken. (The compass was corrected for declination.) At 1/3 tree height a mark was made on the windward and leeward side of the stem to aid in identification of the direction of inclination on a disc cross-section taken at that height. The diameter breast height (DBH) (when breast height was less than 1/3 tree height) was measured with a steel diameter tape and recorded. The maximum leeward and windward branch extension from the trunk, and immediately above the shrub layer, was measured with a steel tape and recorded. A photograph was taken at right-angles to the direction of stem inclination. Before photographing, a clinometer range-finder rod was placed in a vertical position near the stem in the line-of-sight between camera and tree. The presence of the rod in the photograph was to provide a plumb-line when measuring the angle of stem deflection from vertical.

Because the greatest proportion of compression wood is formed near the centre of mass of the trunk (Low, 1964), i.e. ≈ 1/3 trunk height, it is assumed that this would also be the appropriate height to measure the compression index. For reasons discussed in the previous chapter, it was in this region that the maximum geotropic righting process occurs through the production of compression wood (Low, 1964). Therefore, it is reasonable to suggest that the compression index at this point is proportional to the deformation caused by wind. Therefore disc samples were taken at 1/3 tree height. A pencil line with an arrow to indicate the direction of stem inclination was drawn across the top of the disc

and through the pith. Location, date, plot and tree number were written on the bottom of the disc. All discs were placed in a paper bag and temporarily stored in a refrigerator within 12 hours until laboratory analysis.

3.3 LABORATORY ANALYSIS

3.3.1 Deformation Ratio

The crown deformation and angle of stem deflection from plumb line of sample trees was plotted from photographic images projected onto graph paper with 10x10 cells.

Tree heights and branch extensions were converted to relative dimensions by scaling the silhouette of the tree to fit the length of the graph paper, i.e. 10 inches. The clinometer range-finder rod in each photograph was aligned with the vertical axis of the graph paper. The centerline of the stem and main branches of the silhouette were traced onto the graph paper. A straight line or curve, whichever was appropriate, was fitted through the extremities of the branch traces. A straight line was drawn with a ruler from 1/3 height on the stem to the tip of the stem. This line represents the angle of deflection. An example of the graphical procedure is shown in Figure 3.7.

The angle of stem deflection was measured with a protractor. The relative extension of leeward and windward branches from the stem centerline was read from the graph at 1/3 and 2/3 heights, respectively. The mean deformation ratio ($\bar{D}'_r$) was computed from a modified Wade-Hewson formula.

$$D'_r = B + \frac{A}{45^\circ}$$

Figure 3.7 Graphical representation of the deformation ratio adapted for tamarack.

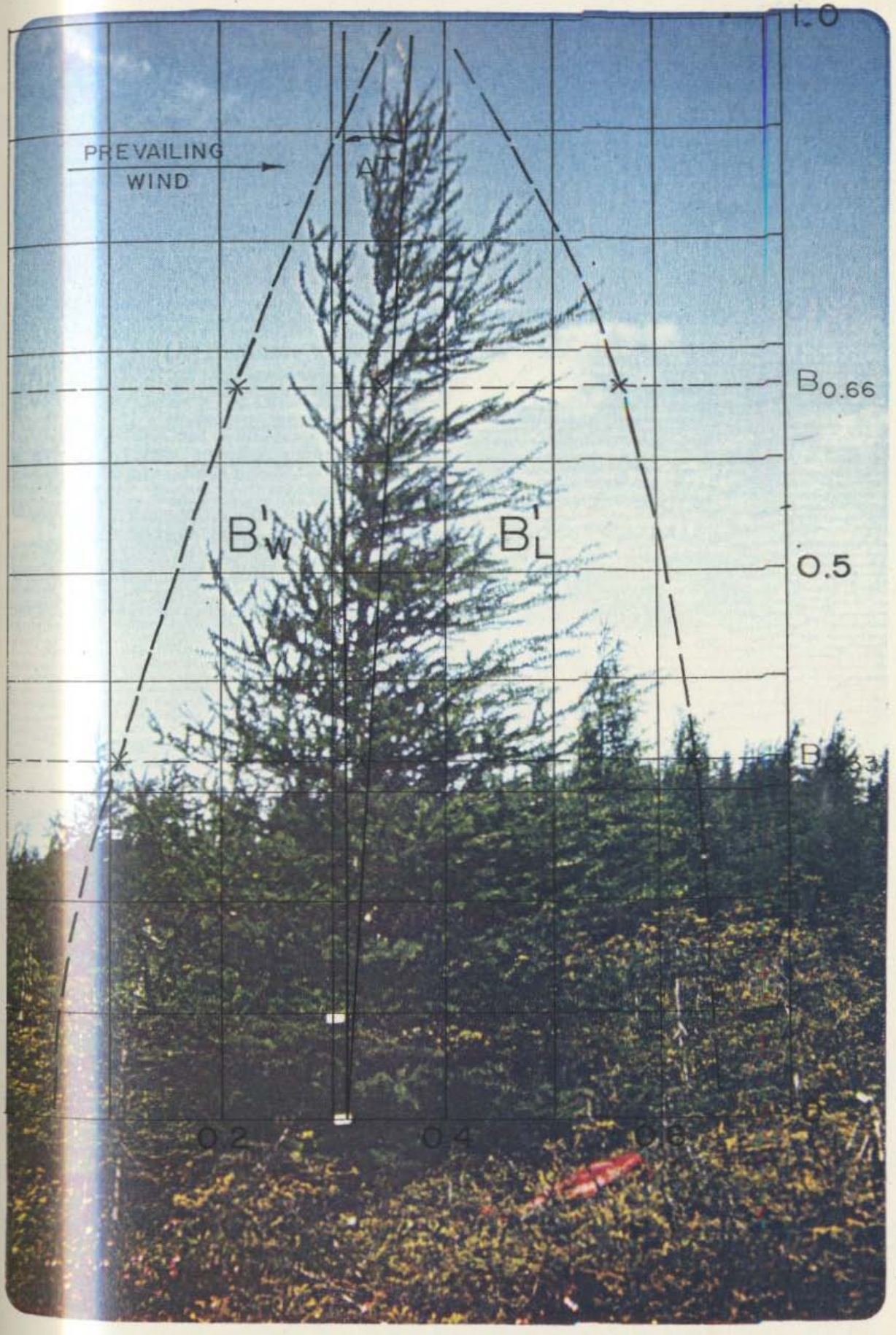
PREVAILING
WIND
AT
1.0
$B_{0.66}$
B'_W
B'_L
0.5
0.2
0.4
0.6

where $D'_r = B' = B'_L/B'_W$ A = angle of stem deflection

3.3.2 Tree-Ring Asymmetry

Tree-ring widths of disc samples were measured by a DIGI-MIC microcomputer system (Jordan and Balance, 1983). Traverses of ring-width measurements were made across the direction of inclination from the pith leeward and in the opposite direction from the pith windward. The compression index (C_i), as defined by Wade and Hewson (1979), is the ratio of tree-rings on the compression side (leeward of the pith) to tree ring widths on opposite side, i.e.

$$C_i = \frac{\text{Tree ring width leeward of pith}}{\text{Tree ring width windward of pith}}$$

Since all discs had asymmetric tree rings the highest compression index did not always lie in the direction of stem inclination. Therefore, where applicable the maximum compression index was determined from an additional pair of traverses from the pith in line with the maximum width of tree-ring asymmetry.

3.3.3 Wind Data

Mean annual wind speed for each calibration site was obtained from the Canadian Climate Normals 1957-80 (A.E.S., 1982).

Computer facilities at the Atmospheric Environment Service laboratories at Downsview, Ontario was used to access wind data for several periods of the year. The Land Statistics System (LAST), an interactive computer program designed by A.E.S., was used to plot wind roses and other graphics relating to the calibration data.

The mean annual wind speed for the calibration sites was adjusted to 2/3 of average tree height by a power law, viz.

$$\bar{V}_Z = \bar{V} \left(\frac{H_A}{H_T} \right)^{\alpha}$$

where $\bar{V}_{AT}$ = mean annual wind speed at 2/3 tree height

$\bar{V}$ = mean annual wind speed at meteorological station

H_A = anemometer height at meteorological station

H_T = 2/3 of average tree height

α = constant = 0.14 for unstable conditions in flat, grass-covered terrain (Sellers, 1965)

Aerial reconnaissance, using hand-held 35mm photographic equipment and light aircraft, was undertaken in several parts of Newfoundland to record various features of the relationship between wind and trees. The general techniques for oblique aerial photography with respect to tree deformation surveys are described in Wade and Hewson (1980).

A terrestrial reconnaissance along major highways and logging roads to map the general wind flow patterns, as shown by tamarack, was undertaken. A compass, hand-held 35mm photographic equipment and 1:50 000 topographic map were utilized to obtain direction of inclination, a photographic record of sample trees (as described above) and the precise location, aspect and elevation of selected tamarack trees.

A detailed tree deformation survey was undertaken on an area, 2 km x 3 km, on the Avalon Peninsula containing two adjacent bell-shaped hills with tamarack as the main forest species. The area is approximately 20 km southwest of St. John's airport. Stratified sampling was conducted along several transects throughout the area. Stratified

sampling areas were identified on forest vegetation and topographic map reflecting the trends in variation of tree deformation. A preliminary sampling site within each stratification was marked on the map. The intensity of sampling was determined by a ground reconnaissance of the variability of deformed tamaracks within each stratified area. The most open-growing, single-stemmed tamarack at each sampling site was selected for sampling. A total of 59 trees were selected and photographed according to the modified deformation ratio described for sampling trees at the calibration sites. Detailed measurements of 28 of the 59 trees included other measurements such as leeward and windward branch extension, height, direction of stem inclination and disc sample according to the methods described above.

4.0 RESULTS

4.1 CALIBRATION

4.1.1 Relationship between Crown Deformation and Tree-ring Asymmetry

Table 2 shows the mean deformation ratio, $\bar{D}'_r$, mean compression index, $\bar{C}_i$, mean direction of stem inclination, $\bar{S}_{DIR}$, and mean direction of maximum width of tree-ring asymmetry, $\bar{C}_{DIR}$.

Table 2. Mean deformation ratio, $\bar{D}'_r$, mean compression index, $\bar{C}_i$, mean direction of stem inclination, $\bar{S}_{DIR}$, and mean direction of maximum tree-ring asymmetry, $\bar{C}_{DIR}$, for each calibration site.

CALIBRATION SITE	$\bar{D}'_r$	$\bar{C}_i$	$\bar{S}_{DIR}$	$\bar{C}_{DIR}$
STEPHENVILLE	1.33	1.35	200	212
DEER LAKE A	1.40	1.56	193	235
BUCHANS A	1.60	1.53	213	214
TWILLINGATE	2.33	1.74	267	256
GANDER	1.76	1.34	232	198
BONAVISTA	1.95	1.66	268	235
ST. JOHN'S A	3.78**	1.75	240	224

**Means between calibration sites significantly different at 1%.

Only the $\bar{D}'_r$ value for St. John's A is significantly different from $\bar{D}'_r$ values of the other calibration sites. For $\bar{C}_i$, $\bar{S}_{DIR}$, $\bar{C}_{DIR}$, there is no significant difference between calibration sites (5% level).

There is a non-significant correlation between the mean deformation ratio, $\bar{D}'_r$, and the mean compression index, $\bar{C}_i$, expressed by the equation

$$\bar{D}'_r = 50.1 - 66.7\,\bar{C}_i + 23.0\,\bar{C}_i^2 \qquad (R^2 = 0.76,\ F = 4.08)$$

There is also a non-significant correlation between the mean direction of stem inclination, $\bar{S}_{DIR}$, and the mean direction of maximum tree-ring asymmetry, $\bar{C}_{DIR}$, where

$$\bar{C}_{DIR} = 1266.1 - 9.4\,\bar{S}_{DIR} + 0.21\,\bar{S}_{DIR}^{2} \quad (R^2 = 0.71,\ F = 6.19)$$

4.1.2 Deformation Ratio, D'_r

Tables A1-A6 summarize the data used to calculate the deformation ratio. Table 3 compares the mean annual wind speed, $\bar{V}_A$, recorded by the station anemometer and the mean annual wind adjusted to 2/3 mean tree height at each site, $\bar{V}_{AT}$. The value of Z^{α} used to adjust mean annual wind speed at each station is shown in Table A4.

Table 3. Mean annual wind speed, $\bar{V}_A$, obtained from Canadian Normals (A.E.S., 1982), mean annual wind speed adjusted to 2/3 mean tree height, $\bar{V}_{AT}$, at each calibration site and student's t-test of mean monthly wind speed and mean monthly wind speed adjusted to 2/3 tree height.

CALIBRATION SITE	$\bar{V}_A$	$\bar{V}_{AT}$	Student's -t (22 Df.)
STEPHENVILLE	4.3	3.7	1.59 NS
DEER LAKE A	4.3	4.0	2.45*
BUCHANS	5.9	5.1	2.79*
TWILLINGATE	7.3	5.4	3.94**
GANDER	5.8	5.2	2.17*
BONAVISTA	7.8	6.3	3.38**
ST. JOHN'S	6.8	6.4	1.61 NS

95% Confidence limits $\bar{V}_A$ = 5.19 to 6.87

95% Confidence limits $\bar{V}_{AT}$ = 4.26 to 5.94

*Significantly different at 5%

**Significantly different at 1%

NS - Non-significant at 5% level

At five stations the mean annual wind speed adjusted to 2/3 mean tree height is significantly different from the mean annual wind speed recorded at the station.

Table 4 summarizes the mean deformation ratios at each calibration site.

Table 4. Mean deformation ratios at three levels (i.e., near base, $\bar{D}'_r$, at 1/3 tree height, $\bar{D}'_{r\ 0.33}$, and at 2/3 tree height, $\bar{D}'_{r\ 0.66}$) and total mean for calibration sites.

CALIBRATION SITE	$\bar{D}'_{r\ 0.00}$	$\bar{D}'_{r\ 0.33}$	$\bar{D}'_{r\ 0.66}$	TOTAL MEAN ± SD
STEPHENVILLE	1.25	1.47	1.27	1.33 ± 0.10
DEER LAKE	1.37	1.42	1.42	1.40 ± 0.02
BUCHANS A	1.66	1.55	1.59	1.60 ± 0.05
TWILLINGATE	2.49	2.44	2.06	2.33 ± 0.19
GANDER	1.54	1.65	2.08	1.76 ± 0.23
BONAVISTA	1.56	2.21	2.09	1.95 ± 2.03
ST. JOHN'S A	2.13	2.57	6.64	3.78 ± 2.03

A significant correlation exists between the mean deformation ratio and the mean annual wind speed ($R^2 = 0.86$). A non-significant correlation exists between the deformation ratio and the mean annual wind speed adjusted to 2/3 mean tree height ($R^2 = 0.77$). The relationships are expressed by the equations

$$\bar{V}_A = -5.96 + 10.0\ \bar{D}'_r - 1.7\ \bar{D}'^2_r \qquad (R^2 = 0.86,\ F = 16.2^*)$$

and $$\bar{V}_{AT} = -1.5 + 5.2\ \bar{D}'_r - 0.8\ D'_r \qquad (R^2 = 0.77,\ F = 3.87)$$

Table 5 compares the observed unadjusted, $\bar{V}_A$, and adjusted, $\bar{V}_{AT}$, mean annual wind speed with values predicted by the deformation ratio, D'_r.

Table 5. Comparison between observed mean annual wind speed, $\bar{V}_A$, and mean annual wind speed adjusted to 2/3 tree height, $\bar{V}_{AT}$, and value predicted by the deformation ratio.

CALIBRATION SITE	$\bar{V}_A$		$\bar{V}_{AT}$	
	OBS.	PRED.	OBS.	PRED.
STEPHENVILLE	4.3	4.3	3.7	4.0
DEER LAKE A	4.3	4.6	4.0	4.2
BUCHANS A	5.9	5.6	5.1	4.7
TWILLINGATE	7.3	7.8	5.4	6.2
GANDER	5.8	6.2	5.2	5.1
BONAVISTA	7.8	6.9	6.3	5.5
ST. JOHN'S A	6.8	6.8	6.4	6.3

Because there is no significant difference at 5% between observed values of $\bar{V}_A$ and $\bar{V}_{AT}$, nor any significant difference between the values of $\bar{V}_A$ and $\bar{V}_{AT}$ predicted by the deformation ratio, the results indicate there is very little to be gained by readjusting the wind speed data base level to 2/3 mean tree height.

The relationship between deformation ratio and mean vector speed is summarized in Table 6. Figure 4.1 gives a plot of the monthly trend in R^2 values.

There is higher correlation between the mean monthly vector speed and the deformation ratio for the May to December period than the January to April period. Also the deformation ratio has a higher correlation coefficient, (R^2 = 0.83) with the mean annual vector speed than with the mean summer (May-August) vector speed (R^2 = 0.69). Obviously it is difficult to provide a reasonable explanation for such a trend in the correlations. However, it is obvious from the results so far that

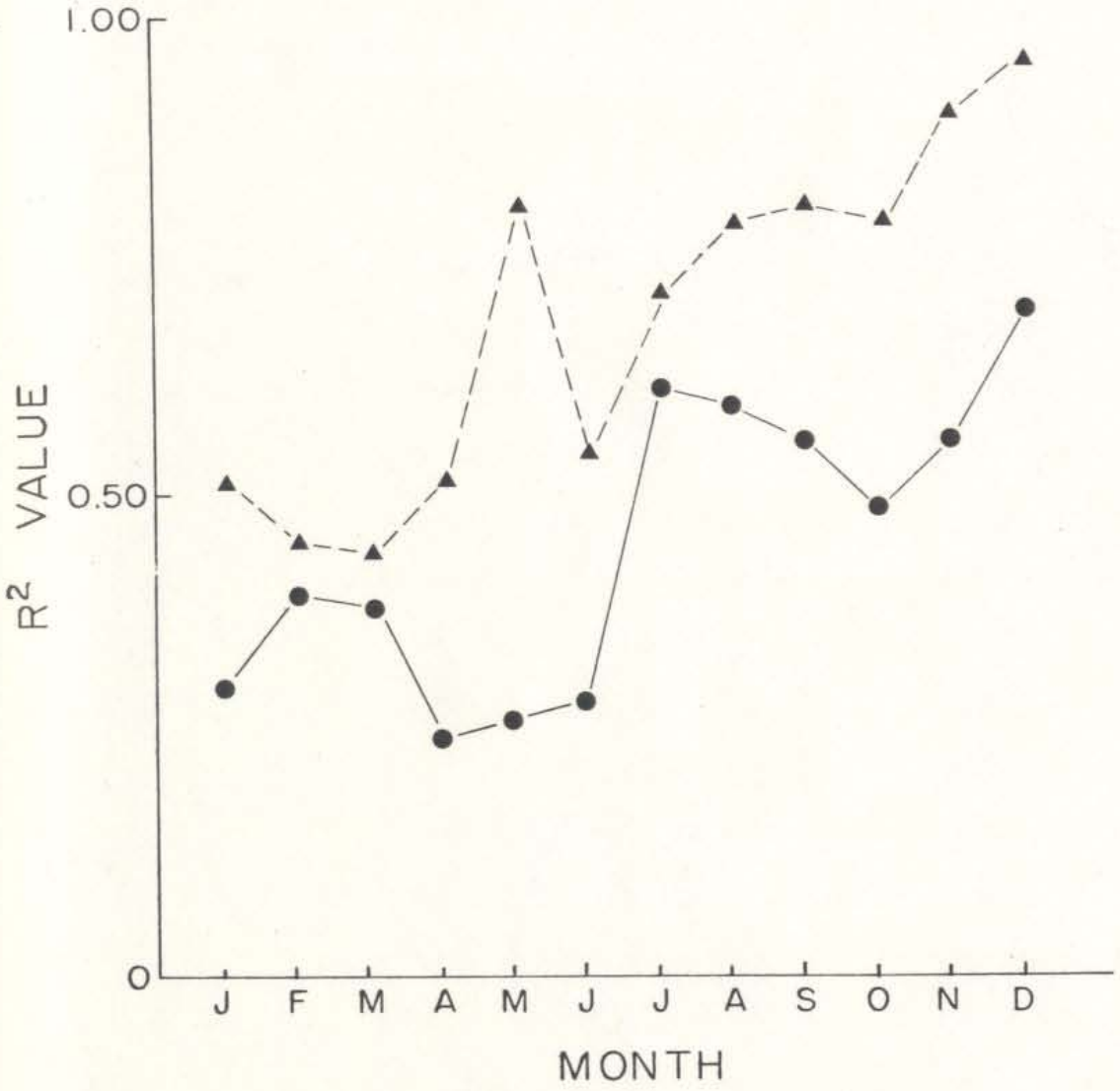

Figure 4.1 Plot of R^2 values relating mean monthly vector winds to the deformation ratio, ▲ , and compression index ● .

the deformation ratio is a good predictor of wind speed and vector speed in general.

Table 6. Polynomial regression analysis of mean vector wind speed, $\bar{v}_{(i)}$, and deformation ratio, D'_r.

$\bar{v}_{(i)}$	REGRESSION EQUATION	R^2
$\bar{v}_{ANNUAL}$	$-8.4 + 13.2\ D'_r - 2.2\ D'^2_r$	0.83
$\bar{v}_{MAY-AUG}$	$-0.4 + 4.7\ D'_r - 0.5\ D'^2_r$	0.69
$\bar{v}_{JAN}$	$-10.2 + 16.9\ D'_r - 2.9\ D'^2_r$	0.52
$\bar{v}_{FEB}$	$-9.4 + 15.5\ D'_r - 2.7\ D'^2_r$	0.67
$\bar{v}_{MAR}$	$-9.2 + 13.6\ D'_r - 2.4\ D'^2_r$	0.46
$\bar{v}_{APR}$	$-6.6 + 9.2\ D'_r - 1.4\ D'^2_r$	0.53
$\bar{v}_{MAY}$	$4.4 - 2.4\ D'_r + 1.0\ D'^2_r$	0.81
$\bar{v}_{JUN}$	$2.9 + 0.7\ D'_r + 0.4\ D'^2_r$	0.55
$\bar{v}_{JUL}$	$-5.3 + 10.7\ D'_r - 1.5\ D'^2_r$	0.71
$\bar{v}_{AUG}$	$-1.2 + 6.9\ D'_r - 1.0\ D'^2_r$	0.79
$\bar{v}_{SEP}$	$-8.5 + 14.4\ D'_r - 2.5\ D'^2_r$	0.81
$\bar{v}_{OCT}$	$-10.9 + 16.8\ D'_r - 2.9\ D'^2_r$	0.79
$\bar{v}_{NOV}$	$-18.4 + 22.9\ D'_r - 4.1\ D'^2_r$	0.92
$\bar{v}_{DEC}$	$-27.4 + 13.5\ D'_r - 5.6\ D'^2_r$	0.96

4.1.3 Compression Index, C_1

Table A8 shows the compression index based on tree-ring widths for the period 1973 to 1983. There is a non-significant correlation between the compression index and unadjusted and adjusted mean annual wind speed, respectively, expressed by

$$\bar{V}_A = 34.4 - 43.1\ C_i + 15.8\ C_i^2 \quad (R^2 = 0.53,\ F = 0.33)$$

$$\bar{V}_{AT} = 27.9 - 34.0\ C_i + 12.3\ C_i^2 \quad (R^2 = 0.49,\ F = 0.34)$$

The results indicate a better relationship between C_i and $\bar{V}_A$ than C_i and $\bar{V}_{AT}$. However, the correlation between the compression index and wind speed is consistently lower than the correlation between the deformation ratio and wind speed. This trend is particularly evident in the relationship between the compression index and mean vector speed (Table 7) which, in most cases, shows a low correlation from January to June and a high correlation coefficient from July to December.

Table 7. Polynomial regression analysis of mean vector wind speed, $\bar{v}_i$, and compression index, C_i.

$\bar{v}_i$	REGRESSION EQUATION	R^2
$\bar{v}_{ANNUAL}$	$53.8 - 70.0\ C_i - 25.7\ C_i^2$	0.64
$\bar{v}_{MAY-AUG}$	$36.4 - 48.0\ C_i + 18.3\ C_i^2$	0.45
$\bar{v}_{JAN}$	$2.4 - 0.5\ C_i + 3.4\ C_i^2$	0.30
$\bar{v}_{FEB}$	$6.8 - 6.8\ C_i + 5.3\ C_i^2$	0.41
$\bar{v}_{MAR}$	$107.7 + 139.6\ C_i - 41.7\ C_i^2$	0.37
$\bar{v}_{APR}$	$48.4 + 63.3\ C_i + 22.6\ C_i^2$	0.24
$\bar{v}_{MAY}$	$13.2 - 18.4\ C_i + 7.9\ C_i^2$	0.26
$\bar{v}_{JUN}$	$15.6 - 22.1\ C_i + 10.1\ C_i^2$	0.27
$\bar{v}_{JUL}$	$42.0 - 57.5\ C_i + 23.2\ C_i^2$	0.62
$\bar{v}_{AUG}$	$24.9 - 31.5\ C_i + 13.2\ C_i^2$	0.61
$\bar{v}_{SEP}$	$27.8 - 35.0\ C_i + 14.5\ C_i^2$	0.56
$\bar{v}_{OCT}$	$3.1 - 3.6\ C_i + 4.8\ C_i^2$	0.59
$\bar{v}_{NOV}$	$44.5 - 60.2\ C_i + 23.6\ C_i^2$	0.65
$\bar{v}_{DEC}$	$216.7 - 288.8\ C_i + 99.2\ C_i^2$	0.69

The results show the compression index is not as good a predictor of mean vector speed but the seasonal trend in R^2 values, with low correlation in the early part of the year to high correlation in the latter part of the year; clearly shows an affinity to the deformation ratio.

Table 8 compares the observed mean wind speed with that predicted by the compression index.

Table 8. Comparison between the observed mean annual wind speed, $\bar{V}_A$, and mean annual wind speed adjusted to 2/3 the tree height, $\bar{V}_{AT}$, and values predicted by the compression index, C_i.

CALIBRATION SITE	$\bar{V}_A$		$\bar{V}_{AT}$	
	OBS.	PRED.*	OBS.	PRED.
STEPHENVILLE	4.3	5.1	3.7	4.4
DEER LAKE A	4.3	5.6	4.0	4.8
BUCHANS A	5.9	5.4	5.1	4.7
TWILLINGATE	7.3	7.3	5.4	6.0
GANDER	5.8	5.0	5.2	4.5
BONAVISTA	7.8	6.4	6.3	5.4
ST. JOHN'S A	6.8	7.4	6.4	6.1

A significance test between columns shows there is no significant difference between the observed and predicted V_{AT}. However, at 5% level, the predicted values of $\bar{V}_A$ differ significantly from the observed values ($t = 2.88$ for 12 DF).

4.1.4 Direction of Stem Deformation, S_{DIR} and C_{DIR}

Table A9 shows the direction of stem inclination and direction of maximum width of tree-ring asymmetry for sample trees at calibration sites. There is no significant difference between direction of stem inclination, S_{DIR}, and direction of maximum tree-ring asymmetry, C_{DIR} ($t = 0.44$ for 12 DF). However, there is a significant difference between $\bar{S}_{DIR}$ and the mean annual vector wind direction ($t = 2.71$ for 12 DF) but no significant difference between $\bar{S}_{DIR}$ and the mean summer (June-Aug.) and fall (Sept.-Oct.) vector directions (Table 9). Also, $\bar{C}_{DIR}$ differs significantly from the annual and fall values of $\bar{v}_{DIR}$ (Table 10).

Table 9. Observed mean direction of stem inclination, $\bar{S}_{DIR}$, and mean wind vector direction, $\bar{v}_{DIR}$.

CALIBRATION SITE	$\bar{S}_{DIR}$	$\bar{v}_{DIR}$		
		ANNUAL*	SUMMER	FALL
STEPHENVILLE	200	285	268	267
DEER LAKE A	193	254	250	243
BUCHANS A	213	272	255	243
TWILLINGATE	267	259	225	233
GANDER	232	258	243	247
BONAVISTA	268	256	225	250
ST. JOHN'S A	240	260	250	250

*Significant at 5%.

Table 10. Observed mean direction of the maximum tree-ring asymmetry, $\bar{C}_{DIR}$, and mean vector wind direction $\bar{v}_{DIR}$.

CALIBRATION SITE	$\bar{C}_{DIR}$	$\bar{v}_{DIR}$		
		ANNUAL*	SUMMER	FALL
STEPHENVILLE	212	285	268	267
DEER LAKE A	235	254	250	243
BUCHANS A	214	272	255	243
TWILLINGATE	256	259	225	233
GANDER	198	258	243	247
BONAVISTA	235	256	225	250
ST. JOHN'S A	224	260	250	250

Much more revealing results were obtained with polynomial regression analysis. Tables 11 and 12 show the regression equations and corresponding R^2 values, predicting the annual, summer, fall and monthly values of mean vector wind direction; and Figure 4.2 gives a plot of the monthly trend in R^2 values. Clearly, there is a higher correlation between the direction of stem inclination and summer vector wind direction but virtually no correlation with the annual or other seasonal vector wind directions. There is a lag apparent in the higher correlations between the direction of maximum width of tree-ring asymmetry and late summer and fall vector wind directions. The reason for this is unclear. However, it is obvious that tree-ring asymmetry is closely associated with the summer, and possibly late fall, vector wind direction.

Table 11. Polynomial regression analysis of mean vector wind direction, $\bar{v}_{DIR}$, and direction of mean stem inclination, $\bar{S}_{DIR}$.

$\bar{v}_{DIR}$	REGRESSION EQUATION	R^2
ANNUAL	$41.0 + 2.1\ S_{DIR} - 4.7\ S^2_{DIR}$	0.14
SUMMER	$-13.2 + 2.7\ S_{DIR} - 6.9\ S^2_{DIR}$	0.85
FALL	$297.1 - 0.3\ S_{DIR} + 2.1\ S^2_{DIR}$	0.21
JAN	$44.2 + 2.0\ S_{DIR} - 4.5\ S^2_{DIR}$	0.04
FEB	$53.8 + 1.8\ S_{DIR} - 3.7\ S^2_{DIR}$	0.08
MAR	$-175.3 + 4.0\ S_{DIR} - 8.2\ S^2_{DIR}$	0.05
APR	$1111.3 - 6.6\ S_{DIR} + 0.0\ S^2_{DIR}$	0.36
MAY	$77.6 + 2.4\ S_{DIR} - 6.7\ S^2_{DIR}$	0.83
JUN	$-246.0 + 4.7\ S_{DIR} + 0.0\ S^2_{DIR}$	0.81
JUL	$119.0 + 1.35\ S_{DIR} - 3.7\ S^2_{DIR}$	0.72
AUG	$18.2 + 2,3\ S_{DIR} - 5.7\ S^2_{DIR}$	0.72
SEP	$-35.3 + 2.6\ S_{DIR} - 5.8\ S^2_{DIR}$	0.29
OCT	$146.2 + 1.2\ S_{DIR} - 3.0\ S^2_{DIR}$	0.12
NOV	$505.5 - 2.2\ S_{DIR} + 4.8\ S^2_{DIR}$	0.10

Table 12. Polynomial regression of mean vector wind direction, $\bar{v}_{DIR}$, and direction of maximum width of tree-ring asymmetry, $\bar{c}_{DIR}$.

$\bar{v}_{DIR}$	REGRESSION EQUATION	R^2
ANNUAL	$183.2 + 1.0\ C_{DIR} - 2.7\ C_{DIR}^2$	0.20
SUMMER	$-454.0 + 6.7\ C_{DIR} + 0.0\ C_{DIR}^2$	0.53
FALL	$-347.3 + 5.5\ C_{DIR} + 0.0\ C_{DIR}^2$	0.42
JAN	$-\ 1.9 + 2.6\ C_{DIR} - 6.2\ C_{DIR}^2$	0.08
FEB	$-22713.5 + 221.8\ C_{DIR} - 0.5\ C_{DIR}^2$	0.09
MAR	$-2096.2 - 15.9\ C_{DIR} + 0.0\ C_{DIR}^2$	0.18
APR	$874.5 - 4.8\ C_{DIR} + 0.0\ C_{DIR}^2$	0.04
MAY	$-327.9 + 6.0\ C_{DIR} + 0.0\ C_{DIR}^2$	0.59
JUN	$-385.1 + 6.1\ C_{DIR} + 0.0\ C_{DIR}^2$	0.59
JUL	$-807.5 + 9.4\ C_{DIR} - 0.2\ C_{DIR}^2$	0.46
AUG	$-470.4 + 6.8\ C_{DIR} + 0.0\ C_{DIR}^2$	0.67
SEP	$-\ 6.1 + 2.6\ C_{DIR} - 6.3\ C_{DIR}^2$	0.56
OCT	$-959.0 + 11.2\ C_{DIR} + 0.0\ C_{DIR}^2$	0.56
NOV	$-188.0 + 3.8\ C_{DIR} - 3.0\ C_{DIR}^2$	0.18
DEC	$51.0 + 2.1\ C_{DIR} - 5.2\ C_{DIR}^2$	0.14

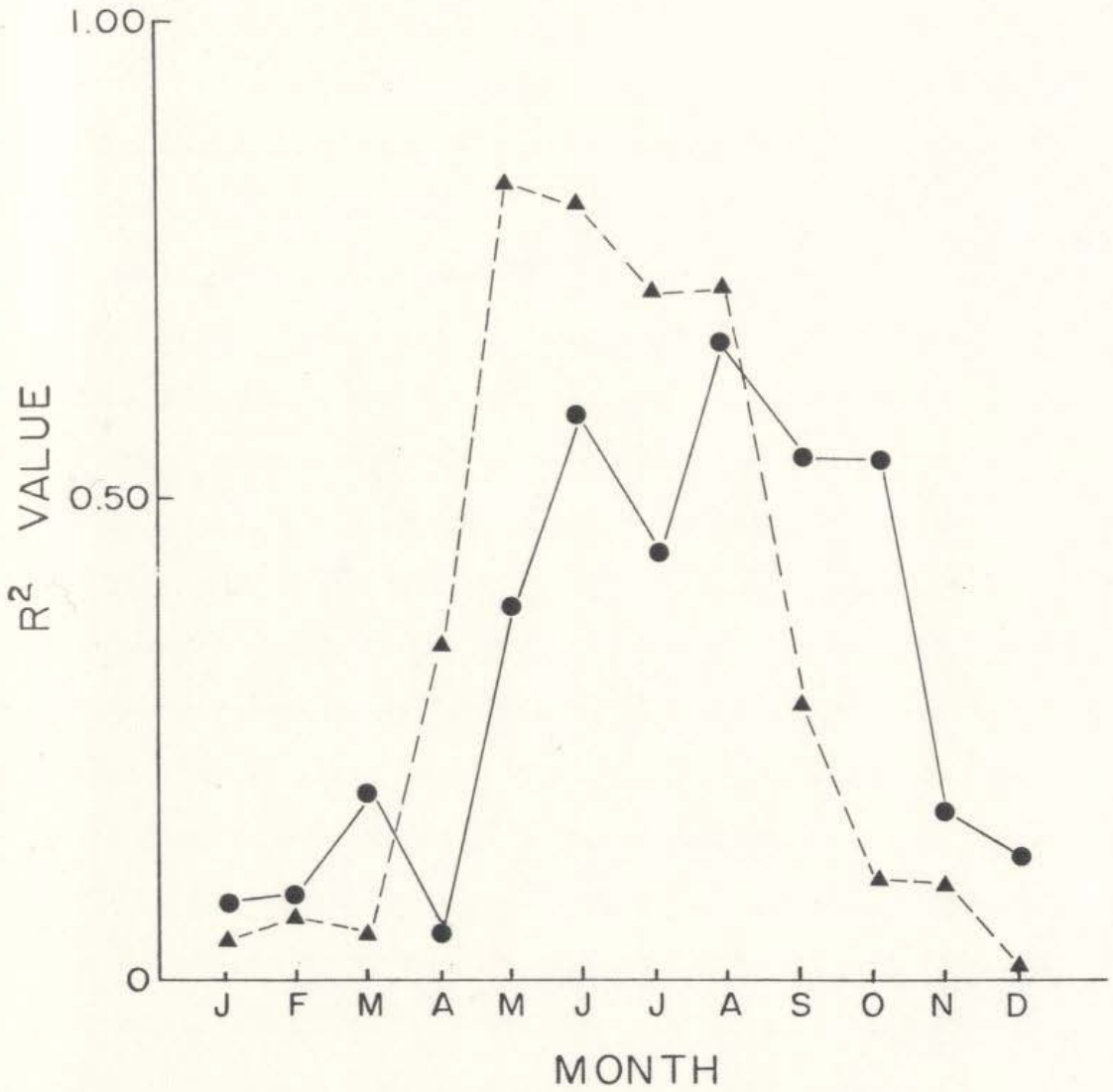

Figure 4.2 Plot of R^2 values relating mean monthly vector wind direction to direction of mean stem inclination, ▲ and maximum width of tree-ring asymmetry, ● .

4.2 TEST OF DEFORMATION INDICES

The location of the Black Mountain area where the deformation indices were tested is shown on the phytogeographic map (Appendix). Figure 4.3 is a detailed topographic map of the area which also shows the location and direction of stem inclination of each sample tree. The area is dominated by three hills rising from 500 feet (153 m) to 850 feet (260 m). Black Mountain is the northernmost hill and has the steepest slopes (approaching 1:1.5 gradient). Between Black Mountain and the second hill in the southwest is a short, narrow valley about 60 m deep. A broad saddle arcs from the second hill to the third, smaller hill in the southeast corner of the map.

Figures 4.4 and 4.5 show that tamarack is the dominant tree species in the area. Forest cover varies from sparse, isolated tamarack in bogs and heath barrens in the southeastern part, to fairly dense forest elsewhere in the area. A distinctive feature of the forest cover is the different distributions of multiple- and single-stemmed tamarack. On the summits of the two highest hills about 80% of the tamarack trees have multiple stems; whereas elsewhere, even on bogs and barrens at lower elevations, multiple-stemmed tamarack trees comprise only about 10-20% of the stand. At the southern end of the valley between the two highest hills (just west of the pond) most of the tamarack were broken by snow- and ice-loading. This phenomenon was not observed elsewhere in the area.

The results of the wind survey based on the deformation of 59 sample trees are shown in Table 13.

Figure 4.6 shows the distribution of mean wind speed classes calculated from the deformation ratio (Table 13). The highest mean wind

Figure 4.3 Topographic map of the Black Mountain area, Avalon Peninsula, Newfoundland, showing the location and direction of stem inclination of sample trees.

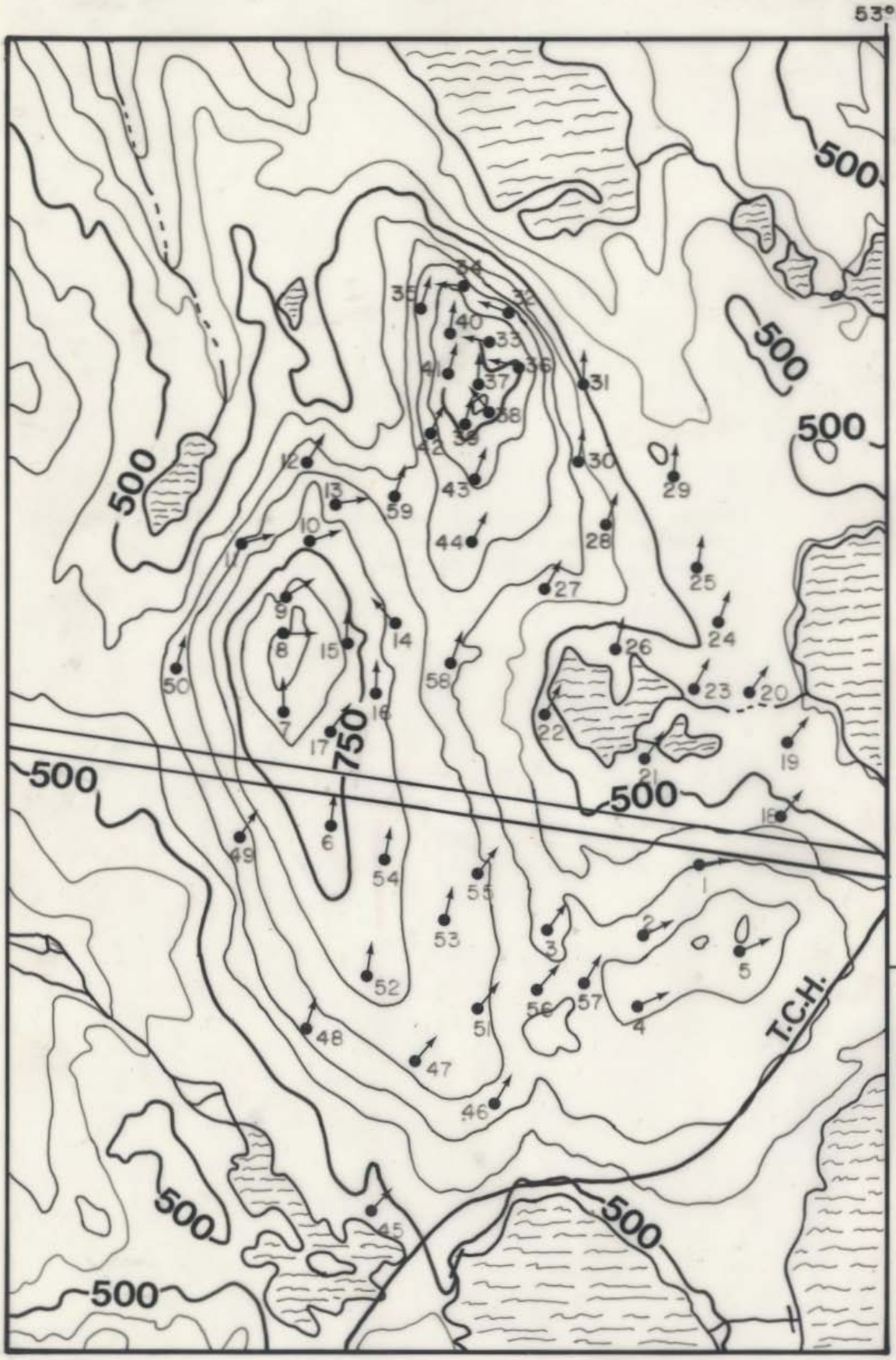
53°00'W
47°25'N
500
750
T.C.H.
0
1KM.
CONTOUR INTERVAL
50 FT.

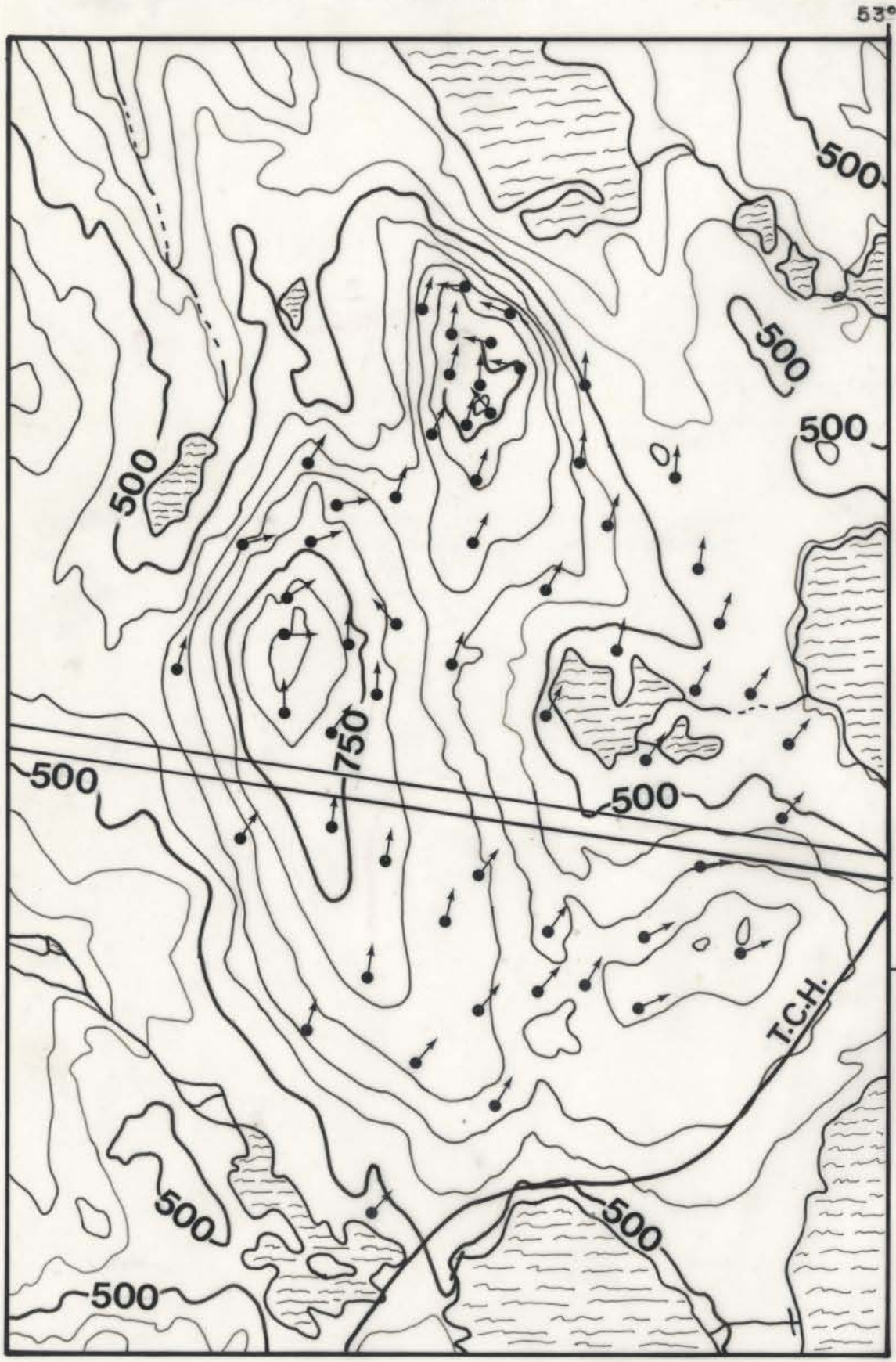
53°00'W
500
500
500
500
750
500
500
500
500
47°25' N
T.C.H.
0
1KM.
CONTOUR INTERVAL
50 FT.

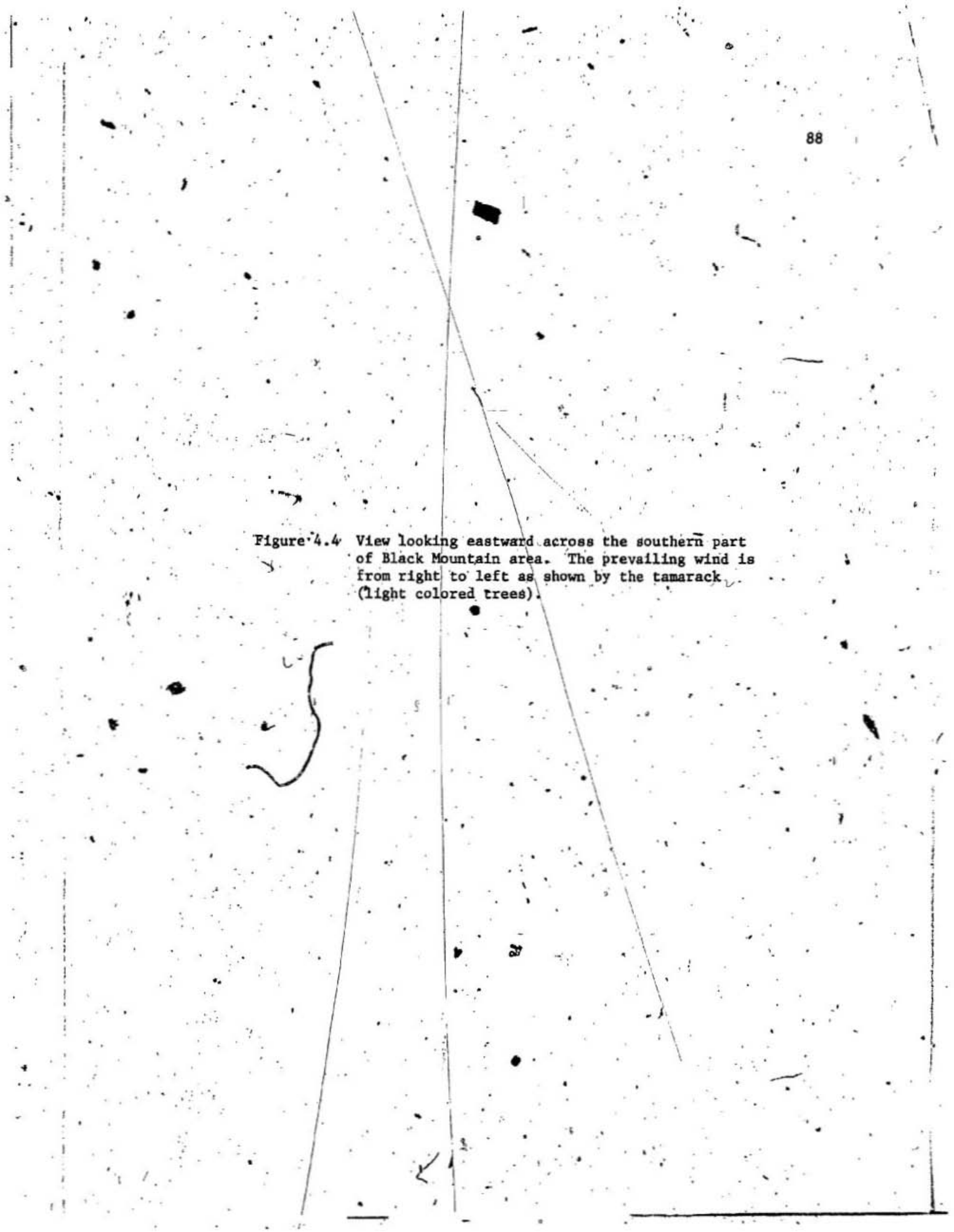

Figure 4.4 View looking eastward across the southern part of Black Mountain area. The prevailing wind is from right to left as shown by the tamarack (light colored trees).

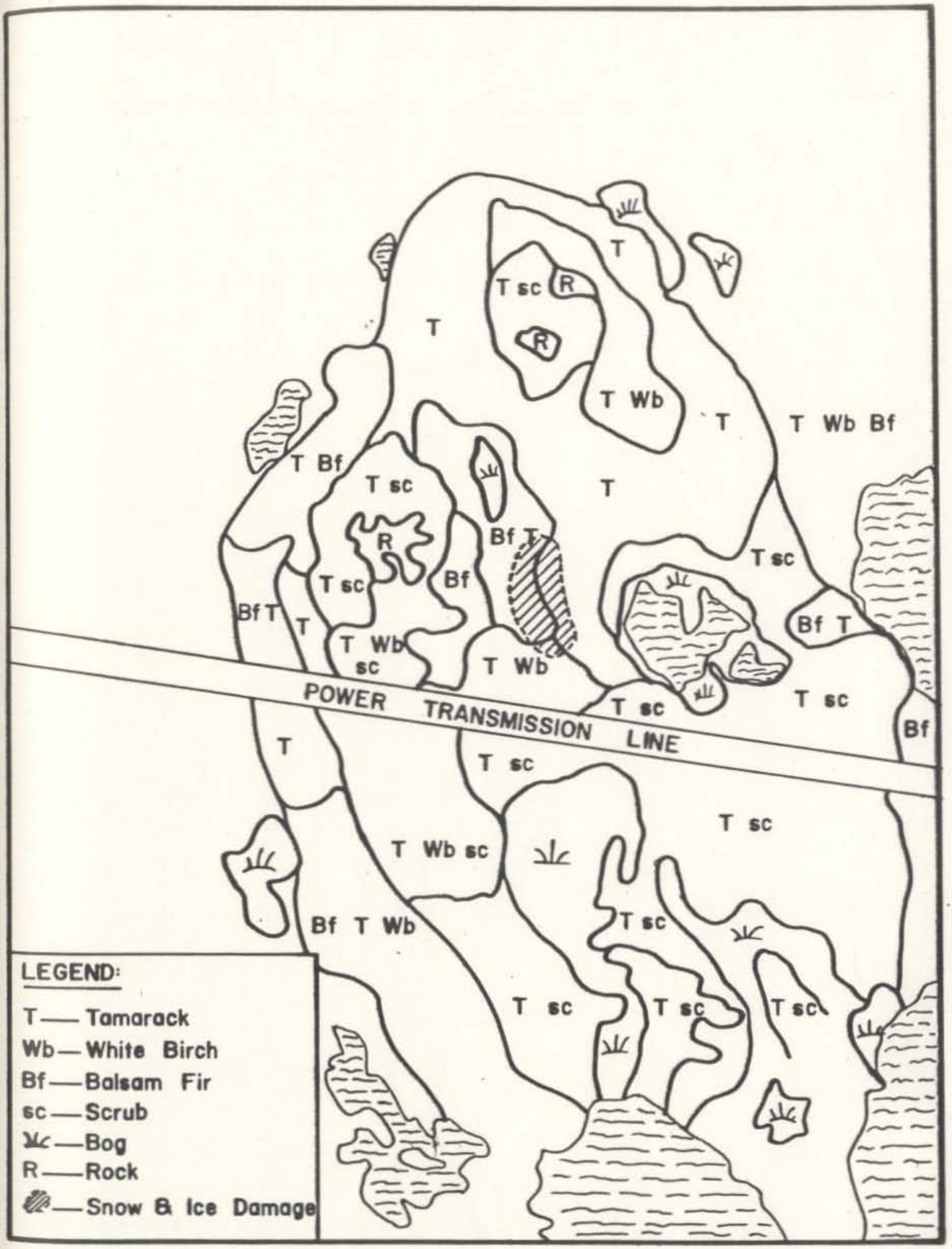

Figure 4.5 Map of the forest types in the Black Mountain area.

Table 13. Results of wind survey of Black Mountain area, Avalon Peninsula, Newfoundland. (Data include tree number, direction of stem inclination, S_{DIR}, deformation ratio, D'_r, compression index, C_i, and mean annual wind speed predicted by the deformation ratio, $\bar{V}_{A(1)}$, and compression ratio, $\bar{V}_{A(2)}$.

TREE #	S_{DIR} (°)	D'_r	C_i	$\bar{V}_{A(1)}^{+}$ ($m\ s^{-1}$)	$\bar{V}_{A(2)}^{++}$ ($m\ s^{-1}$)
1	256	1.44	1.5	5.5	5.7
2	240	2.04	1.2	6.0	4.0
3	224	2.49	1.3	6.5	4.6
4	244	2.13	2.0	6.1	8.5
5	250	4.29	2.0	8.1	8.5
6	185	2.20	1.2	6.2	4.0
7	185	2.01	1.3	6.0	4.6
8	266	1.70	1.5	5.7	5.7
9	236	1.82	1.2	5.8	4.0
10	248	2.00	1.2	6.0	4.0
11	216	2.15		6.1	
12	258	2.04	1.8	6.0	7
13	252	1.77	1.5	5.8	5.7
14	148	1.54		5.6	
15	180	1.15		5.2	
16	185	1.04	1.1	5.1	3.4
17	220	2.37	1.7	6.3	6.8
18	232	1.80		5.8	
19	220	1.68		6.1	
20	220	2.13		5.8	
21	220	1.80		5.8	
22	210	1.80		5.8	
23	212	2.61		6.6	
24	196	1.80	5.8	5.8	
25	184	1.28		5.3	
26	190	1.02	1.7	5.1	6.8
27	212	1.90		5.9	
28	200	1.55	1.3	5.6	4.6
29	184	1.05	1.2	5.1	4.0
30	184	1.30		5.4	
31	184	1.70		5.7	
32	108	1.77	1.4	5.8	5.1
33	97	1.92		5.9	
34	90	3.15		7.1	
35	202	2.42		6.4	
36	90	1.52		5.6	
37	180	1.92		5.9	
38	130	2.51	1.6	6.5	6.2

...continued

Table 13 (continued)

TREE #	S_{DIR} (°)	D'_r	C_i	$\bar{V}_{A(1)}$ + ($m\ S^{-1}$)	$\bar{V}_{A(2)}$ ++ ($m\ S^{-1}$)
39	200	1.73		5.8	
40	192	2.44		6.4	
41	192	4.65		8.5	
42	202	4.10	1.5	8.0	5.7
43	200	1.75		5.8	
44	200	1.75	1.4	5.8	5.1
45	222	1.55		5.6	
46	208	1.40	1.4	5.5	5.1
47	220	2.15	2.1	6.1	9.0
48	194	1.66	1.2	5.7	4.0
49	208	2.10	1.5	6.1	5.7
50	196	1.70	1.5	5.7	5.7
51	212	1.60		5.6	4.6
52	212	1.90		5.9	
53	185	1.52		5.6	
54	185	1.35		5.4	
55	224	1.72		5.7	
56	212	2.15		5.6	
57	220	1.60		5.6	
58	200	1.07		5.1	
59	200	1.09		5.1	
MEAN	200			5.8	5.5*
± SD	38			0.89	1.48

+ $\bar{V}_{A(1)} = 4.1 + 1.0\ D'_r$

++ $\bar{V}_{A(2)} = -2.8 + 5.6\ C_i$

*Significantly different at 10% (t = 1.819 for 84 DF)

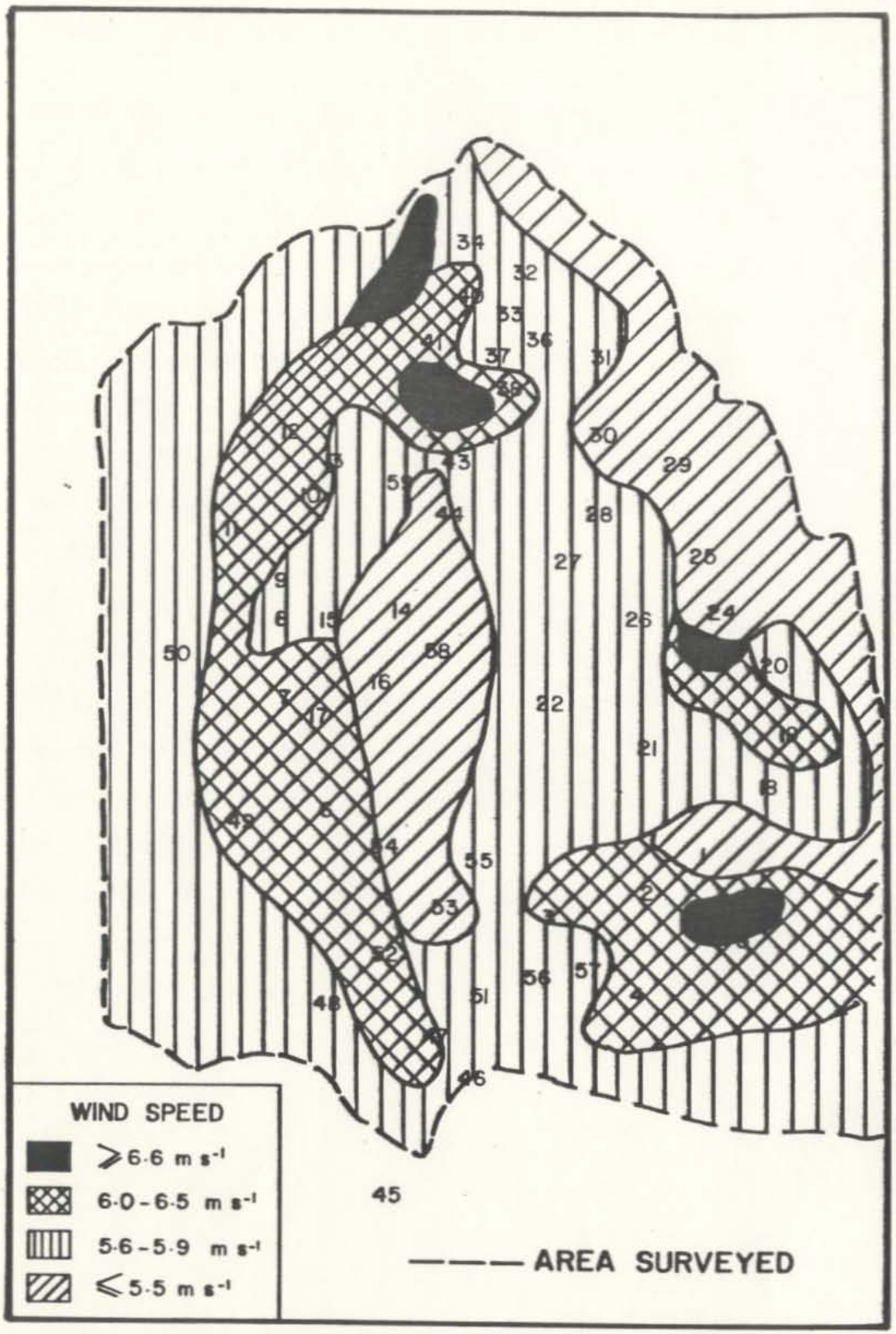

Figure 4.6 Map of the spatial variation of mean wind speed over the Black Mountain area determined from a survey of the deformation ratio, D'_r, of tamarack.

speeds (> 8.0 m S^{-1}) occur on the south side of summits of Black Mountain and the lower hill. High mean wind speeds also occur on the southwest slope of a low ridge above the northeast shore of small pond near the power transmission line and on the northwestern slope of Black Mountain. Moderately strong mean winds (6.0-6.5 m S^{-1}) occur on the ridges, even on comparatively low elevation ridges, between the two ponds near the transmission line. Middle and lower slopes with a south and west aspect, upper slopes with an east aspect and the southern part of the valley between Black Mountain and the neighbouring hill have mean wind speeds in the 5.6-5.9 m S^{-1}) range. Middle and lower slopes with an east aspect have the lowest mean wind speed (≤ 5.5 m S^{-1}).

The mean wind speed calculated for the area from the deformation ratio (5.8 m S^{-1}) is not significantly different from the mean annual wind speed observed at St. John's airport (6.8 m S^{-1}). In terms of similarity in exposure, the calculated mean wind speed for ridges and summits is 6.6 m S^{-1}, which is a 3% difference from mean annual wind speed at St. John's airport. The calculated mean wind speed for the area differs from the mean summer wind speed at St. John's airport by only 3% (i.e., 5.8 m S^{-1} compared to 6.0 m S^{-1}).

Figure 4.7 shows the percentage frequency for 10° classes of direction of stem inclination, S_{DIR}. Seventy-five percent of S_{DIR} values are between 180° and 229°, 16.7% between 230° and 269° and 10.3% between 90° and 149°. The mean S_{DIR} for the Black Mountain area is 200° (± 38°) compared to 240° for St. John's airport, which is significantly different at 2% (t = 2.317 for 62 DF). The difference is interpreted as being the result of differences in topography between the rolling hills of

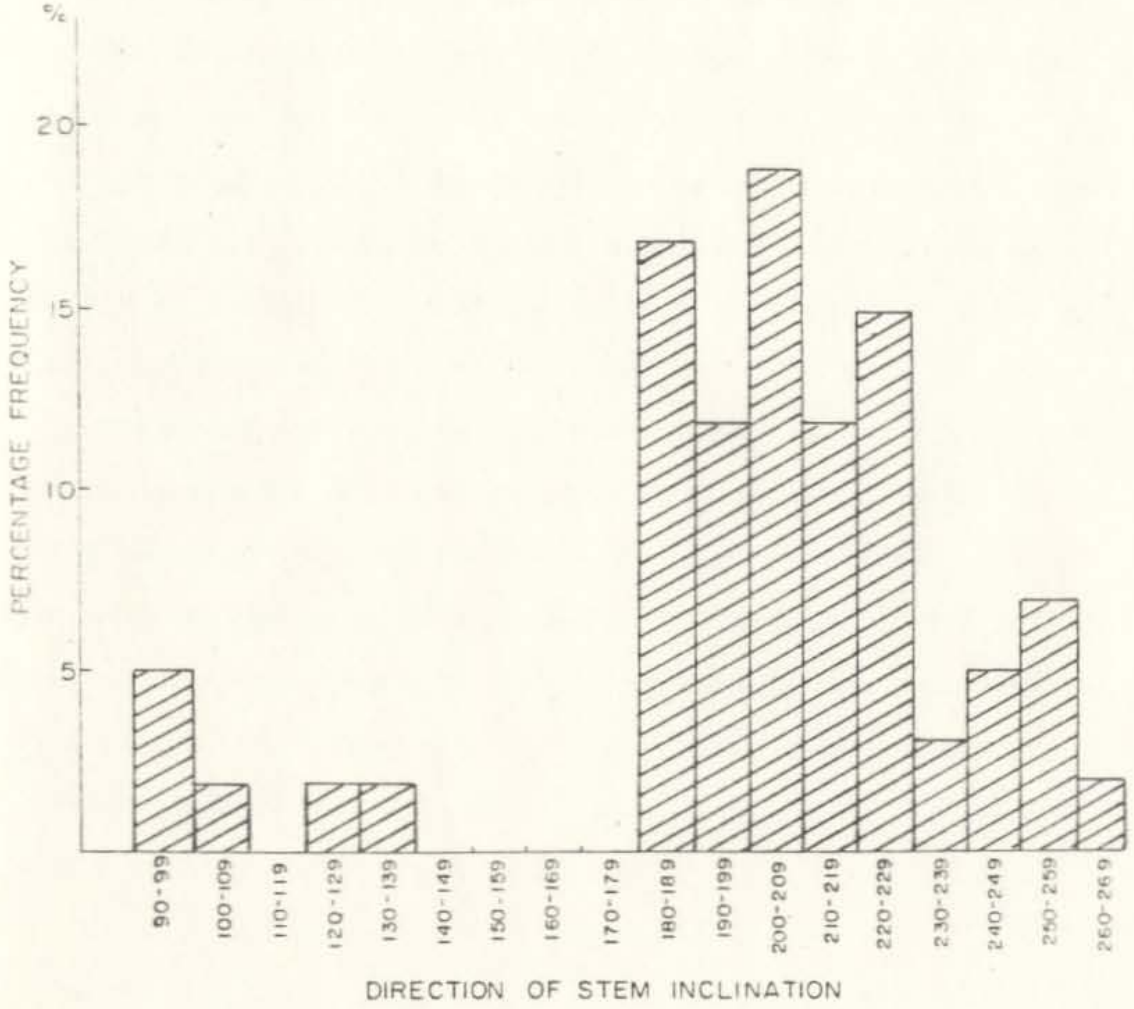

Figure 4.7 Percentage frequency classes of the direction of stem inclination of sample trees in the Black Mountain area.

Black Mountain area compared to the flat terrain of St. John's airport. The effect that topography has on wind direction is most pronounced on the upper slope in the east side of Black Mountain. These dramatic shifts in wind direction are interpreted as the result of vortex systems caused by flow separation. Other notable shifts in mean wind direction were observed on the north side of hill and valley west of Black Mountain. This section is interpreted as a zone of divergence where the velocity of up-slope wind increases with elevation. The flow is interrupted by the north ridge of Black Mountain resulting in another vortex system on the opposite side of the ridge.

The mean wind speed calculated from the compression index is significantly different from the mean wind speed calculated from the deformation ratio ($t = 1.819$ for 84 DF). A preliminary plot of the compression index failed to produce a reliable wind field map. The reason for the poor results is attributed to the influence of snow and soil creep, and snow and ice loading which also contribute to the development of asymmetric tree-rings.

5.0 DISCUSSION

5.1 POWER LAW

Readjusting the mean annual wind speed to a reference height of 2/3 mean tree height by the power law has no real advantage. The principal objection to the use of the power law is the uncertainty of the value of the power α. While $\alpha = 0.14$ is the most widely used, values ranging from $\alpha = 0.12$ (Nakajima, 1973) to as high as $\alpha = 0.69$ (Yoshino, 1975) for complex terrain have been proposed. As shown above, α varies considerably with surface roughness, thermal stability and seasonally and so, in the context of this study, the writer is in agreement with Touma (1977) and Wade and Hewson (1980) who maintain the power law is unreliable. Furthermore, there is no significant difference between the observed and predicted values of $\bar{V}_A$ and $\bar{V}_{AT}$ and therefore the power law is not necessary.

5.2 DIRECTION

The higher correlations between direction of stem inclination and summer vector wind direction, compared to other seasons of the year, indicates that summer southwesterlies are the main cause of tamarack deformation. Mednis (1971) observed that trees on Fogo Island on the north coast of Newfoundland were flagging towards the south. He shows that, although southwesterly winds dominate throughout the year, it is the northeasterlies, laden with ice crystals, which cause tree deformation. However, he was referring to the deformation of balsam fir (Mednis, pers. comm.). Figure 5.1 illustrates a similar situation along the southwest shore of Pistolet Bay, on the Great Northern Peninsula of

Figure 5.1 Tamarack (centre foreground) deformed mainly by summer southwesterlies (i.e. inclined to the left) and balsam fir (background) deformed by dessication and ice abrasion during winter northeasterlies (i.e. flagged to the right). The photo was taken adjacent to the southwest shoreline of Pistolet Bay, Newfoundland.

Newfoundland. The balsam fir exhibits flagging caused by winter northeasterlies as described by Mednis (1971); but the tamarack are deformed by summer southwesterlies. The reason, of course, is that tamarack is a deciduous conifer and, thus, is less affected by dessicating winter winds.

The trend in monthly correlation coeffitients for S_{DIR} vs $\bar{v}_{DIR}$ corresponds to monthly variations of wind speed and direction which is particularly noticeable in the wind roses for St. John's A, Gander and Buchans A (Appendix, Figures A2-A8). Because of coastal and valley influences such trends are less noticeable in the wind roses for the other calibration sites. However, it is clear that the winter northeasterlies have very little influence on the deformation of tamarack.

Apart from statistical relationships, the general trend of wind flow over Newfoundland, as shown on the phytogeographic map (Figure A1) corresponds closely to the strong southwesterlies which dominates the growing season as shown in the wind roses for the calibration sites. The southwesterlies are modified to varying degrees orographically. For example, in coastal areas the onshore southwesterlies are turned to the right where, in extreme cases, they become westerlies. Inland, topography tends to turn the southwesterlies to the left along major geomorphic structures. At the base of the Long Range Mountains, just north of Deer Lake, downslope mountain winds are conspicuous. This is one of the few areas in Newfoundland where downslope mountain winds are strong enough to cause tree deformation on the windward side of mountain. Other reversals of the general trend on wind flow over Newfoundland shown on the phytogeographic map, e.g., near Burgeo and St. John's,

are local topographic effects one would expect along a coast with high cliffs.

5.3 TREE DEFORMATION INDICES

Statistically, the deformation ratio has a consistently higher correlation with mean wind speed than has the compression index. This corroborates the findings of Wade and Hewson (1979, 1980). Apparently, on flat terrain, common to the calibration sites, the mean wind speed predicted by the deformation ratio and the compression index were not significantly different at $P = 0.05$. On flat terrain or even gently rolling topography, especially on forest cutovers, the compression index should provide a reasonably good estimate of mean wind speed and direction; albeit, not as reliable an estimate as the deformation ratio would give.

In complex terrain, however, the results of the Black Mountain wind survey indicate that the compression index is not a practical alternative for estimating wind flow. On steep slopes, snow and soil creep, ice and snow loading and, to some extent, phototropism contribute to the development of tree-ring asymmetry (Wade and Hewson, 1979) and thus tend to mask the contribution of wind. These effects were particularly evident on the steep northeast slopes of Black Mountain.

By contrast, the deformation ratio produced a wind flow map of Black Mountain area that identified many salient features inherent in microscale wind flow theory. These included distinctive zones of convergence and divergence and vortex systems. Figure 5.2 is a schematic representation of streamlines and vortices over the Black Mountain area.

Figure 5.2 Schematic representation of streamlines and vortices, over the Black Mountain area indicated by the deformation of tamarack. View looking northeast.

——— STREAMLINES

– – – VORTICES

Rutter (1968a) observed that eddies occur on lee slopes with a 1:4 gradient but were not detected on lee slopes with a 1:10 gradient. The deformation ratio indicates that the same phenomenon occurs in the Black Mountain area where a persistent vortex wake occurs on the lee slope of Black Mountain which has a 1:2 gradient, but was not discernible on an equally high hill with a similar longitudinal orientation and a lee slope with a 1:7 gradient. Figure 5.3 illustrates the severe deformation caused by a strong, persistent vortex on the northeast slope of Black Mountain. Putnam (1948), Yoshino (1957), Kaiser (1954), Hutte (1968), Gloyne (1957) and others detected an eddy zone on the leeward crest followed by reduced wind speed in the lower slope.

Rutter (1968b) also observed that when an incident wind is oblique to the longitudinal axis of hills, the wind will blow around the (upwind) ridge. This is also indicated by tree deformation where the wind follows the countours along the slopes with a north aspect providing the ridges are well rounded with long slopes. However, it appears when wind flow encounters comparatively sharp ridges with steep slopes a distinctive zone of divergence exists on the middle and lower windward slope which creates a strong vortex system on the upper lee slope of the ridge as a result of flow separation similar to that described by Yoshino (1975). The zone of divergence, indicated by the high wind speed zone on the lower northwest slope of Black Mountain (Figure 4.6) is due also, in part, to the channelization of wind flow along the NE side of the valley separating the two hills which merges with the wind flowing around the back of the hill. Weidman (1930) found that the most extensive wind throw occurs in the section of valleys where the wind

Figure 5.3 Severe flagging of a tamarack (centre) and a balsam fir (left) caused by a persistent vortex on a steep slope on the east side of Black Mountain, Avalon Peninsula, Newfoundland. The flagging is roughly 90^{0} to the prevailing summer wind for the region (which flows directly towards the person in the centre of the photo).

tends to be funneled (i.e., at the up-wind end). While there was no wind throw in the divergence zone, since the trees were adapted by geotropic growth, the degree of deformation appears to corroborate Weidman's hypothesis. Furthermore, the almost complete reversal of direction of stem inclination on the opposite side of the ridge indicates that comparatively strong vortex wake systems can develop on lee slopes on the up-wind end of the longitudinal axis of hills. So far as is known no model exists that involves two airstreams from an oblique incident wind that creates a vortex wake on up-wind lee slopes.

The hanging valley between the two highest hills is oriented roughly NW-SE and the prevailing winds are southwesterlies, which means the incident wind enters the SE end of the valley at 45° to normal. The strongest winds are along the NE side of the valley, while the lower and middle slopes are areas of relative calm, i.e. zones of convergence. However, it should be noted that a long sloping ridge which arcs to the SE extends the zone of convergence on the leeward slope south of the valley. The trees in this zone are tall and thin with comparatively little compression wood and the deformation ratio indicates a low mean annual wind speed. The high percentage of broken tamarack trees indicates severe damage from ice and snow loading which also indicates a low wind speed area.

The high deformation ratios on the ridges and summits is an indication that wind velocity accelerates upslope. This agrees with the models by Jackson and Hunt (1975), Bradley (1980) and Neal (1982) and observation by Gloyne (1957) and Hutte (1968).

The highest deformation ratios on the windward crests of Black

Mountain and the lower hill indicated that exposure on windward slopes is independent of elevation. The mean wind speed between the 750-850 foot (230-260 m) windward contours on Black Mountain is about the same as on the 700-750 foot (214-230 m) windward contour on the lower hill in the southeast part of the area, i.e. 8.0 m S^{-1}. Rutter (1968) also found that low and high elevation windward crests had the same degree of wind exposure within the same topographic unit. He suggested that rapid acceleration of wind upslope was the result of two airstreams, one flowing parallel to the ground and the other blowing over the lee slope vortex wake. In fact, Bradley (1980) and Neal (1982) both observed a 'jet' above the crest of hill which tends to support Rutters' suggestion. The 'jet' effect may not be restricted to crests but may also occur over low elevation water bodies. For example, the high deformation ratios along the northeast 'up wind' shore of the small pond at the base of the south slopes of Black Mountain indicates that wind accelerates rapidly within a comparatively short distance (0.3 km) over water, resulting in a distinctive zone of divergence with wind velocities higher than on windward saddles. It is also noteworthy that the pond is at the base of a long leeward slope where deformation ratios are in the lower range.

5.4 THIGMOMORPHOGENESIS

Because of past logging activities in the Black Mountain area, resulting in uneven-aged natural regeneration, the relationship between forest productivity and wind could not be studied in detail. However, it is clear that height growth is as good, or better, on the middle and

lower windward slopes than in the leeward slopes. Height growth ranged from 8-14 m on lower windward and leeward slopes. On the ridges and summits height rarely exceeded 3 m.

A distinctive feature of tree form above the 750 foot (230 m) contour was the high percentage (= 80%) of multiple-stemmed (shrub-like) tamarack as opposed to single-stemmed (tree-like) tamarack. There is little height difference between the two forms; they both ranged from about 2-3 m in height. In contrast, the multiple-stemmed trees make up about 10-15% of the pure tamarack forest (8-13 m in height) on the south and east slopes of Black Mountain, and somewhat less than 10% on the west and north slopes elsewhere.

The multiple stems appear as if they were a clump of trees that had germinated in the one spot, when in fact they originate from a single shoot. In terms of total biomass they outproduce single-stem forms by a factor of more than 2:1.

Since it has been shown wind promotes lateral growth at the expense of terminal growth, multi-stemmed tamarack can be interpreted as a growth response to wind. Tansley (1939), Wade and Hewson (1980) and Woolley (1980) observed that in continuous forest cover the top of the canopy is smooth in areas dominated by persistent high winds and rough in areas of low wind. In aerial reconnaissance surveys for wind prospecting, Woolley (1980) graded the canopy texture to map spatial variations in wind speed. Therefore the multi-stemmed form which generally produce a smooth textured canopy can also be used as an indication of high wind speed zones.

However, the fact that multi-stemmed forms occur in sheltered

valleys and lee slopes to an extent greater than in lower windward slopes indicates a genetic adaptation to wind. Lawrence (1982), studying wind stress and elfin forest in high altitude tropical rain forests postulated that physiognomic trends could result from phenotypic plasticity, genetic differentiation within a population or a combination of these factors. This would include a post-germination mortality in which tree forms, specially adapted to withstand the rigors of a windy site, would have a higher rate of survival on exposed sites than less well-adapted forms. Considering the order of distribution where multi-stemmed tamarack consist of 80% on exposed ridges and summits, 10-15% on leeward slopes and < 10% on lower windward slopes, Lawrence's theory may be applicable here.

Tree species which are less adapted to severe exposure to wind often develop into slow growing prostrate shrubs. Figure 5.4 illustrates the poor growth of a 17-year-old Sitka spruce in an experimental plantation established on the windward crest of the hill on the southern part of the Black Mountain area. The site lies within the zone of divergence on the windward side of the crest of the small hill south of Black Mountain where mean summer wind speed is > 6.5 m S^{-1} (Figure 4.7). It could be argued that other site factors such as soil type, competition from heath plants, etc. are more important factors limiting tree growth. However, Figure 5.5 shows a replicated plantation on the Avalon Peninsula (near Arnold's Cove) containing the same 17-year-old Sitka spruce seedlot (and other exotic conifers) in which the stunted growth is barely visible. As with the Mountain planting site, pretreatment of the Arnold's Cove site included furrowing with a Cuthbertson forestry

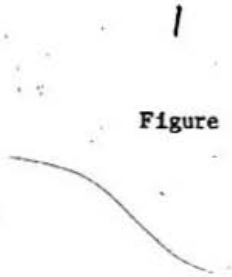

Figure 5.4 17-year-old Sitka spruce planted on the windward crest of hill exposed to a mean summer wind speed > 6.5 m S^{-1} in the Black Mountain area, Avalon Peninsula, Newfoundland.

Figure 5.5 The stunted growth of 17-year-old Sitka spruce and Scots pine is barely discernible from the natural vegetation in this experimental plantation near Arnold's Cove, Newfoundland. The mean summer wind speed at this site, as indicated by tamarack deformation indices, is $\geq$ 5.5 m s^{-1}. Obviously there is not much hope of the spruce and pine progressing beyond low tuckamore.

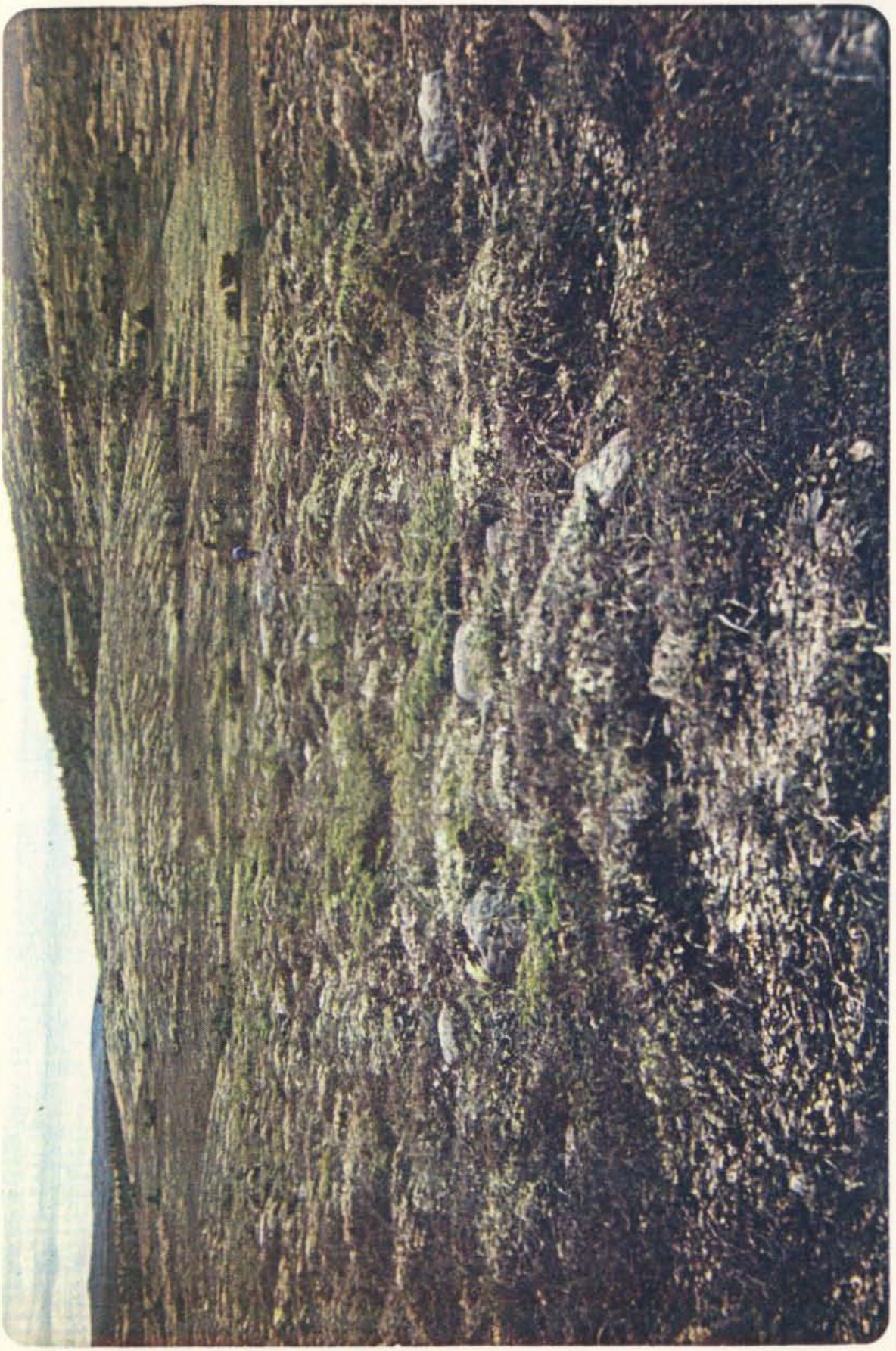

plough (Salter and Evans, 1976). In this case, competition from natural vegetation is not a factor because wind erosion has scoured away the natural vegetation turf around the planted trees exposing bare soil on the windward side of the furrows. The planted trees are able to survive by growing in a low spreading habit where humus is trapped (and accumulated) and thus, at least preventing soil frost-heaving. Here, we can safely assume that a mean summer wind speed of > 5.5 m S^{-1} from a southwesterly direction, as indicated by tamarack deformation in the area, is the major constraint to tree growth.

The results of this study imply that a mean summer wind speed > 5.0 m S^{-1} is a major constraint on productive forest growth. While some coniferous species may be better adapted to wind than others, the amount of compression wood resulting from exposure to mean summer wind speeds of > 5.0 m S^{-1} seriously affects the quality of the wood from a utilization standpoint.

6.0 CONCLUSIONS

The degree of deformation of tamarack can provide a good estimate of mean wind speed and mean summer vector direction based on the five main hypotheses.

1. Mean annual wind speed predicted by the deformation ratio does not differ significantly from the mean annual wind speed recorded by meteorological station.
2. Over flat terrain the mean annual wind speed predicted by the compression index does not differ significantly from the mean annual wind speed predicted by the deformation ratio.
3. Over complex terrain the mean annual wind speed predicted by the compression index differs significantly from the mean annual wind speed predicted by the deformation ratio.
4. The mean direction of stem inclination differs significantly from the mean annual wind vector direction.
5. The mean direction of stem inclination does not differ significantly from the mean summer wind vector direction.

The results show that the deformation ratio is a better estimator of wind speed and direction than the compression index. On flat, or gently rolling terrain, the compression index has the advantage in providing a reliable dendrochronological record of periodic variations in wind flow and, of course, would be the only record of wind in logged or burned areas.

In complex terrain, however, the compression index is unreliable due to other factors contributing to the growth of asymmetric tree-rings. The deformation ratio, on the other hand, is sufficiently sensi-

tive to microscale variations and is able to detect persistent vortex wake systems, zones of divergence and convergence predicted by theoretical models.

The direction of stem inclination shows that summer southwesterlies, associated cyclones, is the main cause of tamarack deformation.

REFERENCES

AANENSEN, C.J.M. (editor) 1965
Gales in Yorkshire in February 1962. Meteor. Office; Geophys. Mem. 108:14-17.

A.E.S. 1982
Canadian Climate Normals 1951-1980: Vol. 5. Wind. Atmospheric Environment Service, Downsview, Ontario.

ALEXANDER, ROBERT R. 1964
Minimizing windfall around clear cuttings in spruce-fir forests. For. Sci. 19(2):130-140.

ALEXANDER, ROBERT R., and JESSE H. BUELL 1955
Determining the direction of destructive winds in a Rocky Mountain timber stand. J. For. 53(1):19-23.

BANFIELD, COLIN 1981
The climatic environment of Newfoundland. In The natural environment of Newfoundland past and present. (Editors A.G. Macpherson and J.B. Macpherson.) Dept. of Geography, Memorial University of Newfoundland.

BANNAN, M.W., and M. BINDRA 1970
Influence of wind on ring width and cell length in conifer stems. Can. J. Bot. 48:255-259.

BARSCH, D. 1963
Wind, Baumform und Landschaft: Eine Untersuchung des windeinflusses auf Baumform und Kulturland schaft am Biespiel des Mistralgebietes in franzosischen Rhonetal. Frieberger Geogr. Hefte, Heft. 1.

BOOTH, T.C. 1976
In 4th Symposium on shelter research. Warwick Sept. 1975. (Editor R.G.A. Lofthouse.) Min. Agric., Fish and Food, London.

BOYD, J.D. 1950
Tree growth stresses. I. Growth stress evaluation. Austr. J. Sci. Res., Ser. B., Biol. Sci. 3:270-293.

BRUNIG, E.F. 1967
Protection against inorganic types of damage other than fire. In F.A.O. World symposium on man-made forests and their industrial importance. Vol. 1:760-772.

BURNS, G.P. 1920
Eccentric growth and the formation of redwood in the main stem of conifers. Vermont Univ. Agric. Exp. Sta., Bull. No. 219.

CASPERSON, G. 1963
Über die Bildung der Zellwand beim Reaktionsholz. II. Zur Physiologie des Reaktionsholes. Holztechnol, Dresden. 4:33-37.

CLAQUE, JOHN, L.A. JOZSO, and M.L. PARKER 1982
Dendrochronological dating of glacier-dammed lakes: An example from Yukon Territory, Canada. Arct. and Alpine Res. 14:301-310.

COCHRANE, WILLIAM G. 1963
Sampling techniques. John Wiley & Son, New York.

COOPER, W.S. 1913
The climax forest of Isle Royale, Lake Superior, and its development. Bot. Gaz. 55:1-44.

COUTANT, V.C.B., and VAL L. EICHENLAUB 1975
De Ventis/Theophrastus. Univ. Notre Dame Press.

CROPPER, JOHN P., and HAROLD C. FRITTS 1981
Tree-ring width chronologies from the North American Arctic. Arct. Alp. Res. 13(3):245-260.

CURTIS, J.D. 1943
Some observations on wind damage. J. For. 41:877-882.

DAUBENMIRE, R.F. 1974
Plants and environment: A textbook on autecology. 3rd Edition. John Wiley & Sons, New York.

DUTTON, JOHN A. 1976
The ceaseless wind: An introduction to the theory of atmospheric motion. McGraw-Hill Co., New York.

EWART, A.J., and A.J. MASON-JONES 1906
Formation of redwood in conifers. Ann. Bot., London, 20:201-204.

FIELDING, J.M. 1940
Lean in Monterey pine (Pinus radiata) plantations. Austr. For. 5:21-25.

FITTING, H. 1905
Untersuchungen über den geotropischen Reizforgang. I. Geotropische Empfindlichkeit der Pflanzen. II. Weiere Erfolge mit der intermittierenden Reizung. Jahrb. Wiss. Bot. 41:221-330, 331-398.

FRANKLIN, JERRY F., T. MAEDA, Y. OHSUMI, M. MATSUI, and H. YAGI 1979
Subalpine coniferous forests of Central Honshu, Japan. Ecol. Mongr. 49(3):311-334.

GILMOUR, J.D. 1926
Clear cutting of pulp woodlands. For. Chron. 2:1-2.

GLOYNE, R.W. 1957
Problems of surface air flow and related phenomena in agriculture, horticulture and forestry. Meteor. Res. Comm., Meteor. Office, Harrow; MRP 1049.

GORCHAKOVSKY, P.L., and S.G. SHIYATOV 1978
The upper forest limit in the mountains of the boreal zone of the USSR. Arct. Alp. Res. 10(2):349-363.

GRACE, J. 1977
Plant response to wind. Academic Press, New York.

GRATKOWSKI, H.J. 1956
Windthrow around staggered settings in old-growth Douglas fir. For. Sci. 2(1):60-74.

GRIGGS, ROBERT F. 1938
Timberlines in the northern Rocky Mountains. Ecology 19:548-564.

HARTIG, R. 1896
Das Rotholz der Fichte. Forst. Naturw. Zeits. 157-169.

HARTIG, R. 1901
Holzuntersuchungen, Altes und Neues. J. Springer, Berlin.

HARTMANN, F. 1942
Statische wuchsgesetz bei Nadel-und Laubbäumen. Springer-Verlag, Vienna.

HEEDE, B.H. 1972
Flow and channel characteristics of two high mountain streams. U.S.D.A., Rocky Mtn. For. Exp. Sta., Res. Paper RM-96.

HOLROYD, E.W. 1970
Prevailing winds in White Mountains as indicated by flag trees. For. Sci. 16:222-229.

HUTTE, PAUL 1968
Experiments on wind flow and wind damage in Germany; site and susceptibility of spruce forests to storm damage. Forestry (Supplement) 41:20-25.

JACCARD, P. 1919
Nouvelles recherches sur l'accroissement en épaisseur des arbres: essai d'une théorie physiologique de leur croissance concentrique et excentrique. Foundation Schnyder von Wartensee, Zurich. 200pp.

JACCARD, P. 1920
Inversion de l'excentricité des branches produité experimentalement. Rev. Gen. Bot. 32:273-281.

JACCARD, P. 1934
Über Versuche zue Bestimmung der Zellsaftkonzentration in der Kambialzone beim exzentrischen Dickenwachstrum. II. Jahrb. wiss Bot. 81:35-58.

JACCARD, P. 1939
Tropisme et bois de réaction provoques par la force centrifuge. Berl Schweiz. Bot. Ges. 50:285-292.

JACKSON, P.S., and J.C.R. HUNT 1975
Turbulent flow over a low hill. Q.J.R.M.S. 101:925-955.

JACOBS, M.R. 1936
Effect of wind on trees. Austr. For. 1(2):25-32.

JACOBS, M.R. 1938
Fiber tension of woody stems, with special reference to the genus Eucalyptus. Comm. For. Bureau, Austr., Bull. No. 22.

JACOBS, M.R. 1939
Study of the effect of sway on trees. Comm. For. Bureau, Austr., Bull. No. 26.

JACOBS, M.R. 1945
Growth stresses of woody stems. Comm. For. Bureau, Austr., Bull. No. 28.

JACOBS, M.R. 1954
Effect of wind sway on the form and development of Pinus radiata D. Don. Austr. J. For. 2:35-51.

JACOBY, G.C., and E.R. COOK 1981
Past temperature variation inferred from 400 year tree-ring chronology from Yukon Territory, Canada. Arct. Alpine Res., 13(4): 409-418.

JAFFE, M.J. 1973
Thigmomorphogenesis: The response of plant growth and development to mechanical stimulation, with special reference to Bryonia dioica. Planta 114:143-157.

JAFFE, M.J. 1980
Morphogenetic responses of plants to mechanical stimuli or stress. Bio Science 30:239-243.

JEFFERSON, MARK S.W. 1904
Wind effect J. Geogr. 3:2-20.

JENSEN, MARTIN 1961
Shelter effect. Danish Technical Press, Copenhagen.

JOHNSON, R.C., G.E. RAMLEY, and D.S. O'HAGAN 1982
Wind-induced forces on trees. J. Fluid Eng. 104:25-30.

JORDAN, G.A., and R.H. BALLANCE 1983
A microcomputer-based annual ring measurement system. For. Chron. 59:21-25.

KAISER, H. 1954
Über die Stromungsverhältnisse im Bergland. Met. Rasch., 7:214-217.

KAY, PAUL A. 1978
Dendroecology in Canada's forest tundra transition zone. Arct. Alpine Res. 10(1):133-138.

KELLOGG, R.M., and G.L. STEUCEK 1980
Mechanical stimulation and xylem production in Douglas fir. For. Sci. 26(4):643-651.

KENNEDY, MICHAEL JOSEPH 1974
Windthrow and windsnap in forest plantations, Northern Ireland. Michigan Georgr. Publ. No. 11. Univ. of Michigan, Ann Arbor.

KIENHOLZ, R. 1930
Wood structure of a 'pistol-butted' mountain hemlock. Amer. J. Bot. 17:739-764.

KIMBAL, M.H., and G.A. BROOKES 1959
Plantclimates of California. California Agric. 13(5):7-12.

KINERSON, RUSSELL S., and LEO J. FRITSCHEN 1973
Modeling air flow through vegetation. Agric. Met. 12:93-104.

KNIGHT, T.A. 1803
Account of some experiments on the descent of the sap in trees. Phil. Trans. Roy. Soc., London. 1803 (pp. 277-279).

KONONCHUK, D.I. 1888
On the local or one-sided "hard-layerness" of trees [in Russian]. Yearbook of the St. Petersburg Forest Institute 2:41-56.

LARSON, PHILIP R. 1953
Influence of gravity on rate of elongation and on geotropic and autotropic reactions in roots. Physiol. Plant., Copenhagen 6:735-774.

LARSON, PHILIP R. 1965
Stem form of young larix as influenced by wind and pruning. For. Sci. 11:412-424.

LAWRENCE, DONALD B. 1939
Some features of the vegetation of the Columbia River Gorge with special reference to asymmetry in forest trees. Ecol. Monogr. 9:217-257.

LAWRENCE, ROBERT O. 1982
Wind stress and elfin stature in a rain forest tree: An adaptive explanation. Amer. J. Bot. 69(8):1224-1230.

LIESE, W., and H.F. DADSWELL 1959
Über den Einfluss der Himmelsrichtung auf die Länge von Holzfäsern und Traheiden. Holz. Roh. Werkstatt 17:421-427.

LORIMER, CRAIG G. 1980
Age structure and disturbance history of a southern Appalachian virgin forest. Ecology 61(5):1169-1184.

LOW, ALLAN J. 1964
A study of compression wood in Scots pine. Forestry 37(2):181-201.

McADAM, J.H. 1980
Tatter flags and climate in the Falkland Islands. Weather 35(11): 321-327.

MEDNIS, ROBERTS JANIS 1971
A phytogeographical analysis of the occurrence of vegetation patterns on Fogo Island, Newfoundland - Labrador, Canada. Dept. of Geography, Boston University. Ph.D. Thesis.

MER, É. 1888
Causes qui produisent l'excentricité de la moelle dans les sapins. C.R. Acad. Sci., Paris 106:313-316.

METSGER, K. 1939
Der Wind als massgebender Faktor für das Waschtum der Bäume. Mündener Forstl., 3:35-86.

MOORE, M.K. 1977
Factors contributing to blowdown in streamside leave strips on Vancouver Island. Land Management Report No. 3. Res. Div., Min. Forests, Victoria, B.C.

MÜNCH, E. 1937
Entstehungsursachen und Wirkung des Druck-und Zugholzes der Bäume. Forst. Wochens. Silva, Tbuingen 25:337-341, 345-350.

NAKAJIMA, S. 1973
[Observed profile of wind velocity in the lower atmospheric layer.] Chôkôsô Tower Kishôshiryô 5:17-32.

NEWNHAM, R.M. 1968
A classification of climate by principal component analysis and its relation to tree species distribution. For. Sci. 14:254-264.

NICHOLS, H. 1976
Historical aspects of the northern Canadian tree line. Arctic 29: 38-47.

NICHOLSON, J., and D.G. BRYANT 1972
Climatic zones of insular Newfoundland: A principal component analysis. Env. Canada, Canadian Forestry Service, St. John's. Publ No. 1299.

NOGUCHI, Y. 1979
Deformation of trees in Hawaii and its relation to wind. J. Ecol. 67:611-628.

OKE, T.R. 1978
Boundary layer climates. Methuen Co., London.

OLIVER, J. 1960
Wind and vegetation in the Dale Peninsula. Field Studies 1(2):1-12.

OLIVER, H.R. 1971
Wind profiles in and above a forest canopy. Agric. Met. 12: 123-130.

OLIVER, H.R., and G.J. MAYHEAD 1974
Wind measurements in a forest during a destructive gale. Forestry. 47(2):185-195.

ONAKA, F. 1935
[On the arrangement of compression wood in conifers.] J. Jap. For. Soc. 17:680-693.

ONAKA, F. 1940
[On the influence of auxin on radial growth, particularly regarding compression wood formation in trees.] J. Jap. For. Soc. 22: 573-580.

ONAKA, F. 1949
[Studies on compression wood and tension wood.] Mokuzai Kenkyu, Bull. No. 1.

OSHIMA, Y., M. KIMURA, H. IWAKE, and S. KUROIWA 1958
Ecological and physiological studies on the vegetation of Mt. Shimagare. I. Preliminary survey of the vegetation of Mt. Shimagare. Bot. Mag. Tokyo 71:289-300.

OWADA, M. 1973
Prevailing winds in the Tshikari Plain, Hokkaido. Geogr. Rev. Japan 44(9):638-652.

PETERSON, K.M., and W.D. BILLINGS 1980
Tundra vegetational patterns and succession in relation to micro-topography near Athasook, Alaska. Arct. Alpine Res. 12(4):473-482.

PETRIE, S.M. 1951
Gale Warning! Windthrow in western spruce plantations. J. For. Comm. 22:81-90.

PILLOW, M.Y. 1931
Compression wood records hurricane. J. For. 29:575-578.

PILLOW, M.Y., and R.F. LUXFORD 1937
Structure, occurrence, and properties of compression wood. U.S.D.A., Tech. Bull. No. 546.

PILLOW, M.Y., E.R. SCHAEFFER, and J.C. PEW 1959
Occurrence of compression wood in black spruce and its effects on properties of ground wood pulp. Paper Trade J. 102(16):36-38.

PLESNIK, P. 1957
[Influence of the wind on the shape of crown and stem of spruce in the region of the upper tree-line in the Mountain Krwanska, Mala Tatra.] Geograf. Casopis, Bratislava 9(4):197-224.

PLESNIK, P. 1971
Horná hranica lesa + Mapova prikola vo Vysokýck a v Belanskýck Tatrák. Vydavaleśtvo Slov. Akad. Vied, Bratislava, 1-238.

PLESNIK, P. 1973
Some problems of the timberline in the Rocky Mountains compared with Central Europe. Arct. Alpine Res. 5:77-84.

PUTNAM, P.D. 1948
Power from the wind. Van Nostrand, New York.

QUIRK, J. THOMAS, and FRANK FREESE 1976a
Effect of mechanical stress on growth and anatomical structure of red pine: Compression stress. Can. J. For. Res. 6:195-202.

QUIRK, J. THOMAS, and FRANK FREESE 1976b
Effect of mechanical stress on growth and anatomical structure of red pine: Stem vibration. Can. J. For. Res. 6:375-381.

QUIRK, J. THOMAS, DIANA M. SMITH, and FRANK FREESE 1975
Effect of mechanical stress on growth and anatomical structure of red pine (Pinus resinosa Ait.): Torque stress. Can. J. For. Res. 5:691-699.

RAWITSCHER, F. 1937
Geotropism in plants. Bot. Rev. 3:175-194.

REES, D.J., and J. GRACE 1980a
The effects of wind on the extension growth of Pinus contorta Doug. Forestry 53(2):145-153.

REES, D.J., and J. GRACE 1980b
The effects of shaking on extension growth of Pinus contorta. Forestry 53(2):155-166.

RUNGE, F. 1957
Windgeformte Bäume in den italienischen Riviera. Met. Rundsch. 10:47-48.

RUTTER, N. 1968a
Tatter of flags at different sites in relation to wind and weather. Agric. Met. 5:163-181.

RUTTER, N. 1968b
Geomorphic and tree shelter in relation to the surface wind conditions, weather, time of day and season. Agric. Met., 5:319-334.

RUTTER, N. 1968c
Shelter effect of an old-established shelter block of European larch on a slope of mean gradient 1 in 4. Agric. Met. 5:335-349.

RYAN, BILL C. 1977
A mathematical model for diagnosis and prediction of surface winds in mountainous terrain. J. App. Met. 16(6):571-584.

RYDBERG, P.A. 1913
Phytogeographical notes on the Rocky Mountain Region 1. Alpine region. Bull. Torrey Bot. Club. 40:677-686.

SALTER, E.C., and C.H. EVANS 1976
Record of silvicultural trials and demonstrations. Env. Can., Forest Service, Nfld. For. Res. Centre, St. John's. Info. Rept. N-X-137.

SCIECZ, G., D.E. PETZOLD, and R.G. WILSON 1979
Wind in the subarctic forest. J. App. Met. 18:1268-1274.

SCOTT, D.R.M., and S.B. PRESTON 1955
Development of compression wood in eastern white pine through the use of centrifugal force. For. Sci. 1:178-182.

SELLERS, W.D. 1965
Physical climatology. Univ. Chicago Press.

SIMARD, ALBERT J. 1969
Variability in wind speed measurement and its effect on fire danger rating. Forestry Branch, Dept. Fish., For., Ottawa. Inf. Rpt. FF-X-19.

SINNOTT, E.W. 1952
Reaction wood and the regulation of tree form. Amer. J. Bot. 39: 69-78.

SMITH, KAN, and R.H. WEITKNECHT 1915
Windfall damage in selection cuttings in Oregon. Proc. Soc. Amer. For. 10:263-265.

SPRUGEL, D.G. 1976
Dynamic structure of wave-generated Abies balsamea forests in the north eastern United States. J. Ecol. 64:889-911.

SPRUGEL, DOUGLAS G., and F.H. BORMANN 1981
Natural disturbance and the steady state in high altitude balsam fir forests. Science 211:390-393.

SUTHERLAND, C.H., B. JANZ, and A.P. MOAKLER 1963
Study of abnormal winds in southwestern Newfoundland and train delays 1956-62. Canada Dept. Transport, Meteorological Branch. CIR 3903 TEC 484.

SWANSON, F.J., G.W. LIENKAEMPER, and J.R. SEDELL 1976
History, physical effects and management implications of large organic debris in western Oregon streams. Pacific Northwest For. & Range Exp. Sta., Gen. Techn. Rept. PNW-56.

TANSLEY, A.G. 1939
The British Islands and their vegetation. Cambridge Univ. Press.

THOM, A.S. 1971
Momentum absorption by vegetation. Q.J.R.M.S. 97:414-428.

THOMAS, D. 1959
Tatter flags as an index of exposure to wind. Met. Mag. 88(1041): 67-70.

THOMAS, J.M. 1973
Tree deformation by wind in Wales. Weather 28(2):46-58.

TOUMA, J.S. 1977
Dependence of wind profile power law on stability for various locations. J. Air Poll. Control Assoc. 27:863-866.

TRANQUILLINI, W. 1963
Water relations of plants. British Ecological Symposium (editors A.J. Rutter and F.H. Whitehead). Blackwell Publ., London.

WADE, JOHN E., and F.W. HEWSON 1979
Trees as a local climate indicator. J. App. Met. 19:1182-1187.

WADE, JOHN E., and F.W. HEWSON 1980a
A guide to biological wind prospecting. Dept. Atmos. Sci., Oregon State Univ., DOE/ET/10316-80-2, UC-60.

WADE, JOHN E., and F.W. HEWSON 1980b
A guide to biological wind prospecting. Final Report. Dept. Atmos. Sci., Oregon State Univ., DOE:EY-76-506-2227.

WARDLE, PETER 1968
Engelmann spruce (Picea engelmanni Engel.) at its upper limits on the Front Range, Colorado. Ecology 49:483-495.

WEIDMANN, ROBERT H. 1930
A study of windfall loss of western yellow pine in selection cuttings fifteen to thirty years old. J. For. 18:616-622.

WEISCHET, W. 1955
Die Baumkronendeformation als physiognomische Beobachtungsgrundlage. In Die Geländeklimate der mederrheinischen Bucht und ihrer Rahmendlandschaften. Münchener Geogr. Hefte., Univ. München 8: 105-114.

WELLS, B.W., and I.V. SHUNK 1937
Sea-side shrubs: Wind forms vs. spray forms. Science 85:499.

WERREN, GARRY L. 1981
Dendroecology of spruce in central Labrador-Ungava. McGill Subarctic Res. Pap. 32:97-116.

WESTING, ARTHUR H. 1959
Studies on the physiology of compression wood formation in Pinus L. Yale Univ. New Haven, Ph.D. Thesis.

WESTING, ARTHUR H. 1961
Changes in radial symmetry in the leaders of eastern white pine following inclination. J. For. 59:17-19.

WESTING, ARTHUR H. 1964
Geotropism: Its orienting force. Science 144:1342-1344.

WESTING, ARTHUR H. 1965
Formation and function of compression wood in gymnosperms. Bot. Rev. 31(3):381-480.

WHITE, J. 1908
Formation of redwood in conifers. Proc. Roy. Soc. Victoria, N.S. 20(2):107-124.

WILTON, W.C. 1964
The forests of Labrador. Canada Dept. of Forestry, Publ. No. 1066.

WOOLLEY, STUART C. 1980
Wind field mapping utilizing flagged trees as indicators of speed and direction. In A guide to biological wind prospecting. (Editors Joseph E. Wade and E.W. Hewson). Dept. Atmos. Sci., Oregon State Univ., DOE:EY-76-306-2227.

YOSHINO, MASATOSHI M. 1957
Local characteristics of surface winds in a small valley. Sci. Rept. Tokyo Kyoiku Diagaku (c), 4(46):129-151.

YOSHINO, MASATOSHI M. 1973
Studies on wind-shaped trees; their classification, distribution and significance as a climatic indicator. Climat. Notes, Hosei Univ. (12):1-52.

YOSHINO, MASATOSHI M. 1975
Climate in a small area: An introduction to local meteorology.
Univ. Yokyo Press, Tokyo.

APPENDIX

Table A1. Ratio of leeward branch extension to windward branch extension near base, B_o, at one-third height, $B_{0.33}$, and two-thirds height, $B_{0.66}$ and angle of stem inclination, AT.

SITE	TREE #	B_0	$B_{0.33}$	$B_{0.66}$	AT
	1	1.21	1.08	1.13	6
	2	1.09	1.65	1.46	5
STEPHENVILLE	3	1.13	1.45	1.25	7
	4	1.14	1.27	0.86	7
	5	1.27	1.27	1.00	4
	X	1.12	1.34	1.14	5.8
	1	1.22	1.13	1.62	5
	2	1.00	1.29	1.38	7
DEER LAKE A	3	1.76	1.63	1.15	7
	4	1.11	1.21	1.11	7
	5	1.04	1.12	1.14	7
	X	1.23	1.28	1.28	6.4
	1	1.10	1.16	1.16	1
	2	1.62	1.26	1.40	5
BUCHANS	3	1.50	1.70	1.54	2
	4	1.56	1.57	1.70	9
	5	2.03	1.56	1.67	5
	X	1.56	1.45	1.49	4.4
	1	1.44	1.56	1.53	6
	2	3.76	4.17	2.40	11
TWILLINGATE	3	3.10	2.06	1.55	5
	4	1.48	1.85	1.80	17
	5	1.51	1.42	1.90	12
	X	2.26	2.21	1.83	10.2
	1	1.42	1.65	2.00	17
	2	1.31	1.35	2.28	7
GANDER	3	1.42	1.38	1.80	9
	4	1.03	1.28	1.41	11
	5	1.35	1.42	1.75	8
	X	1.31	1.42	1.85	10.4
	1	1.52	2.47	1.80	7
	2	1.23	1.50	2.00	9
BONAVISTA	3	1.41	1.62	1.81	9
	4	1.28	1.55	2.00	7
	5	1.48	2.96	1.86	11
	X	1.37	2.02	1.90	8.6
	1	1.16	3.50	11.00	32
	2	1.50	1.50	4.75	26
ST. JOHN'S A	3	1.25	1.43	1.73	23
	4	1.48	1.86	11.00	27
	5	2.17	1.48	1.64	31
	X	1.51	1.95	6.02	27.8

Table A2. Stem length of sample trees at calibration sites

CALIBRATION SITE	STEM LENGTH (m)/TREE NUMBER					
	1	2	3	4	5	MEAN ± SD
STEPHENVILLE	4.21	5.52	5.24	5.12	4.94	5.0 ± 0.44
DEER LAKE	6.27	8.89	9.94	7.28	10.57	8.59 ± 1.61
BUCHANS A	7.69	6.07	5.41	7.90	7.35	6.94 ± 1.00
TWILLINGATE	3.29	2.78	2.76	4.08	4.97	3.60 ± 0.84
GANDER	9.20	7.95	6.41	5.90	5.10	6.93 ± 1.47
BONAVISTA	2.96	3.58	3.58	3.87	3.55	3.51 ± 0.30
ST. JOHN'S	8.70	8.90	13.20	10.60	9.60	10.20 ± 1.64

Table A3. Canadian normals for mean monthly and annual wind speed at calibration sites (m S^{-1})

MONTH	CALIBRATION SITE						
	STEPHENVILLE	DEER LAKE A	BUCHANS A	TWILLINGATE	GANDER	BONAVISTA	ST. JOHN'S A
JAN	5.4	4.6	6.9	9.2	6.8	9.5	7.6
FEB	5.1	4.7	6.9	8.3	6.6	8.9	7.6
MAR	4.7	4.7	7.1	7.6	6.5	8.2	7.5
APR	4.3	4.6	6.2	6.6	6.0	7.2	6.8
MAY	3.9	4.4	5.3	5.7	5.5	6.5	6.4
JUN	3.3	4.3	5.1	5.7	5.2	6.4	6.2
JUL	3.1	4.0	4.8	5.8	4.8	6.3	5.9
AUG	3.5	3.8	5.1	6.1	4.8	6.6	5.9
SEP	3.9	3.9	5.4	7.2	5.3	7.3	6.1
OCT	4.1	3.9	5.7	8.0	5.7	8.4	6.6
NOV	4.7	5.3	6.1	8.6	6.1	8.7	7.0
DEC	5.1	4.3	6.6	9.3	6.3	9.3	7.4
ANNUAL	4.3	4.3	5.9	7.3	5.8	7.8	6.8
± SD	0.72	0.31	0.78	1.30	.66	1.14	0.63

Table A4. Station anemometer height; H_A, mean height of sample trees, $\bar{H}_T$; height to which wind data base is adjusted, $\bar{H}_{T\ 0.66}$; and the adjustment factor,* u^{α}.

CALIBRATION SITE	H_A (m)	$\bar{H}_T$ (m)	$\bar{H}_{T\ 0.66}$ (m)	Z^{α}
STEPHENVILLE	10.1	5.00	3.3	.85
DEER LAKE A	10.1	8.95	5.91	.93
BUCHANS A	13.1	6.94	4.58	.86
TWILLINGATE	19.8	3.60	2.40	.74
GANDER	10.1	6.93	4.57	.90
BONAVISTA	10.1	3.51	2.32	.81
ST. JOHN'S A	10.1	10.20	6.73	.94

*Mean tree height is obtained from Table A3.

**The adjustment factor, Z^{α}, is derived from the power law where

$$u^{\alpha} = (Z_2/Z_1)^{\alpha} = (\bar{H}_{T\ 0.66}/H_A)^{0.14}$$

i.e, the ratio of winds at height Z_2 to anemometer height Z_1. The value of $\alpha = 0.14$ for unstable conditions based on Sellers (1965) and Woolley (1980).

Table A5. Mean annual wind speed adjusted to 2/3 mean tree-height at calibration sites (m S^{-1})

MONTH	CALIBRATION SITE						
	STEPHENVILLE	DEER LAKE A	BUCHANS A	TWILLINGATE	GANDER	BONAVISTA	ST. JOHN'S A
JAN	4.6	4.3	5.9	6.8	6.1	7.7	7.1
FEB	4.3	4.3	5.9	6.1	5.9	7.2	7.1
MAR	4.0	4.3	6.1	5.6	5.9	6.6	7.0
APR	3.7	4.3	5.3	4.9	5.4	5.8	6.4
MAY	4.6	4.1	4.6	4.2	4.9	5.3	6.0
JUN	3.8	4.0	4.4	4.2	4.7	5.2	5.8
JUL	2.6	3.7	4.1	4.2	4.3	5.1	5.0
AUG	3.0	3.5	4.4	4.5	4.3	5.3	5.5
SEP	3.3	3.6	4.6	5.3	4.8	5.9	5.7
OCT	3.5	3.6	4.9	5.9	5.1	6.8	6.2
NOV	4.0	4.0	5.2	6.4	5.5	7.0	6.6
DEC	4.3	4.0	5.6	6.9	5.7	7.5	7.0
± SD	0.60	0.28	0.65	0.97	0.60	0.92	0.60

Table A6. Mean monthly vector speed at calibration sites (Source: Anon, 1981)

MONTH	MEAN VECTOR SPEED (km/hr)						
	STEPHENVILLE	DEER LAKE A	BUCHANS A	TWILLINGATE	GANDER	BONAVISTA	ST. JOHN'S A
JAN	6.3	7.2	9.6	10.1	9.9	15.7	11.8
FEB	5.1	7.1	9.4	10.0	9.5	12.8	11.1
MAR	2.9	4.6	10.5	8.5	6.7	8.1	8.4
APR	2.0	2.1	7.7	6.1	5.8	4.9	7.8
MAY	1.4	3.0	4.9	2.7	4.0	4.4	7.7
JUN	2.3	5.5	5.0	3.5	6.0	8.6	11.0
JUL	4.2	9.0	7.3	9.9	8.9	11.9	13.6
AUG	5.0	7.1	8.4	8.6	7.8	9.7	11.5
SEP	4.9	7.4	10.0	11.5	8.8	9.[illegible]	10.8
OCT	5.0	7.8	9.2	11.1	8.9	12.4	10.9
NOV	4.0	5.8	9.2	12.4	8.5	11.1	10.0
DEC	5.5	5.6	7.6	16.1	10.0	13.2	11.8
MEAN	4.1	6.0	8.2	9.2	7.9	10.2	10.5
± SD	1.48	1.90	1.70	3.58	1.80	3.21	1.70

Table A7. Sum of tree ring width for years 1973-1983 on windward side (TW_{10}) and leeward side (CW_{10}) across the maximum width of disc, and their compression ratio ($C_i = CW/TW$)

SITE	TREE #	TW_{10}	CW_{10}	Ci	MEAN ± SD
	1	8.11	12.36	1.52	
	2	15.97	19.01	1.19	
STEPHENVILLE	3	12.04	19.74	1.64	1.35 ± 0.22
	4	6.74	8.46	1.26	
	5	17.05	19.36	1.12	
	1	19.86	22.63	1.14	
	2	16.62	22.85	1.37	
DEER LAKE A	3	14.84	24.53	1.65	1.56 ± 0.39
	4	12.66	18.31	1.45	
	5	14.98	32.46	2.17	
	1	11.94	25.37	2.12	
	2	8.54	11.58	1.35	
BUCHANS A	3	11.91	17.25	1.45	1.53 ± 0.34
	4	20.95	27.93	1.33	
	5	15.83	21.80	1.38	
	1	12.64	23.20	1.84	
	2	10.26	13.44	1.31	
TWILLINGATE	3	7.11	16.34	2.30	1.74 ± 0.37
	4	22.70	37.01	1.63	
	5	15.32	24.91	1.62	
	1	21.30	27.81	1.31	
	2	29.43	31.15	1.06	
GANDER	3	22.72	34.44	1.52	1.34 ± 0.18
	4	11.48	15.26	1.33	
	5	15.12	22.44	1.48	
	1	13.11	16.08	1.23	
	2	7.97	16.99	2.13	
BONAVISTA	3	7.86	16.83	1.71	1.66 ± 0.34
	4	11.85	28.85	2.43	
	5	29.10	44.20	1.50	
	1	23.64	40.19	1.70	
	2	23.59	34.47	1.46	
ST. JOHN'S A	3	29.10	44.20	1.50	1.75 ± 0.39
	4	11.85	18.85	2.43	
	5	29.10	44.20	1.50	

Table A8. Mean monthly vector direction at calibration sites (Degrees). (Source, Anon, 1981)

	VECTOR DIRECTION						
MONTH	STEPHENVILLE	DEER LAKE A	BUCHANS A	TWILLINGATE	GANDER	BONAVISTA	ST. JOHN'S A
JAN.	290	250	290	270	260	270	270
FEB	290	250	300	290	270	280	270
MAR	320	250	330	330	290	280	280
APR	360	310	320	320	300	290	280
MAY	310	280	290	250	270	240	270
JUN	260	240	250	220	240	220	250
JUL	240	240	230	210	220	210	240
AUG	260	240	250	220	240	230	240
SEP	260	240	240	240	250	250	260
OCT	280	250	240	240	250	270	260
NOV	260	250	260	260	240	260	250
DEC	290	250	260	260	260	270	260
ANNUAL"	285	254	272	259	258	256	260
MAY-JUN	268	250	255	225	243	225	250
+ SD	31.8	19.8	31.8	36.6	21.7	24.7	13.5

Table A9. Direction of stem inclination, S_{DIR}, and direction of maximum width of tree ring asymmetry, C_{DIR}, of sample trees at calibration sites

CALIBRATION SITE		DIRECTION (°)					
		SAMPLE TREE NUMBER					
		1	2	3	4	5	MEAN
STEPHENVILLE	S_{DIR}	200	200	200	200	200	200
	C_{DIR}	200	200	200	260	200	212
DEER LAKE A	S_{DIR}	194	192	194	192	194	193
	C_{DIR}	194	250	223	280	229	235
BUCHANS A	S_{DIR}	212	212	212	214	211	213
	C_{DIR}	267	167	165	214	257	214
TWILLINGATE	S_{DIR}	260	264	270	270	270	267
	C_{DIR}	260	228	235	250	308	256
GANDER	S_{DIR}	231	232	232	231	231	232
	C_{DIR}	231	188	232	191	149	198
BONAVISTA	S_{DIR}	270	270	267	268	266	268
	C_{DIR}	270	226	267	228	184	235
ST. JOHN'S A	S_{DIR}	240	240	240	240	240	240
	C_{DIR}	240	240	203	220	215	224

S_{DIR} = Direction of stem inclination of sample trees,

C_{DIR} = Direction of maximum compression ratio, C.

PHYTOGEOGRAPHIC MAP OF NEWFOUNDLAND

by Alexander Robertson

ENVIRONMENT CANADA
CANADIAN FORESTRY SERVICE
St. John's, Newfoundland
Canada

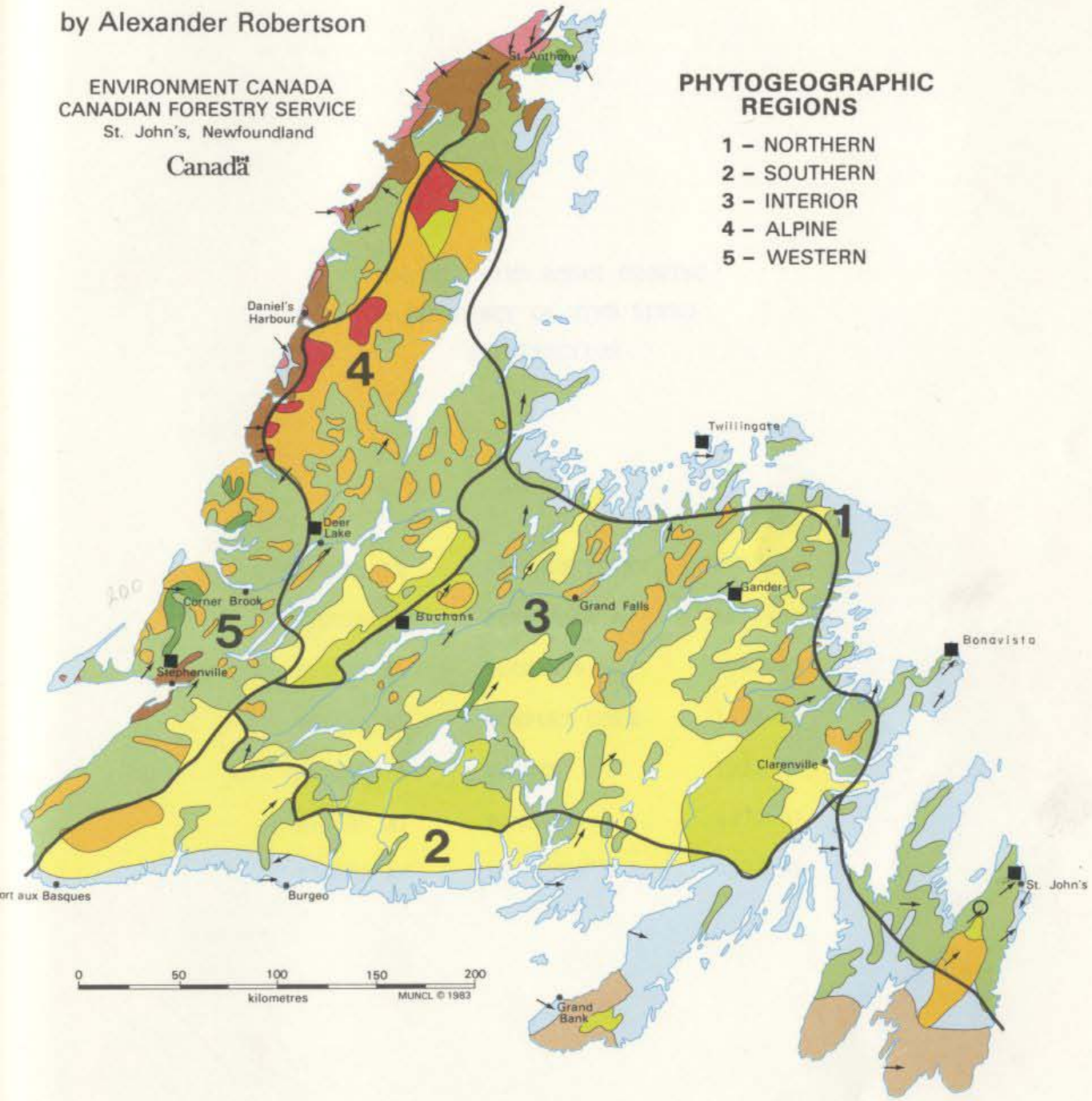

VEGETATION TYPES

- Alpine
- Subalpine
- Interior Barren
- Coastal Barren
- Limestone Barren
- Serpentine Barren
- Blanket Bog
- Plateau Raised Bog
- Patterned Fen
- Forest

→ WIND DIRECTION INDICATED BY TAMARACK TREES
■ CALIBRATION SITES
○ BLACK MOUNTAIN WIND SURVEY SITE

MONTHLY WIND ROSES SHOWING
FREQUENCY OF WIND SPEED
BY DIRECTION

FIGURE A2	STEPHENVILLE	1972-81
FIGURE A3	DEER LAKE A	1972-81
FIGURE A4	BUCHAN'S A	1962-65
FIGURE A5	COMFORT COVE	1972-81
FIGURE A6	GANDER	1972-81
FIGURE A7	BONAVISTA	1972-81
FIGURE A8	ST. JOHN'S A	1972-81

ST JOHN'S A 1972-81

BONAVISTA **1972-81**

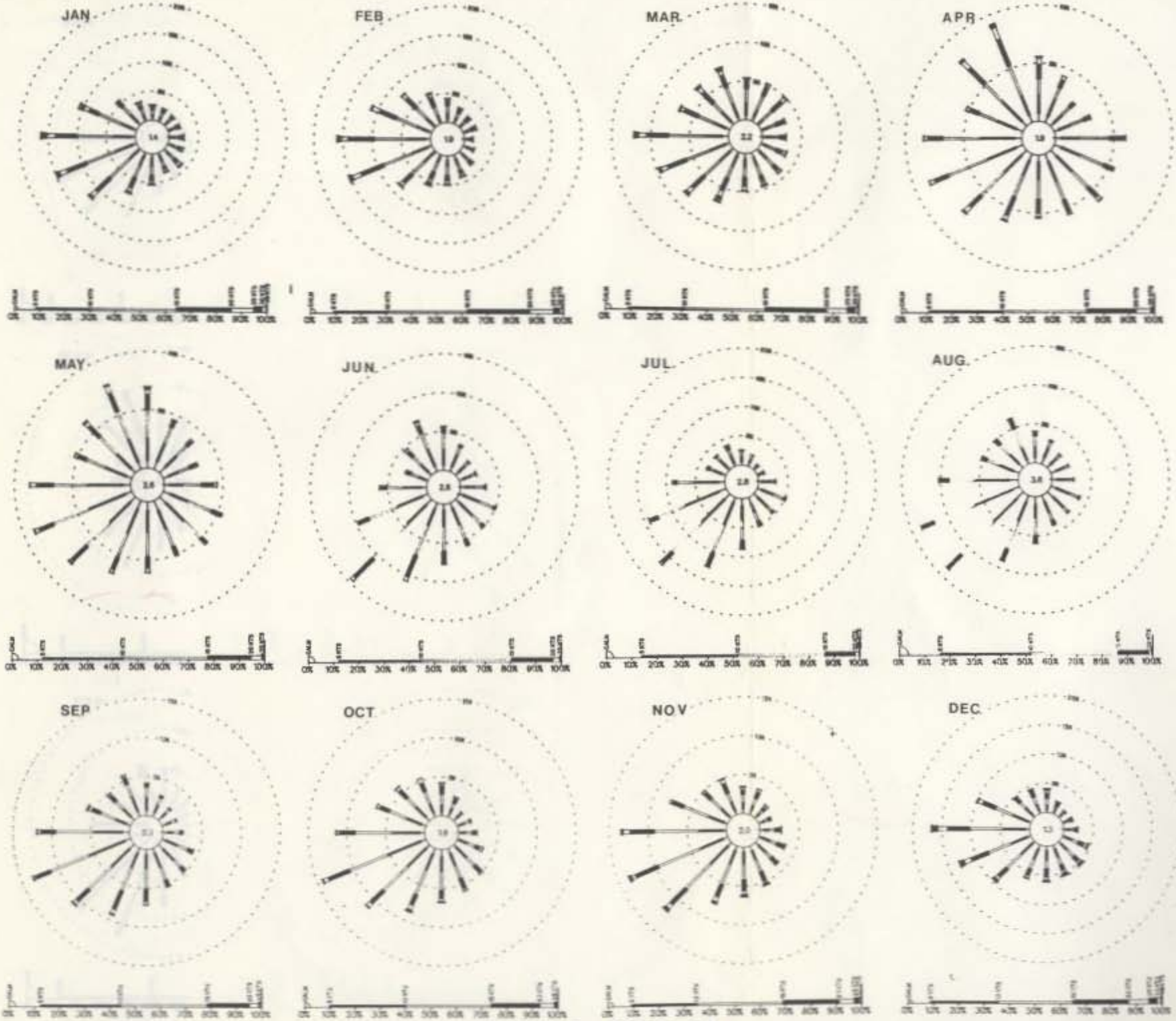

GANDER 1972-81

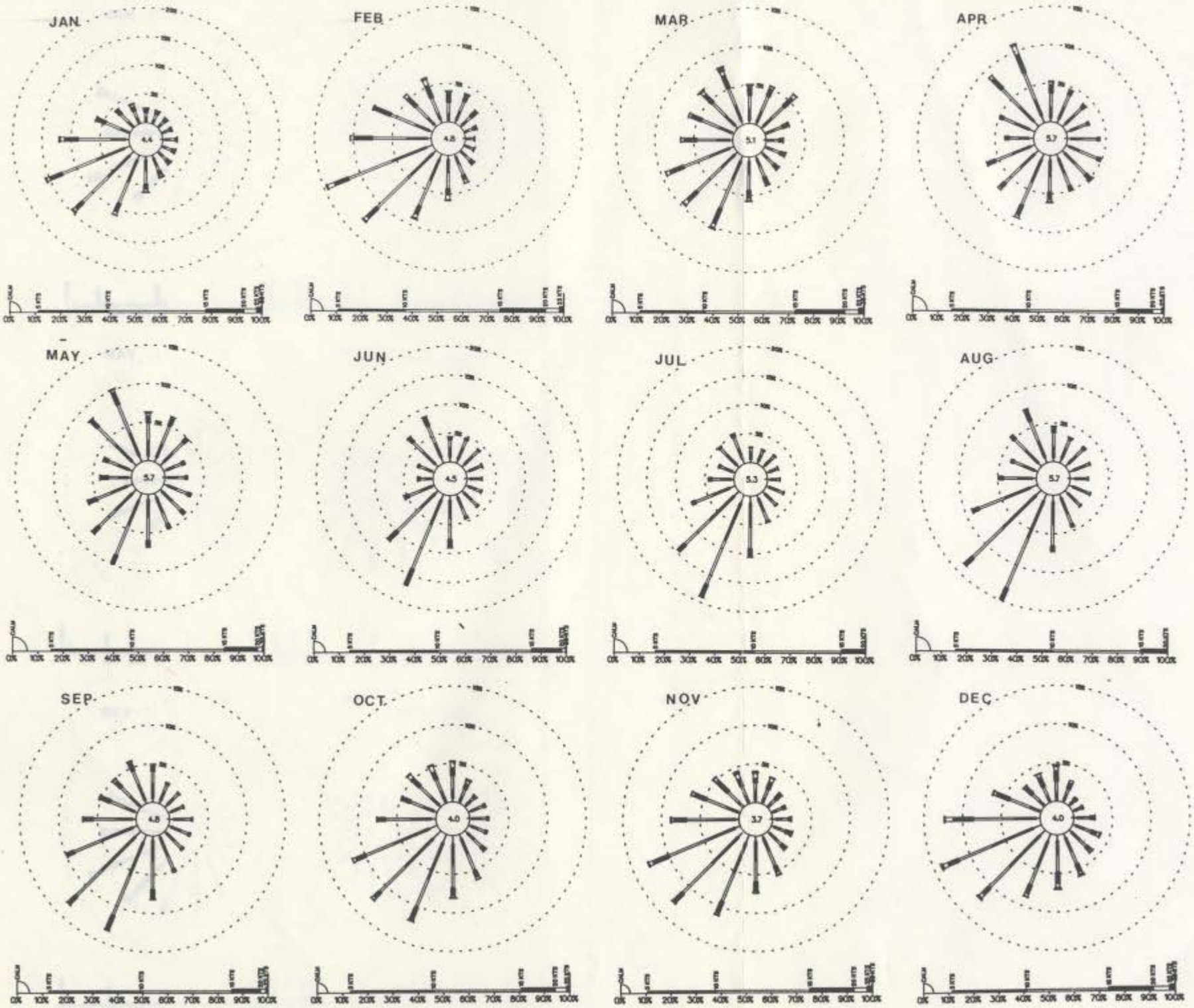

COMFORT COVE **1972-81**

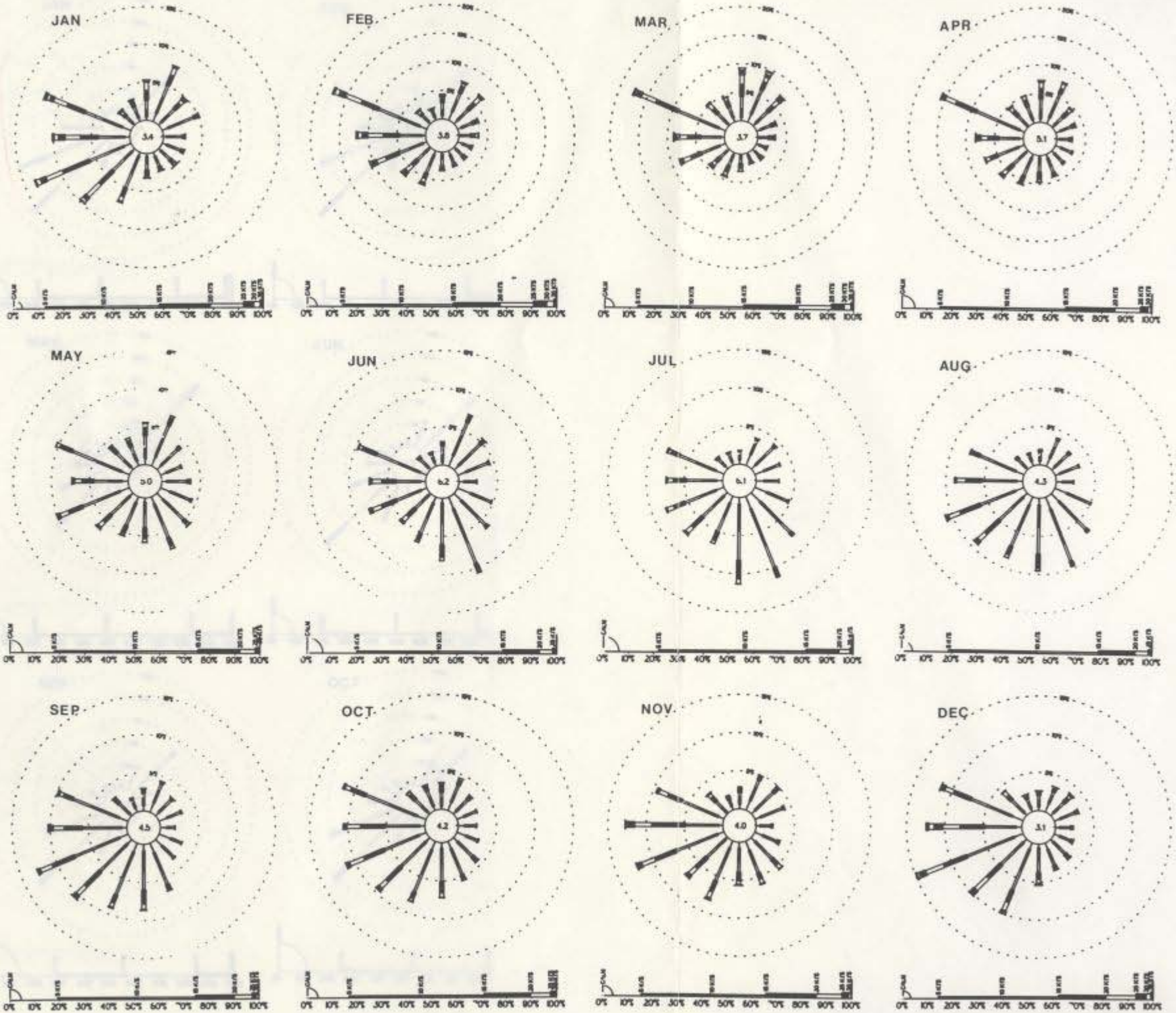

BUCHANS A 1962-65

DEER LAKE A 1971-81

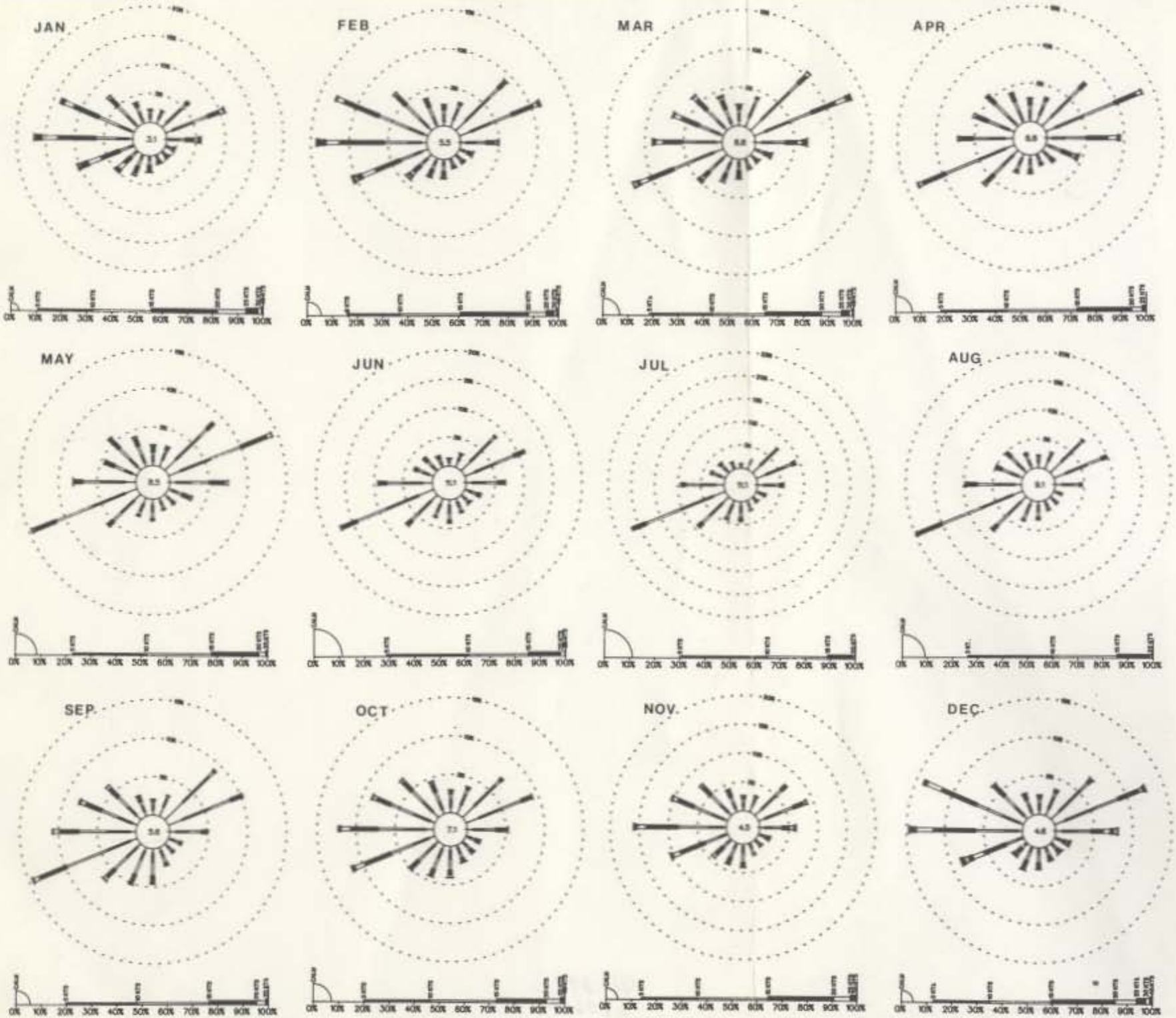

STEPHENVILLE **1972-81**